

# Stable Isotope Hydrology

Roger E. Diamond

# *Stable Isotope Hydrology*

*The Groundwater Project*

i

*Roger E. Diamond*

*Senior Lecturer  
Department of Geology  
University of Pretoria  
Pretoria, South Africa*

*Stable Isotope Hydrology*

*The Groundwater Project  
Guelph, Ontario, Canada*

All rights reserved. This publication is protected by copyright. No part of this book may be reproduced in any form or by any means without permission in writing from the authors (to request permission contact: [permissions@gw-project.org](mailto:permissions@gw-project.org)). Commercial distribution and reproduction are strictly prohibited.

Groundwater-Project (The GW-Project) works are copyrighted and can be downloaded for free from [gw-project.org](http://gw-project.org). Anyone may use and share [gw-project.org](http://gw-project.org) links to download GW-Project's work. It is neither permissible to make GW-Project documents available on other websites nor to send copies of the documents directly to others. Kindly honor this source of free knowledge that benefits you and all those who want to learn about groundwater.

Copyright © 2022 Roger E. Diamond (The Author)

Published by the Groundwater Project, Guelph, Ontario, Canada, 2022.

Diamond, Roger E.

Stable Isotope Hydrology / Roger E. Diamond - Guelph, Ontario, Canada, 2022

102 pages

ISBN: 978-1-77470-043-3

DOI: <https://doi.org/10.21083/978-1-77470-043-3>

Please consider signing up for the GW-Project mailing list to stay informed about new book releases, events and ways to participate in the GW-Project. When you sign up for our email list it helps us build a global groundwater community. [Sign up](#).

**Citation:** Diamond, Roger E., 2022, [Stable Isotope Hydrology](#). The Groundwater Project, Guelph, Ontario, Canada. doi: <https://doi.org/10.21083/978-1-77470-043-3>.



*Domain Editors:* Robert Kalin, Eileen Poeter, and John Cherry

*Board:* John Cherry, Paul Hsieh, Robert Kalin, Ineke Kalwij, Stephen Moran, Everton de Oliveira and Eileen Poeter

*Steering Committee:* John Cherry, Allan Freeze, Paul Hsieh, Ineke Kalwij, Douglas Mackay, Stephen Moran, Everton de Oliveira, Beth Parker, Eileen Poeter, Ying Fan, Warren Wood, and Yan Zheng.

*Cover Image:* Roger Diamond, 2022. Schematic diagram of typical hydrogen and oxygen isotope ratios for major water types in the global hydrological cycle.

## Dedication

To all those friends, family, colleagues, students, climbers, weeders and hackers who have shared time with me outdoors, enjoying and puzzling over the wonders of nature.

# Table of Contents

<b>DEDICATION</b> .....	<b>IV</b>
<b>TABLE OF CONTENTS</b> .....	<b>V</b>
<b>THE GROUNDWATER PROJECT FOREWORD</b> .....	<b>VII</b>
<b>FOREWORD</b> .....	<b>VIII</b>
<b>ACKNOWLEDGEMENTS</b> .....	<b>IX</b>
<b>1 INTRODUCTION</b> .....	<b>1</b>
<b>2 ISOTOPES AND ISOTOPOLOGUES</b> .....	<b>4</b>
<b>3 MEASUREMENT AND STANDARDS</b> .....	<b>7</b>
3.1 MASS SPECTROMETRY .....	8
3.2 LASER CAVITY SPECTROSCOPY.....	9
<b>4 ISOTOPE FRACTIONATION</b> .....	<b>11</b>
4.1 KINETIC FRACTIONATION .....	11
4.2 EQUILIBRIUM FRACTIONATION.....	12
4.3 FRACTIONATION AND ENRICHMENT FACTORS .....	13
4.4 RAYLEIGH DISTILLATION.....	15
<b>5 METEORIC WATER LINES</b> .....	<b>17</b>
5.1 THE GLOBAL METEORIC WATER LINE.....	17
5.2 LOCAL METEORIC WATER LINES.....	18
5.3 CALCULATION OF METEORIC WATER LINES .....	20
5.3.1 <i>Least Squares Regression</i> .....	21
5.3.2 <i>Reduced Major Axis Regression (RMA)</i> .....	21
5.4 WEIGHTED REGRESSION LINE EQUATIONS.....	21
<b>6 STABLE ISOTOPE HYDROLOGY</b> .....	<b>23</b>
6.1 ENVIRONMENTAL FACTORS AFFECTING WATER ISOTOPES (ISOTOPE EFFECTS).....	27
6.1.1 <i>The Temperature Effect</i> .....	27
6.1.2 <i>The Latitude Effect</i> .....	28
6.1.3 <i>The Continental Effect</i> .....	29
6.1.4 <i>The Altitude Effect</i> .....	31
6.1.5 <i>The Amount Effect</i> .....	31
6.2 THE DEUTERIUM EXCESS .....	33
6.3 EVENT VARIATION .....	35
6.4 MASS BALANCE .....	37
6.5 HYDROGRAPH SEPARATION.....	39
6.6 GEOTHERMAL WATERS .....	43
6.7 PALEOWATERS.....	46
6.8 PLANT WATERS .....	53
<b>7 CASE STUDIES</b> .....	<b>56</b>
7.1 MOISTURE SOURCE REGION .....	56
7.2 RECHARGE AREA.....	57
7.3 SELECTIVE RECHARGE OF HEAVY RAINS .....	59
7.4 RECHARGE ESTIMATION .....	60
7.5 PISTON FLOW OF GROUNDWATER DURING A STORM.....	61
7.6 GROUNDWATER CIRCULATION AND AGE.....	64

7.7	DETECTING SURFACE WATER IN GROUNDWATER .....	64
7.8	DETECTING GROUNDWATER IN SURFACE WATER .....	66
7.9	RESIDENCE TIME .....	67
<b>8</b>	<b>WATER SAMPLING FOR STABLE ISOTOPE ANALYSIS .....</b>	<b>68</b>
8.1	PRACTICAL CONSIDERATIONS .....	68
8.2	PRECIPITATION .....	68
8.2.1	<i>Spatial and Temporal Variation in Precipitation</i> .....	68
8.2.2	<i>Standard Daily or Cumulative Monthly Collectors</i> .....	69
8.3	SURFACE WATER .....	70
8.4	GROUNDWATER.....	71
8.4.1	<i>Natural Groundwater Sources: Springs and Seeps</i> .....	71
8.4.2	<i>Artificial Groundwater Sampling Points: Wells, Boreholes and Piezometers</i> .....	72
<b>9</b>	<b>FURTHER READING .....</b>	<b>74</b>
<b>10</b>	<b>WRAP-UP .....</b>	<b>75</b>
<b>11</b>	<b>EXERCISES.....</b>	<b>77</b>
	EXERCISE 1 - METEORIC WATER LINE CALCULATIONS .....	77
	EXERCISE 2 - CALCULATION OF RECHARGE ALTITUDE .....	78
	EXERCISE 3 - HYDROGRAPH SEPARATION.....	80
<b>12</b>	<b>REFERENCES .....</b>	<b>81</b>
<b>13</b>	<b>EXERCISE SOLUTIONS .....</b>	<b>94</b>
	SOLUTION EXERCISE 1 - METEORIC WATER LINES .....	94
	SOLUTION EXERCISE 2 - RECHARGE ALTITUDE.....	96
	SOLUTION EXERCISE 3 - HYDROGRAPH SEPARATION .....	98
<b>14</b>	<b>NOTATIONS .....</b>	<b>99</b>
<b>15</b>	<b>ABOUT THE AUTHOR .....</b>	<b>101</b>

## The Groundwater Project Foreword

The Year 2022 marks as an important year for groundwater because the United Nations Water Members and Partners chosen the theme of this year's March 22 World Water Day to be: "Groundwater: making the invisible visible". The goal of the Groundwater Project (GW-Project) is in sync with this theme.

The GW-Project, a registered charity in Canada, is committed to contributing to advancement in groundwater education and brings a unique approach to the creation and dissemination of knowledge for understanding and problem solving. The GW-Project operates the website <https://gw-project.org/> as a global platform for the democratization of groundwater knowledge, founded on the principle that:

*"Knowledge should be free and the best knowledge should be free knowledge." Anonymous*

The mission of the GW-Project is promoting groundwater learning. This is accomplished by providing accessible, engaging, high-quality, educational, copyrighted materials, free-of-charge online in many languages, to all who want to learn about groundwater. In short, providing essential knowledge tools for developing groundwater sustainably for humanity and ecosystems.

This is a new type of global educational endeavor in that it is based on volunteerism of professionals from different disciplines and includes academics, consultants and retirees. The GW-Project involves many hundreds of volunteers associated with more than 200 hundred organizations from 27 countries and six continents, with growing participation.

The GW-Project is an on-going endeavor and will continue with hundreds of books being published online over the coming years, first in English and then in other languages, for downloading wherever the Internet is available. An important tenet of the GW-Project books is a strong emphasis on visualization via clear illustrations that stimulate spatial and critical thinking to facilitate absorption of information.

The GW-Project publications also include supporting materials such as videos, lectures, laboratory demonstrations, and learning tools in addition to providing, or linking to, public domain software for various groundwater applications supporting the educational process.

The GW-Project is a living entity, so subsequent editions of the books will be published from time to time. Users are invited to propose revisions.

We thank you for being part of the GW-Project Community. We hope to hear from you about your experience with using the books and related material. We welcome ideas and volunteers!

The GW-Project Steering Committee

January 2022

## Foreword

Isotope hydrology uses isotopic measurements of water constituents for understanding of hydrology, and its most diverse applications are those directed at groundwater. Given the importance of this topic, the Groundwater Project (GW Project) has launched a series of books about isotopes, starting with *Introduction to Isotopes and Environmental Tracers as Indicators of Groundwater Flow* by Peter Cook, which will be followed by in-depth books. *Stable Isotopes Hydrology* by Roger Diamond is the first in depth book of the series.

This book concerns the most fundamental isotopes for groundwater studies, the non-radioactive elements of oxygen and deuterium in water molecules. The analysis of oxygen and deuterium give water a voice. Since the first use of these isotopes for research in the 1960s, their application has become routine in the pursuit of answers to many groundwater questions. Use of these isotopes, and a few others, became more feasible as water analysis laboratories became more common and the cost of running such tests ceased to be restrictive. Subsequent tests showed a number of successful applications resulting in increased use of the technique. Of the many isotopes useful in groundwater studies, the stable isotopes of water are the easiest to use because the required sample size is small and sampling methods are uncomplicated. In many circumstances, these water isotopes identify the geographic or temporal origin of the water, such as paleowater, or distinguish water zones of different origins in an aquifer. The small sample volume needed for analysis enables study of aquifer-aquitard systems to address questions relevant to water resources and contamination. Of the many techniques that have been added to the hydrogeologist's toolbox over the past half century, the stable isotopes of water are amongst the most essential.

The author of this book, Roger Diamond, is a Senior Lecturer in Hydrogeology and Geochemistry at the University of Pretoria in South Africa. He has published extensively on a wide variety of applications of these isotopes in the southern part of Africa. Isotopic tools have proven to be especially effective in this region where there is much complexity in the hydrogeology and diversity in groundwater.

John Cherry, The Groundwater Project Leader  
Guelph, Ontario, Canada, September 2022

## Acknowledgements

I deeply appreciate the thorough and useful reviews of and contributions to this book by the following individuals:

- ❖ John Cherry, G360 Institute for Groundwater Research, University of Guelph, Ontario, Canada;
- ❖ Robert Kalin, Department of Civil and Environmental Engineering, University of Strathclyde, Glasgow, Scotland;
- ❖ Peter Cook, National Centre for Groundwater Research and Training, Flinders University, South Australia;
- ❖ Ian Clark, Department of Earth Sciences, University of Ottawa, Canada;
- ❖ Warren Wood, Department of Earth and Environmental Sciences, Michigan State University, USA;
- ❖ Johannes Barth, Department of Geography and Earth Sciences, Friedrich-Alexander-University of Erlangen-Nürnberg;
- ❖ Everton de Oliveira, Hidroplan and Instituto Água Sustentável (Sustainable Water Institute), Brazil; and,
- ❖ Ferdinando Manna, G360 Institute for Groundwater Research, University of Guelph, Ontario, Canada.

I appreciate the contributions of Peter Cook and John Cherry on the genesis of this book. I am grateful for Amanda Sills and the Formatting Team of the Groundwater Project for their oversight and copyediting of this book. I thank Eileen Poeter (Colorado School of Mines, Golden, Colorado, USA) for reviewing, editing, and producing this book.

# 1 Introduction

Stable isotope hydrology is the study of water using the stable isotopes of the hydrogen and oxygen making up the water molecule. Many other stable isotopes can also be used to understand water, but are not part of the actual water molecule and are found within the dissolved matter (carbonate, nitrate, sulphate among others) in water.

As explained later in this book, the abundances of the different isotopes of hydrogen and oxygen vary as water moves through the water cycle. These variations are caused by reactions and transitions (e.g., evaporation and condensation). By measuring these variations, we are able to say something about the history of the water before it arrived at the point where we sampled it (Figure 1).



**Figure 1** - The author collecting samples of snow for stable isotope analysis for his PhD, from Waaihoek Peak in the Hex River Mountains, Western Cape, South Africa. The snow was cored to enable analysis of the layers of snow from consecutive weather events and from the melted/evaporated surface layer between snow storms.

Many other chemical and isotopic methods are available to help us understand water and the processes it undergoes. However, all of the methods other than stable isotopes of water make use of dissolved substances or isotopes that occur in minor to trace quantities. For example, Cl is typically in the range of 1 ppm to 10,000 ppm, NO<sub>3</sub> is seldom above 100 ppm, Sr isotopes occur at ppb levels, and <sup>14</sup>C or <sup>222</sup>Rn (radioactive isotopes) occur at even smaller fractions of the water being sampled. These tracers can therefore more easily be affected by precipitation, adsorption, dissolution and other reactions than the H and O isotopes of water.

The stable isotopes of water constitute nearly 100 percent of the water molecule and therefore suffer far less from reactions that might disturb the isotope abundances. For example, weathering of minerals will release Mg or Sr and change the chemical or isotopic

abundance of such tracers as groundwater moves through an aquifer. The release of oxygen into the groundwater in the form of  $\text{HCO}_3$ ,  $\text{H}_4\text{SiO}_4$  or other species, although able to exchange oxygen with  $\text{H}_2\text{O}$ , will do so in such minor quantities relative to the circulating groundwater, that the stable isotope abundances of the water will not be affected. This behavior, where the species of interest conserves its composition through space and time, is called conservative behavior.

The main exception to the conservative behavior of stable isotopes of groundwater is in geothermal environments, where high temperatures increase the rate of reaction between rock and water, shifting the isotope abundances, particularly oxygen, due to its dominance in almost every mineral. Another exception to conservative behavior is where dissolved gases, such as  $\text{H}_2\text{S}$  or  $\text{CO}_2$  interact with  $\text{H}_2\text{O}$ , either chemically or through isotopic exchange, and thereby change the isotope composition of the water. These environments aside, the other main way in which the stable isotopes in groundwater may change over time is due to mixing with other groundwaters, which may or may not have different isotope abundances.

In many groundwater systems though, neither geothermal or geochemical reactions nor mixing occur, and the stable isotope composition of groundwater remains fairly constant from recharge point to discharge location. In these instances, variations in the stable isotope composition of groundwater must be due to variations in the recharge, or input to the system. Therefore, in order to understand the hydrogeology, we look to both surface and atmospheric waters to find the source of stable isotope variations. This means that, as hydrogeologists, we need to consider the complete water cycle and not only the portion occurring below ground, in order to make full use of stable isotopes. This is why we talk about *stable isotope hydrology* and not stable isotope hydrogeology (Figure 2).

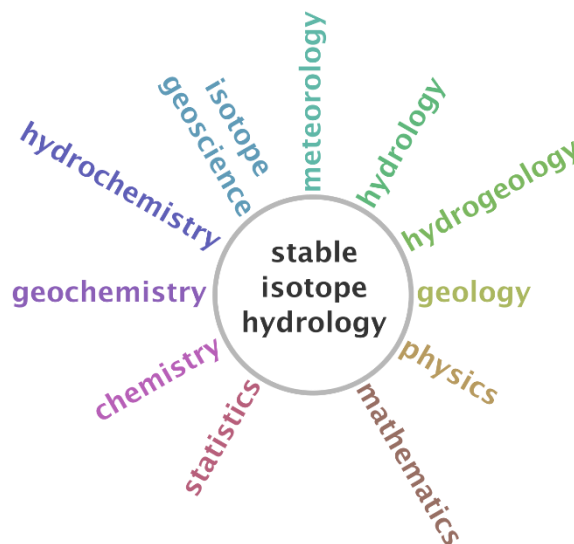


**Figure 2** - Stable isotope hydrology interfaces with many other branches of earth science and the fundamental sciences, such as mathematics and chemistry.

The value of the preserved stable isotope compositions of groundwater is that they can then tell us something about the conditions at and prior to recharge. This is useful for understanding recharge and precipitation processes, including evaporation, intensity of precipitation, altitude of recharge and temperature of condensation. For example, if the groundwater is old, then it may provide insight into past climates and therefore forms one avenue in which scientists conduct paleoclimatic research.

This book outlines stable isotope hydrology at an introductory level as well as including some more advanced applications, aimed at students and professionals with a good understanding of hydrogeology, but little prior knowledge of isotopes. A good grounding in geology along with basic chemistry and physics is essential to being a good hydrogeologist. Knowledge of subjects such as meteorology, hydrology and geochemistry are also helpful at times. This book explains the occurrence of stable isotopes in water molecules and how they change abundance through the water cycle. Sections include measurement and reporting of data, calculation of meteoric water lines, the deuterium excess and other ratios, trends and patterns. The main body of the book explains how to use stable isotopes to perform various hydrogeological investigations and gives a series of case studies to show how these are done. This book also contains practical advice on water sampling for stable isotopes, some worked examples and exercises, as well as suggested reading for those wishing to delve deeper.

The overall intention of this book is that the reader will not only understand the theory, but also learn how to collect water samples, have them analyzed for stable isotope compositions, interpret the data and make conclusions useful for hydrogeologists or other earth scientists. This information, in turn, can be used by those managing natural resources, conducting site investigations or site rehabilitation and many other aspects of the ever-increasing field of environmental management.

## 2 Isotopes and Isotopologues

An isotope is an atom of an element with a specific number of neutrons. An element is defined by the number of protons, for example hydrogen has 1 proton, helium has 2 and uranium has 92. Each of these elements, however, has a few possible isotopes - the isotopes of an element will all have the same number of protons, but a variable number of neutrons, which determine the isotope. For example, hydrogen has 1 proton, but with different numbers of neutrons: protium has 0 neutrons, deuterium has 1 neutron and tritium (radioactive) has 2 neutrons (Figure 3). As the mass of protons and neutrons is very similar, the mass of each of these hydrogen isotopes is approximately 1, 2 and 3 amus (atomic mass units), respectively. These are depicted as  $^1\text{H}$ ,  $^2\text{H}$  and  $^3\text{H}$ . Hydrogen notation is slightly complicated by the alternative notation of H, D and T. Similarly, oxygen has 3 stable isotopes,  $^{16}\text{O}$ ,  $^{17}\text{O}$  and  $^{18}\text{O}$ , all with 8 protons, but 8, 9 and 10 neutrons.

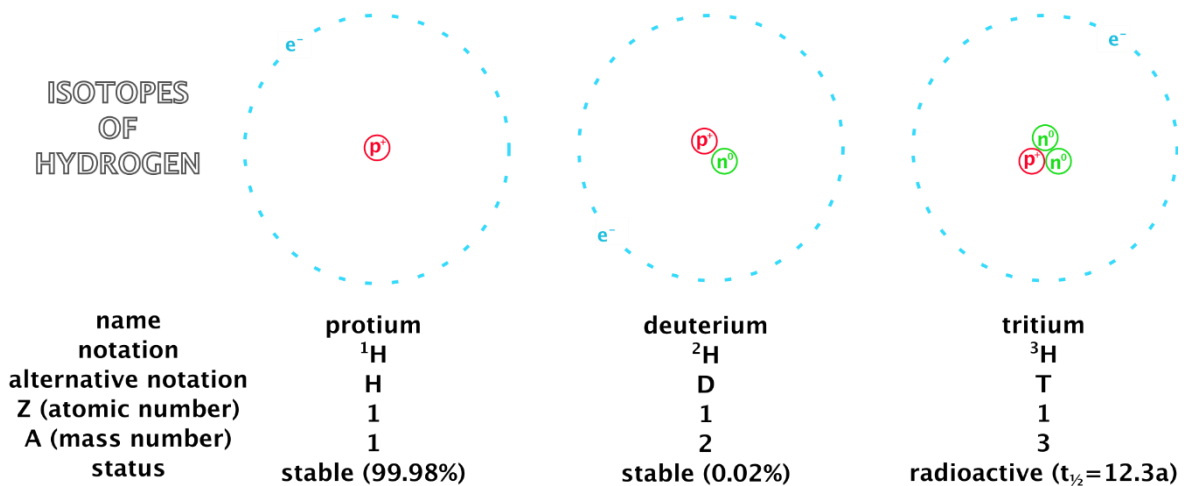


**Figure 3** - The isotopes of hydrogen, including the two stable isotopes, protium and deuterium, and the radioactive isotope, tritium.

Isotopes can be stable, radioactive (decay to another element) or radiogenic (product of decay), or both radioactive and radiogenic, if they are part of a decay chain (Figure 4). In this book we will focus on only stable isotopes, which neither decrease nor increase in abundance, as they are not part of any radioactive decay chain. Note that radiogenic isotopes are "stable" from a physics definition, but as their abundance changes due to being daughters of radioactive isotopes, they are not called stable in a geochemical definition. As the abundance of stable isotopes on Earth is fixed, the ratios of their average global abundances are constant. For example, for oxygen, which occurs as  $^{16}\text{O}$ ,  $^{17}\text{O}$  and  $^{18}\text{O}$ , as these are all stable, their relative abundances are 99.76 percent, 0.04 percent and 0.20 percent.

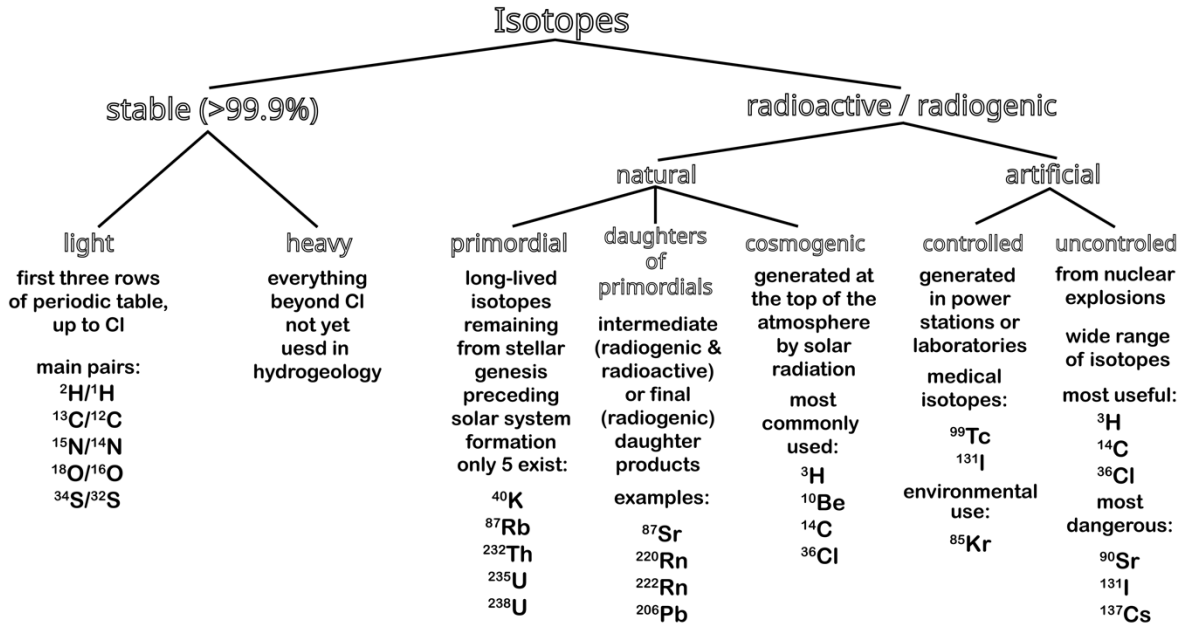


**Figure 4** - Examples of the different types of isotopes, especially those of interest in hydrogeology. Geochemists define stable isotopes as those that are not only physically stable, but also neither increase (radiogenic) nor decrease (radioactive) in abundance.

Hydrogen is somewhat more complex, as <sup>3</sup>H (tritium) is radioactive, with a half-life of 12.3 years. Protium and deuterium, however, are both stable, and on average make up 99.98 percent and 0.02 percent of hydrogen in natural waters, respectively. As with oxygen, you may notice that the lighter stable isotope is by far the most abundant. This is true for C and N and in all other light stable isotopes, but not always for the heavier stable isotopes. When displayed as a ratio, by convention the heavier isotope is always the numerator and the lighter isotope the denominator, for example <sup>18</sup>O/<sup>16</sup>O or <sup>17</sup>O/<sup>16</sup>O.

An isotopologue is an isotopic species of a molecule. For example, a water molecule can include 2 stable hydrogen isotopes, in 2 possible positions and 3 stable oxygen isotopes, giving 9 possible isotopologues (Table 1). If the possibilities with tritium (the radioactive isotope of hydrogen) were added, then the isotopologues increase to 18, but many of these are virtually non-existent. For example, the theoretical abundance of TD<sup>17</sup>O would be the theoretical abundances of each of the isotopes multiplied together, giving:

$$10^{-17} \times 2 \times 10^{-4} \times 4 \times 10^{-4} = 8 \times 10^{-25} \approx 10^{-24}$$

for modern waters, which means it exists in extremely small quantities!

**Table 1** - List of stable isotopologues for water and their theoretical abundances, as calculated from global average abundances of these stable isotopes (Emiliani, 1987). Isotopologues with tritium ( $^3\text{H}$ , radioactive) have been excluded.

Isotopologue	Mass	Abundance (%)
$^1\text{H}^1\text{H}^{16}\text{O}$	18	99.732
$^1\text{H}^1\text{H}^{18}\text{O}$	20	0.200
$^1\text{H}^1\text{H}^{17}\text{O}$	19	0.038
$^1\text{H}^2\text{H}^{16}\text{O}$	19	0.015
$^1\text{H}^2\text{H}^{18}\text{O}$	21	0.00003
$^1\text{H}^2\text{H}^{17}\text{O}$	20	0.0000057
$^2\text{H}^2\text{H}^{16}\text{O}$	20	0.0000022
$^2\text{H}^2\text{H}^{18}\text{O}$	22	0.0000000045
$^2\text{H}^2\text{H}^{17}\text{O}$	21	0.00000000086

A short note on jargon. Isotope scientists often refer to heavier or lighter isotope compositions as enriched or depleted, respectively. The convention here is that the words "in heavier isotopes" have been left out. So, an "enriched sample" actually means a sample that is enriched in heavier isotopes, and *not* a sample enriched in lighter isotopes. This slightly confusing jargon can be avoided by referring to samples with more of the heavier isotope (enriched) as having:

- heavier isotope compositions; and,
- more positive/higher delta values (delta,  $\delta$ , will be explained below).

Similarly, for water with more of the lighter isotopes (depleted), we can say:

- lighter isotope compositions; and,
- more negative/lower delta values.

### 3 Measurement and Standards

Isotope ratios are, by convention, the ratio of the heavier isotope to the lighter one. The differences in isotope ratios between materials are slight and are not easily measured in an absolute sense. However, if measured as a relative difference between the sample and a standard of known isotope ratio, then the precision increases substantially. Thus measurements in stable, light-isotope mass spectrometers are made by comparing the sample to a standard, using either a dual inlet or continuous flow system.

*Stable isotope ratios are reported as deviation from an international standard.*

For both hydrogen and oxygen in water, the standard is SMOW, Standard Mean Ocean Water. SMOW was devised by Harmon Craig in 1961 (Craig, 1961) as an average of previous ocean water samples from Epstein and Mayeda (1953) and Horibe and Kobayakawa (1960), but no actual sample existed. Because of this, SMOW was defined relative to NBS1 (National Bureau of Standards, standard 1), a United States administered sample from the Potomac River. Because of the difficulties of not having an actual standard to analyze, the International Atomic Energy Agency in Vienna commissioned the creation of VSMOW in 1966, which was to mimic SMOW. Although VSMOW is not isotopically identical to SMOW (Clark and Fritz, 1997), it is similar enough (within laboratory error) to be treated as the same. Even though VSMOW may have been used in their laboratories to enable calibration of their local laboratory standards (Gonfiantini, 1981; Sharp, 2007), workers should not report the deviation from VSMOW, as this merely enables correction to SMOW. Data corrected to VSMOW should be reported as deviation from SMOW.

Some natural waters are very isotopically different from ocean water, particularly those at very high latitudes, altitudes and low temperatures, in other words, high mountains or polar areas. For this reason, the Standard Light Antarctic Precipitation (SLAP) standard was created. This standard should be used to calibrate isotopically light working standards for use in high altitude or high latitude environments.

The Greek lower-case delta,  $\delta$ , is used to denote the deviation of a sample from a standard, as shown in Equation 1.

$$\delta = \frac{(R_{\text{sample}} - R_{\text{standard}})}{R_{\text{standard}}} \quad (1)$$

where:

$R$  = isotope ratio such as  $^2\text{H}/^1\text{H}$  (dimensionless)

When relatively more of the heavy isotope (e.g.,  $^{18}\text{O}$ ) is present in the sample than the standard, then the  $\delta$  value will be greater than zero, whereas samples relatively depleted in the heavy isotope will have negative  $\delta$  values. The  $\delta^{18}\text{O}$  and  $\delta^2\text{H}$  values of SMOW are equal to 0. As the variations in isotope ratios are generally quite small, these  $\delta$  values are reported

in permil (parts per thousand), using the ‰ notation. The equation combining these definitions is shown as Equation 2.

$$\delta^{18}O_{sample-SMOW} = \left( \frac{\left(\frac{^{18}O}{^{16}O}\right)_{sample}}{\left(\frac{^{18}O}{^{16}O}\right)_{SMOW}} - 1 \right) \times 1000 \quad (2)$$

### 3.1 Mass Spectrometry

Mass spectrometers were first developed in the early part of the 20<sup>th</sup> century, but the precision was only sufficient for application to natural stable isotope variations after World War II. Thus, was born the field of stable isotope hydrology (Gat, 1981; Sharp, 2007). Today there are many types of mass spectrometers, with specialized designs and features enabling a wide variety of analyses to be performed on samples as diverse as rocks, gases, proteins and teeth. The laboratory preparation procedures are equally diverse for all these substances. Hydrogen and oxygen isotopes of water are typically analyzed in gas-source, light-isotope ratio, mass spectrometers (IRMS) specially adapted for the stable and light isotopes, which include carbon, nitrogen and sulfur.

Mass spectrometers work in the following general way (Figure 5). First, the sample is introduced into the machine, either as a gas, or by vaporizing a liquid or solid sample. This gas or vapor is then ionized using a variety of techniques, such as chemical ionization, electrospray ionization or inductively coupled plasma. The ions are then accelerated and focused down the flight tube and through a strong magnet, where electrical and magnetic fields cause deflection of the ions. This deflection is dependent upon the charge of the ion, as well as its mass. For ions of the same charge, the heavier ions will deflect less, as they possess more momentum than the lighter ions. The last part of the process is the detector, containing collector cups, amplifiers and other electronics to record, process the signal, and output ratios of the various masses of ions being emitted from the source.

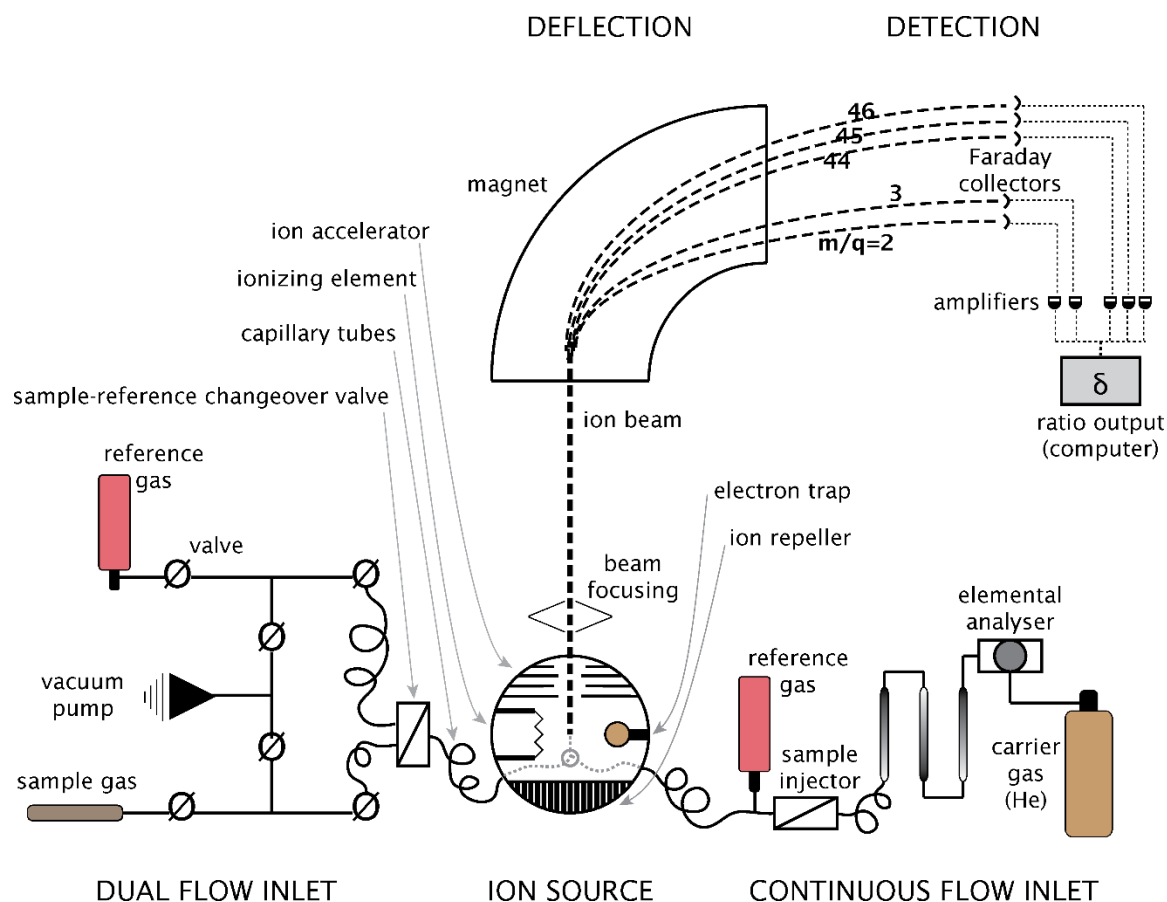


**Figure 5** - Schematic diagram of a gas-source, light-isotope-ratio, mass spectrometer, including the two main types of sample injection setups, continuous-flow and dual-inlet. The  $m/q$  (mass/charge) ratios are illustrative of the paths taken by various ions. Ions with lower  $m/q$  ratios are deflected more by the magnet.

For water, the gases  $H_2$  (for  $\delta^2H$ ) and  $CO_2$  (for  $\delta^{18}O$ ) are used as the inputs to the mass spectrometer. Sample preparation procedures are outlined in Schimmelmann and others (1993) and Socki and others (1992), although other methods are available.

IRMS makes use of either a dual-inlet system, or a continuous flow system. Water has generally been converted to gases, so the dual-inlet system is mostly used. For the dual-inlet system, the samples are alternated with the reference gases, providing a high level of precision. For the continuous flow system, a sample is analyzed only once and the precision is therefore not as good. Laboratory standards are inserted every ten to twenty samples, allowing correction of any drift in the reference gases. These laboratory standards are calibrated to the international standards, such as SMOW, allowing the researcher to present their data in an internationally recognizable form. Paul and others (2007) discuss normalization of the sample data to the standards.

### 3.2 Laser Cavity Spectroscopy

This method is more recent than mass spectrometry and was developed in the 1980's (O'Keefe, 1988). The first form of this method was known as cavity ringdown spectroscopy (CRDS) and is still used, but more recent developments have broadened the method and

its application. One of the more recent modifications is called off-axis integrated cavity output spectroscopy (OA-ICOS) and reduces the need for highly accurate mirror alignment (Los Gatos Research, 2020). As with mass spectrometry, CRDS is not only used for isotopic measurements, as it can be set up to determine the quantities of different gases in a sample, or when modified with a plasma source can analyze for heavy element concentrations (Wang, 2007).

CRDS works in roughly the following way (Figure 6). A cavity containing an inert gas (He, N, etc.) is injected with the gaseous phase of a sample. A short burst of laser light is emitted into the cavity, which contains at least 2 high reflectivity mirrors. The light bounces between the mirrors to give an effective path length of many kilometers, in which the light decays due to mirror inefficiency and absorption by the sample gas. By monitoring wavelengths which are both affected and not affected by the sample absorption, the instrument can compare the decay of light due only to reflection losses and that due to absorption by the sample as well. This means variations in laser intensity and power that occur between measurements are corrected for. Multiple measurements are taken of the time taken for the light to diminish (the ringdown time) and therefore the strength of the sample absorption can be calculated. This absorption factor can be converted into an isotopic composition, as the different isotopic species have different absorptivity.

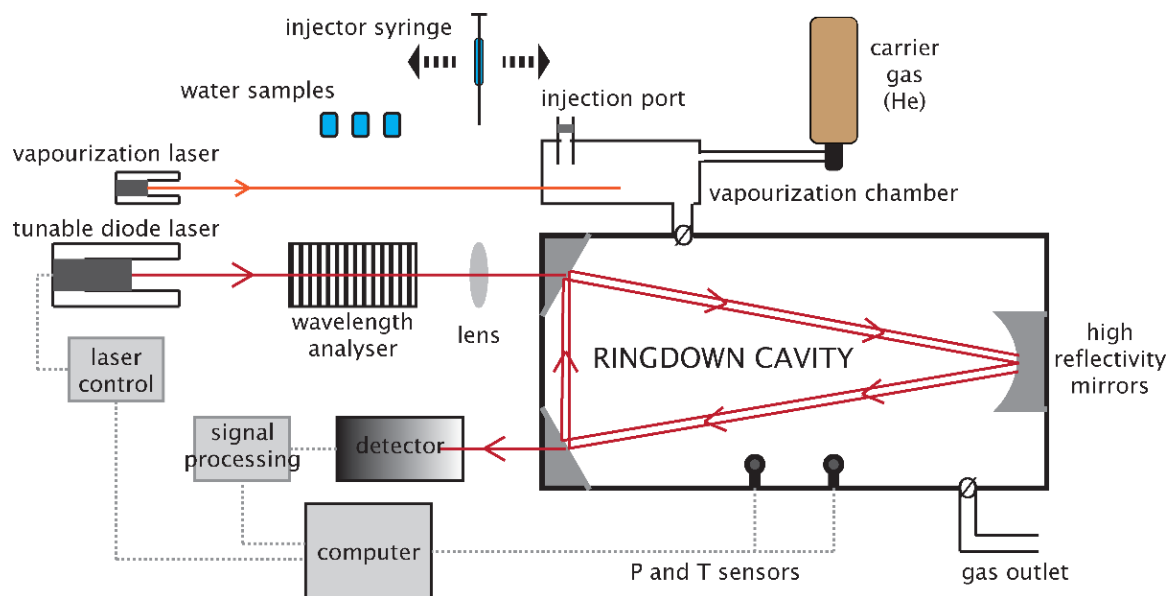


**Figure 6** - Schematic diagram of a laser cavity ringdown instrument.

As with mass spectrometry, laboratory standards are inserted every ten or so samples, to allow final corrections to be made to the CRDS results, and allow reporting to the international standards, SMOW or SLAP.

## 4 Isotope Fractionation

The ratios of one isotope to another, such as  $^{18}\text{O}/^{16}\text{O}$ , vary slightly between different materials or even different reservoirs of the same substance. The magnitude of these variations depends on the element concerned, the compounds, reactions and environmental conditions, but typically range up to around 10‰. The variations are greatest for hydrogen isotopes, up to 1000‰, because the mass difference is 2-fold, or 100 percent, for  $^2\text{H}/^1\text{H}$ . As the mass difference decreases, so the isotopic variations tend to decrease, such as with oxygen 18/16, which is a mass difference of an eighth, or 12.5 percent.

These differences in isotope ratios come about through various processes or reactions, including chemical reactions, physical reactions (changes of state), diffusion and exchange. A chemical reaction is when two or more elements or compounds react to form different compounds; a physical reaction is where an element or compound undergoes a change of state (gas to liquid to solid); diffusion is when atoms or molecules disperse from high to low concentration through other material; exchange is when atoms of the same element swap places from one compound to another without causing any chemical changes. In all of these processes, molecules or atoms bearing different isotopes will proceed through these reactions at different speeds, creating differences in isotope ratios in the different materials.

Preferential location of the heavier or lighter isotopes (or isotopologues) will change the isotopic abundances from the normal ratio. For example,  $^1\text{H}_2$  will preferentially diffuse and escape to space at the top of the atmosphere, compared to  $^1\text{H}^2\text{H}$  or  $^2\text{H}_2$ . Isotopic exchange is where atoms of the same element swap places in different molecules, for example oxygen in  $\text{H}_2\text{O}$  and dissolved  $\text{CO}_2$  in the ocean. Preferential location of the lighter or heavier isotope occurs due to different bond energies, related to mass, for example the preferential condensation of  $^1\text{H}_2^{18}\text{O}_{(v)}$  relative to  $^1\text{H}_2^{16}\text{O}_{(v)}$  during cloud formation ( $_{(v)}$  indicates a vapor phase, and  $_{(l)}$  a liquid phase). These processes of differential accumulation of isotopes are known as fractionation.

### 4.1 Kinetic Fractionation

For physical, chemical and exchange reactions, the dissociation energy of molecular bonds controls the reaction rate. A bond involving lighter isotopes has a lesser dissociation energy and can break more easily than the same bond involving a heavier isotope. One can think of this as requiring more energy to break the bond with a heavier than a lighter isotope. For example, when a body of liquid water evaporates into air, the resultant water vapor ( $\text{H}_2\text{O}$  gas mixed in air) will be relatively enriched in the lighter isotopes and therefore have lower values for the ratios  $^2\text{H}/^1\text{H}$  and  $^{18}\text{O}/^{16}\text{O}$  than the source body. This isotopic fractionation will be exaggerated if the vapor is being removed rapidly, as happens in

windy situations or at low humidity when water evaporates from natural water bodies, and is known as kinetic fractionation. When the air is drier or the wind is stronger, removal of  $^1\text{H}$  and  $^{16}\text{O}$  bearing water molecules will increase, because there is less opportunity for the evaporated water to react backwards with the liquid water body. Bear in mind, that on the other hand, a lack of mixing in the source water body will result in a lesser fractionation effect, because the surface water layer will become depleted in  $^{16}\text{O}$  with time.

For diffusion, the diffusive velocity is inversely proportional to the mass of the molecule and therefore molecules with lighter isotopes will diffuse faster. For the above example, if there is no wind, but diffusion is high because humidity is low, then again, the increased diffusion of water molecules containing  $^1\text{H}$  and  $^{16}\text{O}$  will increase the kinetic effect.

For kinetic fractionation there is no fixed difference in isotope ratios between the source and receptor reservoirs, as this is dependent upon factors such as time, degree of removal of one reservoir and degree of mixing of the reservoirs (i.e., wind or diffusivity), as well as the type of reaction, or change of state, that is taking place.

## 4.2 Equilibrium Fractionation

If chemical, physical or exchange reactions are allowed to run to completion, then there will be a fixed isotope difference between the source and receptor reservoirs, at a given temperature. Temperature plays an important role in fractionation. The higher the temperature, the less the degree of fractionation (Figure 7). Once equilibrium is reached, reactions will continue, but backward and forward reactions will occur at an equal rate, with no net effect on isotopic composition of either reservoir. For example, at a given temperature, there is a fixed difference between the  $^{18}\text{O}/^{16}\text{O}$  ratio in  $\text{H}_2\text{O}_{(l)}$  and  $\text{H}_2\text{O}_{(v)}$  in equilibrium with each other. In this situation, the kinetic effects of reaction rate are not important, and it is the relative preference for a heavier or lighter isotope within a chemical bond that determines which isotopes are located where, with heavier isotopes favored in bond positions with higher strength. To continue the above example, the hydrogen bonds between water molecules are stronger between  $\text{H}_2^{18}\text{O}-\text{H}_2^{16}\text{O}$  than  $\text{H}_2^{16}\text{O}-\text{H}_2^{16}\text{O}$ , and so evaporation will preferentially select for  $\text{H}_2^{16}\text{O}$  in the vapor mass, resulting in the  $\text{H}_2\text{O}_{(v)}$  having lower values for  $^{18}\text{O}/^{16}\text{O}$  than the  $\text{H}_2\text{O}_{(l)}$ .

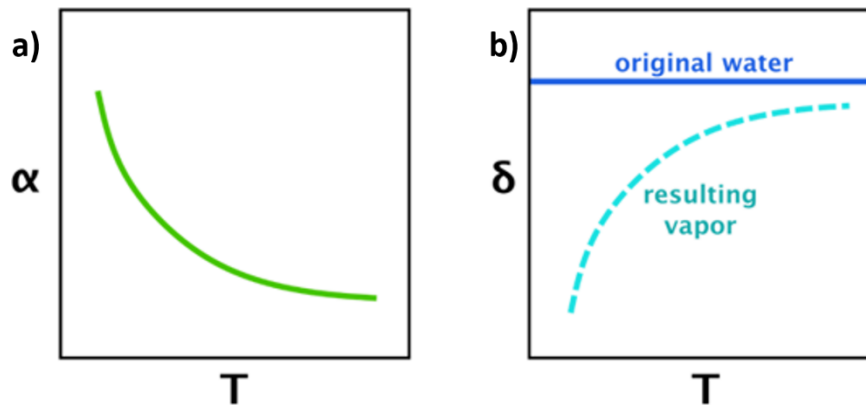


**Figure 7** - Temperature dependence of fractionation. Graph a) shows the fractionation factor decreasing with rising temperature, and b) shows the difference in isotopic composition between a water source and its evaporated moisture becoming less at higher temperatures, assuming equilibrium conditions.

### 4.3 Fractionation and Enrichment Factors

To quantify the fractionation of isotopes between two phases or compounds, the fractionation factor,  $\alpha$ , is used as shown in Equation 3.

$$\alpha = \frac{R_{reactant}}{R_{product}} \quad (3)$$

where:

$R$  = isotope ratio, such as  $^2\text{H}/^1\text{H}$  (dimensionless)

For example, as expressed by Equation 4.

$$\alpha_{^2\text{H}(\text{water-vapor})} = \frac{\left(\frac{^2\text{H}}{^1\text{H}}\right)_{\text{water}}}{\left(\frac{^2\text{H}}{^1\text{H}}\right)_{\text{vapor}}} \quad (4)$$

This factor describes the partitioning of an isotope between two phases or compounds, which is determined by the temperature, chemical bonds and other atomic scale properties of the element. Importantly, the fractionation factor is temperature dependent; in other words, at equilibrium, the isotope ratios in the reactant and product vary with temperature (Figure 7), as was first outlined by Urey (1947). Chacko and others (2001) provide more recent and detailed information on fractionation factors and their calculation.

Calculating the fractionation factor for a given temperature is usually done experimentally with enough measurements at different temperatures to develop an equation such as Equation 5.

$$\ln \alpha_{X-Y} = aT^{-2} + bT^{-1} + c \quad (5)$$

where:

$\alpha_{X-Y}$  = fractionation factor for transition from X to Y (dimensionless)

$x$  = subscript indicating reactant compound or state

$y$  = subscript indicating product compound or state

$T$  = temperature (K)

$a, b, c$  = fitting constants ( $K^2, K$ , dimensionless, respectively)

For most isotopic reactions, the fractionation factor,  $\alpha$ , is close to 1, meaning  $\ln(\alpha)$  will be close to 0. If this is multiplied by 1000, then permil units are obtained.  $\delta$  values are given in permil units. As long as  $\alpha$  is indeed near 1, an enrichment factor ( $\epsilon$ ) can be calculated (Figure 8). The enrichment factor expresses the difference in  $\delta$  values between reactants and products (Clark, 2015), as shown in Equation 6.

$$\epsilon = 1000(\alpha - 1) \approx 1000\ln(\alpha) \tag{6}$$

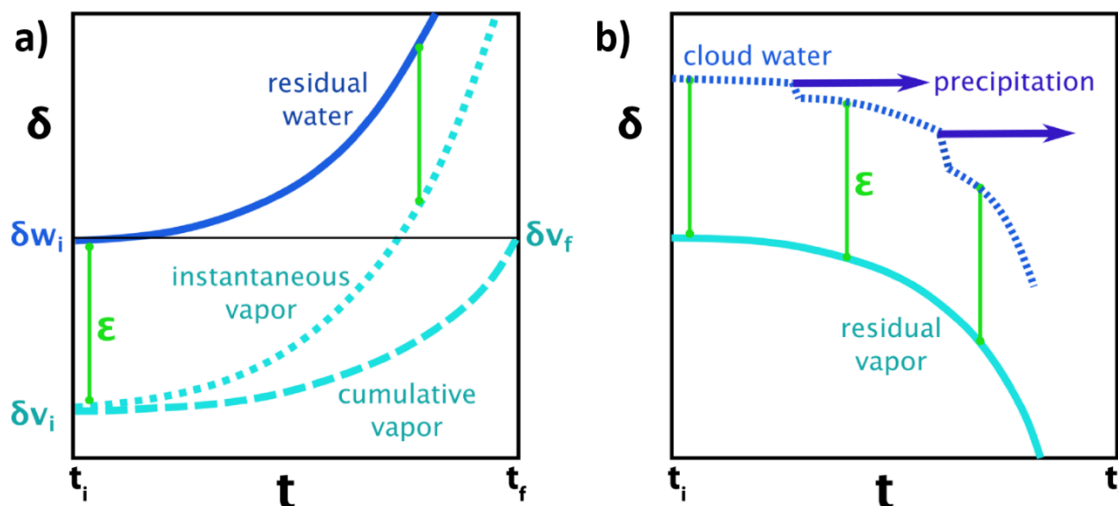


**Figure 8** - Graph a) shows the isotopic evolution of a body of water evaporating to vapor over time, at a set temperature and under equilibrium conditions. In this case, the enrichment factor remains constant as the remaining water and the instantaneous vapor evolve. Also, eventually the final total vapor body, assuming no losses from the system, has the same isotope composition as the initial water body. Graph b) shows the isotopic evolution of vapor, cloud and precipitation, for constant temperature and equilibrium condensation.

Importantly the variation in equilibrium fractionation factors is systematic, because lower temperatures always result in higher fractionation factors and vice versa. This temperature dependence is the fact enabling paleoclimate work. The isotopic composition of a material, such as ice in a glacier, depends on the temperature at which the snow or ice crystallized. Calcite in a speleothem can also be used, as the calcite crystallization occurs at a given temperature in the presence of groundwater, which once was precipitation. With enough measurements to establish an accurate average, the isotopic composition of the original precipitation will be known, and if an age can be calculated for the glacier or speleothem, then the temperature at a specific time and place can be reconstructed.

## 4.4 Rayleigh Distillation

Around the turn of the 20<sup>th</sup> century, Lord Rayleigh proposed a law to describe the changing composition of an original pool of mixed liquids as it is progressively distilled (Lord Rayleigh, 1902). This law relied on the fact that the differential rate of evaporation of the two liquids is known. This was before stable isotopes had been discovered, but it turns out to perfectly predict the theoretical rate at which a reservoir of water will change isotope composition as it loses water to another reservoir through evaporation, freezing, etcetera. The equation Rayleigh proposed is shown here as Equation 7 (Clark, 2015).

$$r_{final} = r_{initial} \times f^{(\alpha-1)} \quad (7)$$

where:

$r_{final}$  = isotope composition of the pool of water with fraction  $f$  remaining (dimensionless)

$r_{initial}$  = original isotope composition of the pool (dimensionless)

$f$  = fraction (1 to 0) of water that remains (dimensionless)

$\alpha$  = equilibrium fractionation factor for the reaction at a given temperature for example,  $^2\text{H}/^1\text{H}$  in liquid to water vapor (evaporation) at 25 °C (dimensionless)

If an imaginary block of moisture laden atmosphere (a vapor body) has water removed by condensation to form a cloud, there will be an isotopic difference between the vapor and cloud exactly equivalent to the equilibrium fractionation factor, for both H and O isotopes. However, this only holds for the first batch of condensation, because the remaining vapor will immediately change its isotope composition due to the fractionation factor causing heavier isotopes to preferentially condense into cloud droplets. This leaves the vapor body isotopically lighter, which means future condensate will be lighter (Figure 8).

If we envision someone fishing tries to catch the biggest fish in the sea, even though she consistently catches fish that are 1 kg heavier than the average weight of all the fish (the fractionation factor), then as those fish are removed, the average weight of fish in the sea decreases, and so will the weight of each fish in her catch. Sadly, this analogy for Rayleigh distillation is also the true story of fish in the oceans over the last century or so.

Rayleigh distillation is applicable to equilibrium situations, such as cloud formation, where vapor and cloud droplets are in contact long enough for equilibrium fractionation to apply. In settings with orographically driven rainout in a high precipitation location such as the Azores in the north Atlantic which receives 1500 mm/a (Antunes et al., 2019) or for heavy frontal precipitation in California (Mix et al., 2019), Rayleigh distillation gives a reasonable approximation of the stable isotope behavior. In higher latitudes and

deeper continental locations, for example the Canadian Rockies (Figure 9), an orographically adjusted Rayleigh model is better for predicting isotope composition of precipitation than a linear Rayleigh distillation (Sinclair et al., 2011).

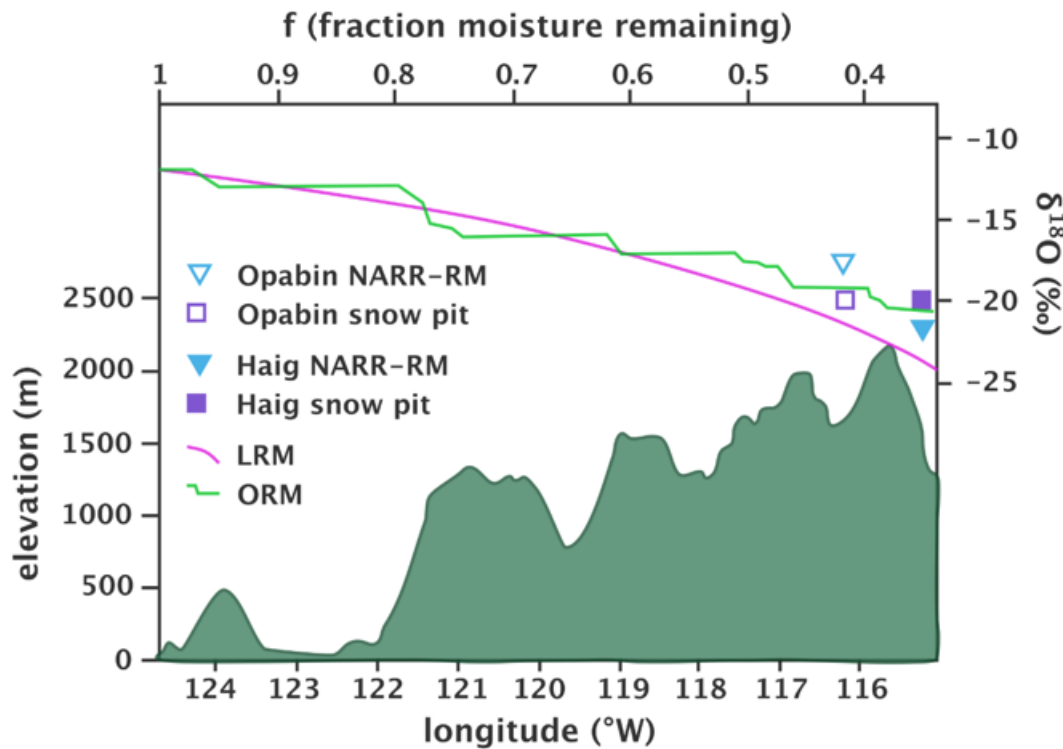


**Figure 9** - Regional investigation of the applicability of Rayleigh distillation models to predict stable isotope content of precipitation. This study used three models to predict the stable isotope composition of snowfall in the Canadian Rockies, at two sites, the Opabin and Haig Glaciers. Actual measurements from snow pits are precipitation weighted means. The three models are the NARR-RM (North American Regional Reanalysis - Rayleigh model), the LRM (linear Rayleigh model) and the ORM (orographic Rayleigh model). The ORM can be seen to produce values closest to the actual precipitation seen in the snow pits (after Sinclair et al., 2011).

For a fractionating process, such as a chemical reaction or diffusion in a porous medium like an aquifer, Rayleigh distillation overestimates the changes to the original reservoir, or the reactants. This is due to the rate limiting effects of transport through the aquifer matrix or kinetic reaction effects. Use of a lower fractionation factor partly resolves this problem, but calculation of this lower fractionation factor is complex (Druhan and Maher, 2017).

## 5 Meteoric Water Lines

### 5.1 The Global Meteoric Water Line

Stable isotope data from precipitation samples fall on a line known as a meteoric water line. This line is usually plotted with data from local, regional or global precipitation samples, but can include surface and groundwater samples. The Global Meteoric Water Line (GMWL) was first recognized by Craig (1961), based on fresh surface water samples from around the world (Figure 10), and is represented by Equation 8.

$$\delta^2\text{H} = 8 \delta^{18}\text{O} + 10 \quad (8)$$

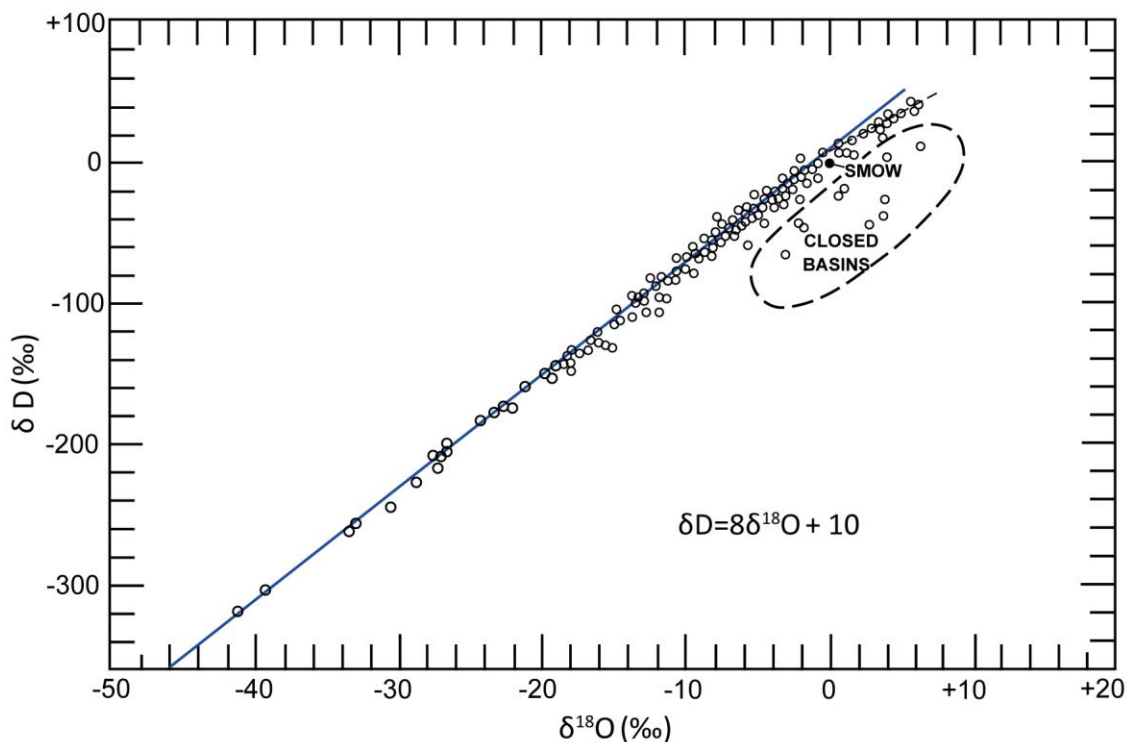


**Figure 10** - The Global Meteoric Water Line (GMWL) as discovered by Craig (1961).

The spread of data along the GMWL is influenced by several meteorological processes or factors, such as humidity and temperature, but it is probably rainout of atmospheric moisture, as air masses move from the tropics to the poles, that accounts for the bulk of the variation in  $\delta$  values (Rozanski et al., 1993; Yurtsever and Gat, 1981). As a moisture laden air mass moves from the tropics to the poles, moisture is removed by precipitation and the temperature tends to be lower. These lower temperatures not only encourage further condensation causing more precipitation, but enhance the removal of heavy isotopes by increasing the equilibrium isotope fractionation factors. As the process of rainout is governed by condensation, which is an equilibrium process,  $\delta^2\text{H}$ - $\delta^{18}\text{O}$  co-vary, but with a factor of 8 difference. This factor of 8 difference is due to the ratio of the

fractionation factors for H and O during rainout, which in turn is due to the difference in mass of  $^2\text{H}/^1\text{H}$  being 8 times greater than the difference in mass of  $^{18}\text{O}/^{16}\text{O}$ .

$$\frac{^{18}\text{O} - ^{16}\text{O}}{^{16}\text{O}} = \frac{2}{16} = \frac{1}{8} \text{ and } \frac{^2\text{H} - ^1\text{H}}{^1\text{H}} = \frac{2-1}{1} = 1$$

Thus, the variations in  $\delta^2\text{H}$  will be roughly 8 times those of  $\delta^{18}\text{O}$ . The difference in mass causes a difference in energy needed to break the bonds, and that is the ultimate cause of fractionation. However, temperature changes the  $^2\text{H}/^1\text{H}$  and  $^{18}\text{O}/^{16}\text{O}$  equilibrium fractionation factors differently, so the gradient of 8 steepens in colder regions and lessens in warmer regions (Clark, 2015). The value of 10 is the intercept, or the  $\delta^2\text{H}$  value when  $\delta^{18}\text{O}$  is 0.

The GMWL was updated by Rozanski and others (1993) and then again by Araguas-Araguas and others (2000) to  $\delta^2\text{H} = 7.96 \delta^{18}\text{O} + 8.86$ .

## 5.2 Local Meteoric Water Lines

A meteoric water line for a region is known as the Local Meteoric Water Line (LMWL) and is usually essential for interpreting stable isotope data. It is ideally generated by using only precipitation samples (not surface or groundwater samples), and samples that capture all of the precipitation in a region over several years, to be representative of unusual weather events and climatic oscillations, such as El Niño or the North Atlantic Oscillation.

The LMWL can be thought of as representing the default or input stable isotope values to the local hydrological cycle. It is different from the GMWL because the local area has a limited range of climatic conditions and weather systems, thus produces a limited and more specific range of stable isotope values compared to the global dataset (Araguas-Araguas et al., 2000). Comparison of groundwater, surface water and particular precipitation events to the LMWL allows investigation of processes such as water-rock interaction, evaporation, recharge and mixing (Jasechko, 2019) as illustrated in Figure 11.

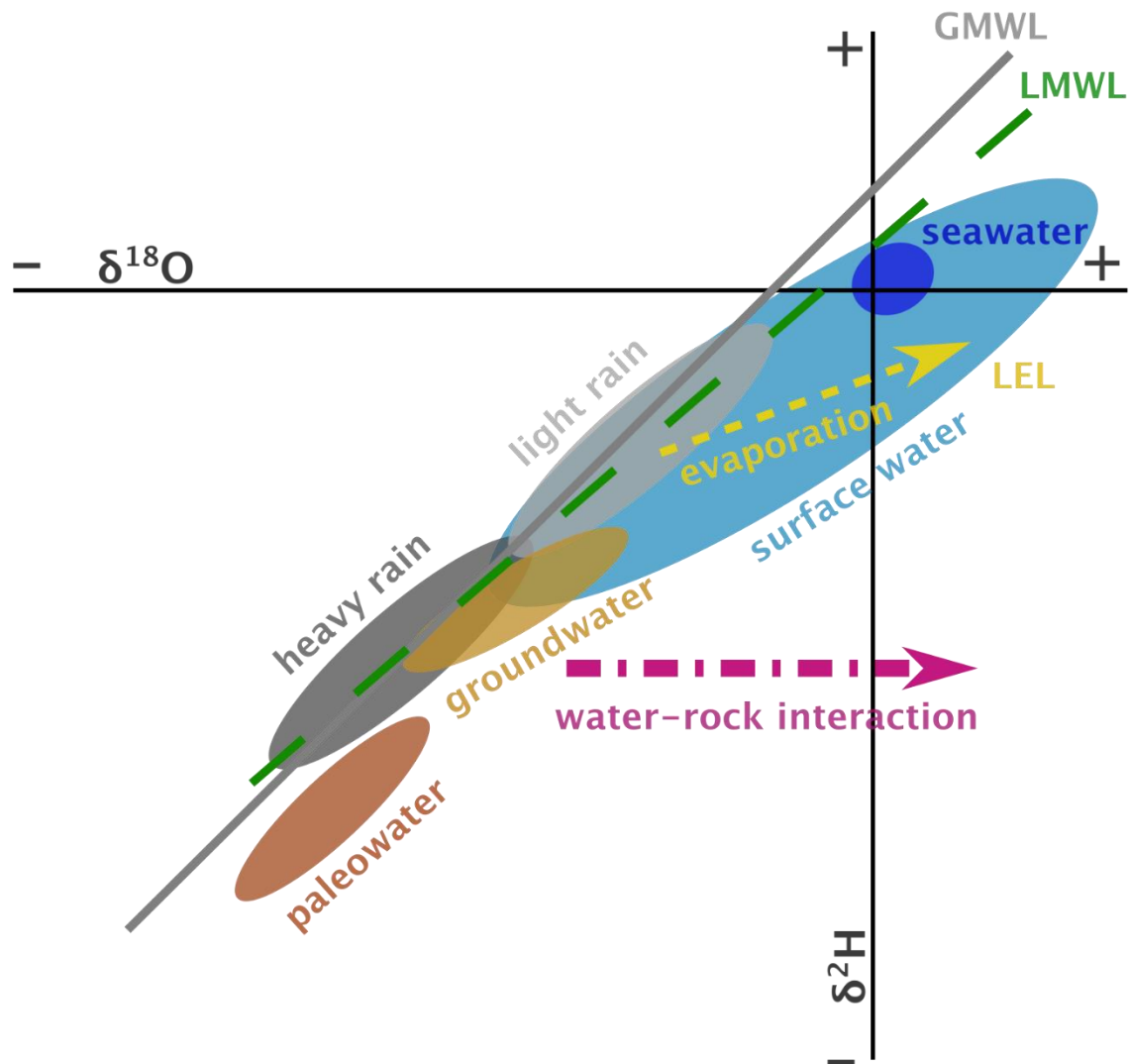


**Figure 11** - A conceptual diagram showing typical isotope compositions of various water bodies and differences in the LEL (local evaporation line), LMWL (local meteoric water line) and GMWL (global meteoric water line) for a specific region. These differences in slope and position allow interpretation of stable isotope data so as to begin formulating hypotheses about water sources, sinks and interactions in a study region.

Most LMWLs have slopes of  $< 8$ , usually around 5 to 7 and a notably limited range of  $\delta^2\text{H}$  and  $\delta^{18}\text{O}$  values compared to the GMWL. When several LMWLs for areas with different climates are drawn, these lines lie semi-parallel, but are displaced 'up' or 'down' on a  $\delta^2\text{H}$ - $\delta^{18}\text{O}$  plot and stack adjacent to each other to form the GMWL, as shown in Figure 12. The GMWL is the cumulative result of all the LMWLs for regions of different climate, with degree of rainout being the main discriminant for the position of each LMWL. LMWLs for higher latitude regions tend to plot lower on a  $\delta^2\text{H}$ - $\delta^{18}\text{O}$  diagram whereas LMWLs for lower latitude and more arid regions tend to plot higher on the diagram.

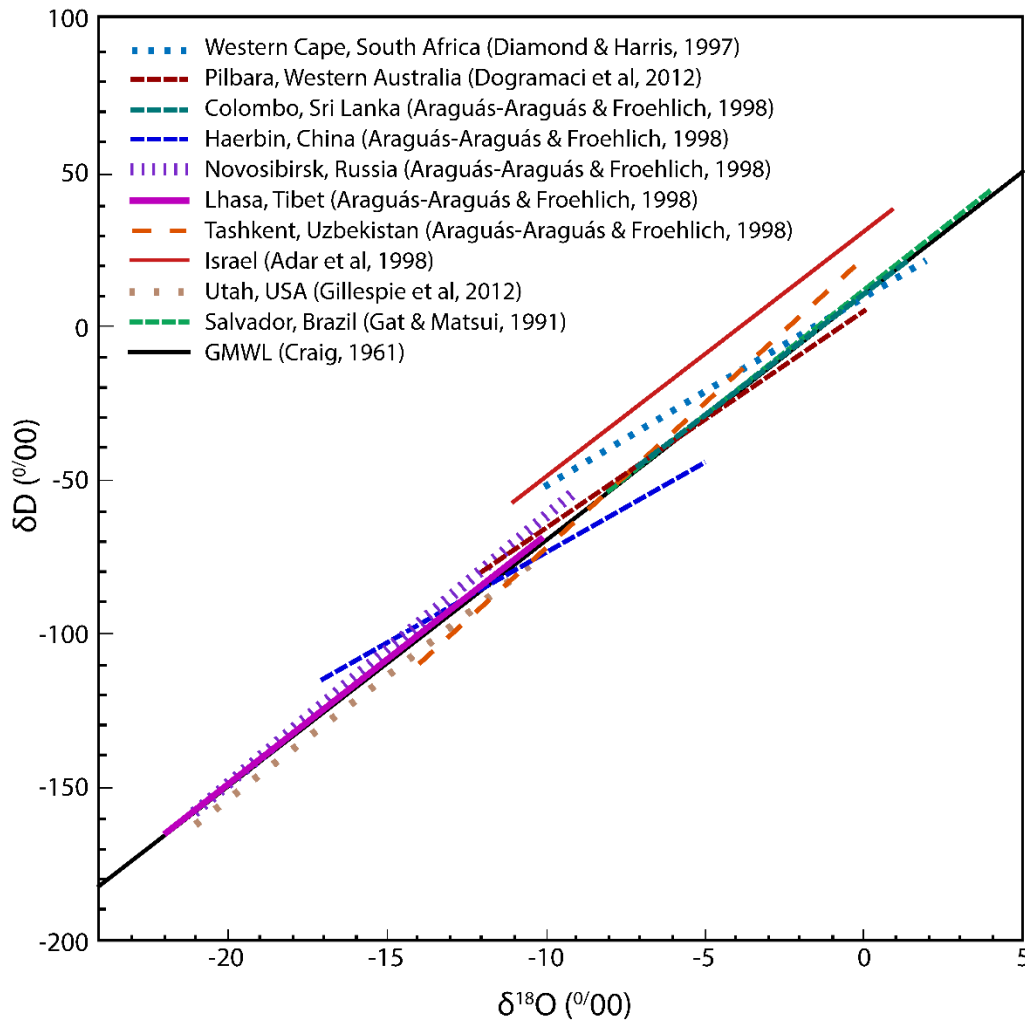


**Figure 12** - Local meteoric water lines (LMWLs) for various regions of the world, and the GMWL.

### 5.3 Calculation of Meteoric Water Lines

A meteoric water line is a best fit line (i.e., a regression line) for a set of points in x-y space. The most common regression analysis is known as the *least squares method*. This assumes the x-variable is independent and accurately known, whereas the y-variable depends upon the x-value and has errors and random variations. An example of an independent x-variable would be time or distance, and a dependent y-variable could be temperature, precipitation or an isotope ratio. For analysis of one stable isotope ratio, say  $\delta^2\text{H}$  against one of these independent variables, like time, a *least squares regression* is a suitable representation of the relationship. However, where both variables are dependent, such as  $\delta^2\text{H}$  and  $\delta^{18}\text{O}$ , neither one should be treated as more certain than the other and so the *reduced major axis* form of a structural regression is suitable (Ma, 2019).

### 5.3.1 Least Squares Regression

The straight-line regression is of the form shown in Equation 9.

$$y = mx + c \quad (9)$$

where:

$m$  = gradient, i.e., slope of the line (dimensions of y-axis values over dimensions of x-axis values)

$c$  = y-intercept (dimensions of y-axis values)

$x, y$  = regression variables

the least squares regression approach produces Equation 10.

$$\begin{aligned} m &= \frac{SP_{xy}}{SS_x} \\ c &= \bar{y} - m\bar{x} \\ SS_x &= \sum_{i=1}^n (x_i - \bar{x})^2 \\ SP_{xy} &= \sum_{i=1}^n (x_i - \bar{x})(y_i - \bar{y}) \end{aligned} \quad (10)$$

where:

$SS_x$  = sum of the squared deviations from the mean of x (squared dimensions of the x variable)

$SP_{xy}$  = sum of product of deviations from the mean of x and deviations from mean of y (dimensions are product of x and y dimensions)

### 5.3.2 Reduced Major Axis Regression (RMA)

The RMA regression line is calculated in a manner similar to that shown in Section 5.3.1, with the single difference that the gradient,  $m$ , is calculated as shown in Equation 11.

$$m_{RMA} = \sqrt{\frac{SS_y}{SS_x}} \quad (11)$$

$$SS_y = \sum_{i=1}^n (y_i - \bar{y})^2$$

## 5.4 Weighted Regression Line Equations

As noted by Hughes and Crawford (2012), weighting of isotopic values for monthly cumulative precipitation by the precipitation amount produces regression lines (meteoric water lines) with higher gradients, as a result of minimizing the influence of evaporated

samples from low precipitation events. The difference in gradient and intercept between weighted and unweighted regression lines depends on the dataset and the regression method, and although the differences are generally minor, they can be significant (Boschetti et al., 2019). These meteoric water lines better characterize the average precipitation and especially heavier events that are more likely to play an important role in hydrological processes such as groundwater recharge (Li et al., 2018). These weighted regressions use methods similar to those presented in Section 5.3, but include a precipitation term in the statistical quantities as shown in Equation 12.

$$\begin{aligned}
 SS_x &= \sum_{i=1}^n (rain_i)(x_i - \bar{x})^2 \\
 SS_y &= \sum_{i=1}^n (rain_i)(y_i - \bar{y})^2 \\
 SP_{xy} &= \sum_{i=1}^n (rain_i)(x_i - \bar{x})(y_i - \bar{y})
 \end{aligned} \tag{12}$$

It is useful to be aware that some computer statistical programs will perform *least squares regression* as their standard method to produce a best fit line. Thus, it is essential to either: 1) know what the program is doing; or, 2) set up the calculations in a spreadsheet using the formulae of Equations 10 - 12.

## 6 Stable Isotope Hydrology

The global water cycle is extremely complex if all the interactions with geological and biological materials are taken into account. The water cycle includes processes as diverse as weathering and volcanic eruptions in the geosphere, and organic decay and drinking by animals in the biosphere. Fortunately, the flows of water involved in those geological and biological interactions are orders of magnitude less than the major flows of water, such as evaporation from the oceans or precipitation over land, except for transpiration by plants (Jasecko et al., 2013). This global flow of water is known as the hydrological cycle. A simplified quantification of the hydrological cycle is shown in Figure 13.

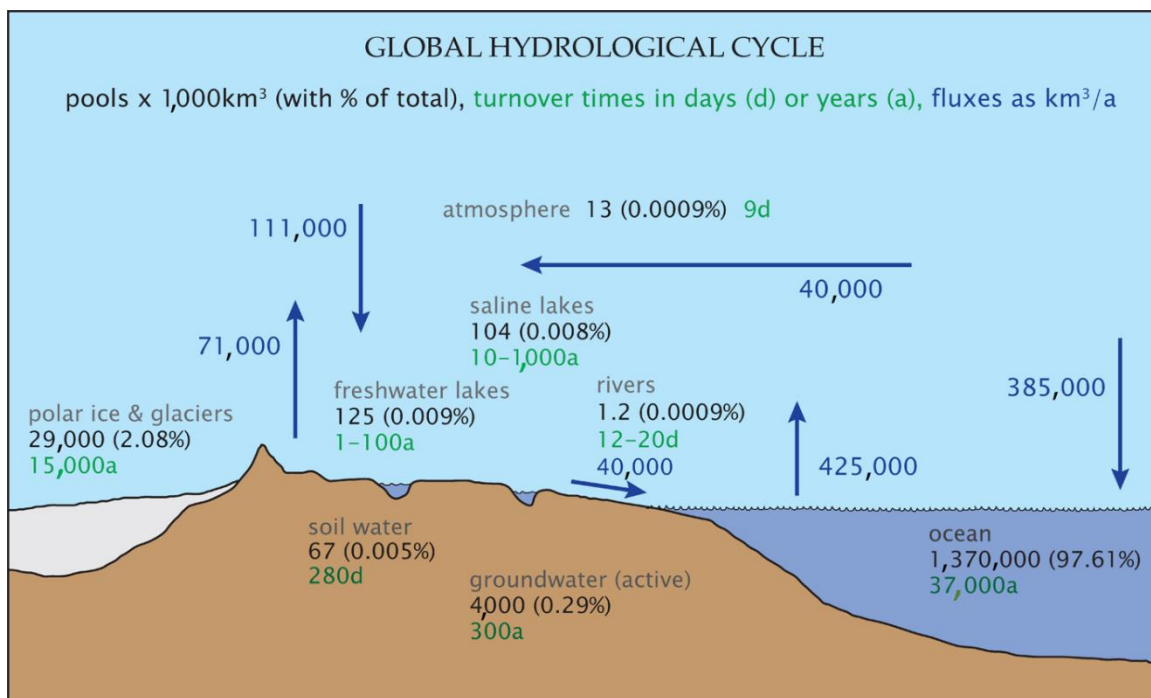


**Figure 13** - A simplified quantification of the global hydrological cycle (after Reeburgh, 1994). Pools are reservoirs that store water such as the atmosphere, glaciers, lakes, rivers, soil water, groundwater and the ocean. Fluxes between pools are indicated by arrows.

Most of the fluxes from one pool to another are key points where the isotopic composition of parcels of water change. An approximation of the range of isotope compositions across the hydrological cycle is depicted in Figure 14.

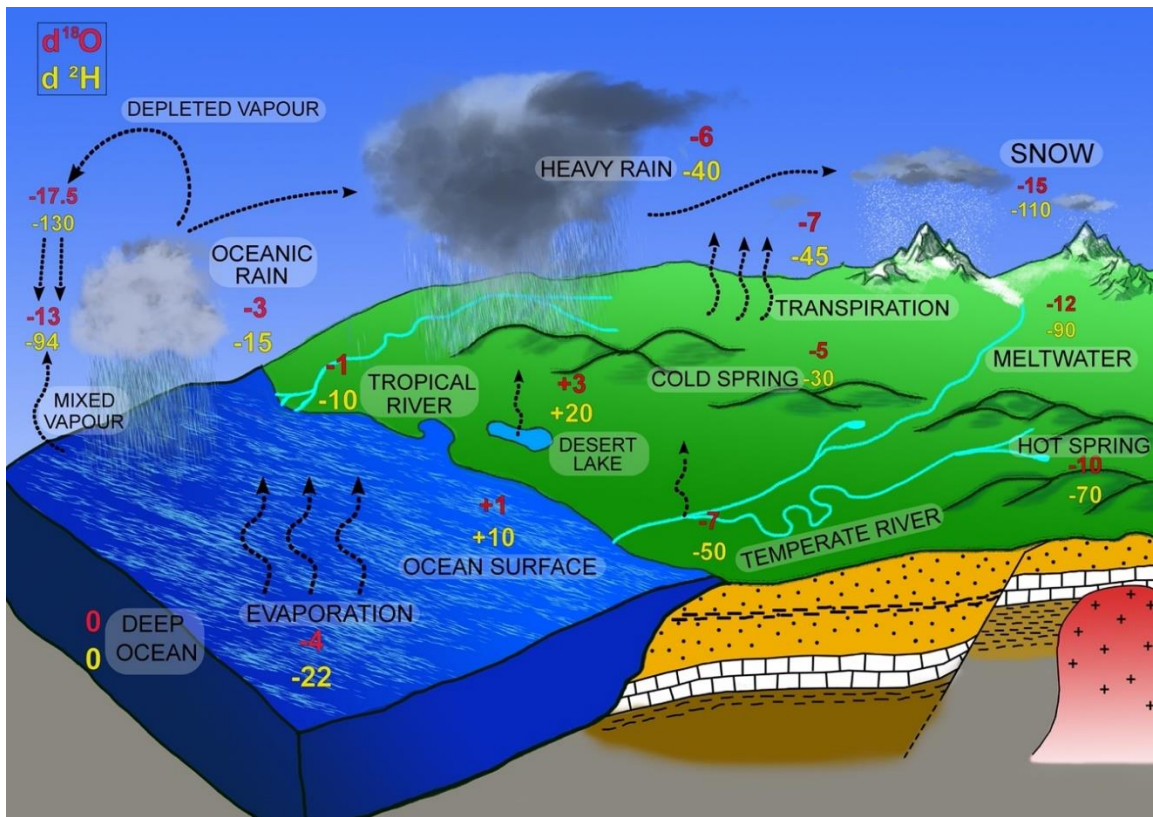


**Figure 14** - Estimates of typical stable isotope compositions of a variety of water sources, reservoirs and flows:  $\delta^2\text{H}$  in yellow,  $\delta^{18}\text{O}$  in red. Values are approximations based on information in relevant literature so, the values may differ widely from actual values for specific locations. The range of isotopic compositions shown here is less than those that occur in field settings, because these are averaged values. Nonetheless they provide an indication of the range of  $\delta^2\text{H}$  and  $\delta^{18}\text{O}$  values that occur in the hydrological cycle. This wide range of values, especially where there is a large change in climate, elevation or distance, is what makes stable isotopes useful for tracing water sources and movement.

With such complexity in the hydrological cycle, it is perhaps surprising that the variation in  $\delta^2\text{H}$ - $\delta^{18}\text{O}$  is very defined, as shown in Figure 10 from the landmark article in *Science* by Harmon Craig in 1961. The most important feature of note in Figure 10 is that most precipitation has  $\delta^2\text{H}$  and  $\delta^{18}\text{O}$  values less than zero. This is primarily because evaporation from the oceans produces vapor that is depleted in the heavier isotopes relative to sea water (which is very similar to SMOW and has  $\delta^2\text{H}$  and  $\delta^{18}\text{O}$  values close to zero).

Evaporation from the oceans is a two-stage process. Initially, equilibrium fractionation occurs where water evaporates into a saturated boundary layer over the ocean surface. Then, from this saturated layer, diffusion and wind continuously remove vapor and mix it upward into the atmosphere, causing an additional kinetic fractionation (Craig and Gordon, 1965). Thus water vapor in the atmosphere is more depleted in the heavier isotopes than would occur if only equilibrium fractionation was taking place (Clark and Fritz, 1997). The measured values of  $\delta^{18}\text{O}$  in vapor over the oceans vary from about -10 to -15‰, as latitude increases (temperature decreases). These values are about 4‰ less than the equilibrium values would be. The values for  $\delta^2\text{H}$  are similarly lower than theoretical equilibrium values and range from -70 to -100‰ (Sharp, 2007).

Generation of atmospheric water vapor occurs mainly over the warmer oceans and it has been estimated that around 65 percent is generated between 30°S and 30°N (Peixoto and Oort, 1983). Once an air mass is cooled, either by advection over a cool surface in colder climates or by convection, the air can become saturated and condensation may commence. Condensation is dependent not only on temperature and humidity, but on the availability of condensation nuclei of the correct type (Sumner, 1988). Condensation generally proceeds slowly in response to reduced pressure or further cooling and this takes place in the presence of the vapor. In other words, cloud droplets are surrounded by vapor when they form and continuously exchange with the vapor, thus condensation is an equilibrium fractionation process.

Only general statements can be made about the causes of the distribution of isotope ratios in meteoric water because the hydrological cycle is complex. Attempts have been made to develop equations or conceptual models that can predict isotopic values for precipitation, but these have not been adequate (Sharp, 2007 and Yurtsever and Gat, 1981). However, several key factors have been identified by the first workers to interpret stable isotopes in water samples, for instance Friedman (1953), Epstein and Mayeda (1953) and Craig (1961), culminating in Dansgaard (1964). Some of these have been alluded to in previous sections. Subsequent workers continued to develop the understanding of these key factors, until they became widely accepted as a fundamental part of isotope hydrology (Gat, 1996). These factors, or isotope effects, are known as the temperature effect, latitude effect, continental effect, altitude effect and amount effect. With decreasing temperature, increasing latitude, increasing distance from the coast, increasing altitude or increasing amount of rain in a precipitation event, the isotopic composition of the precipitation becomes lighter (depleted in  $^2\text{H}$  and  $^{18}\text{O}$ ). The cumulative result of all these effects, and others specific to local settings, can be seen in the global distribution of stable isotope compositions in groundwater, superbly collated by Jasechko (2019) and shown in Figure 15.

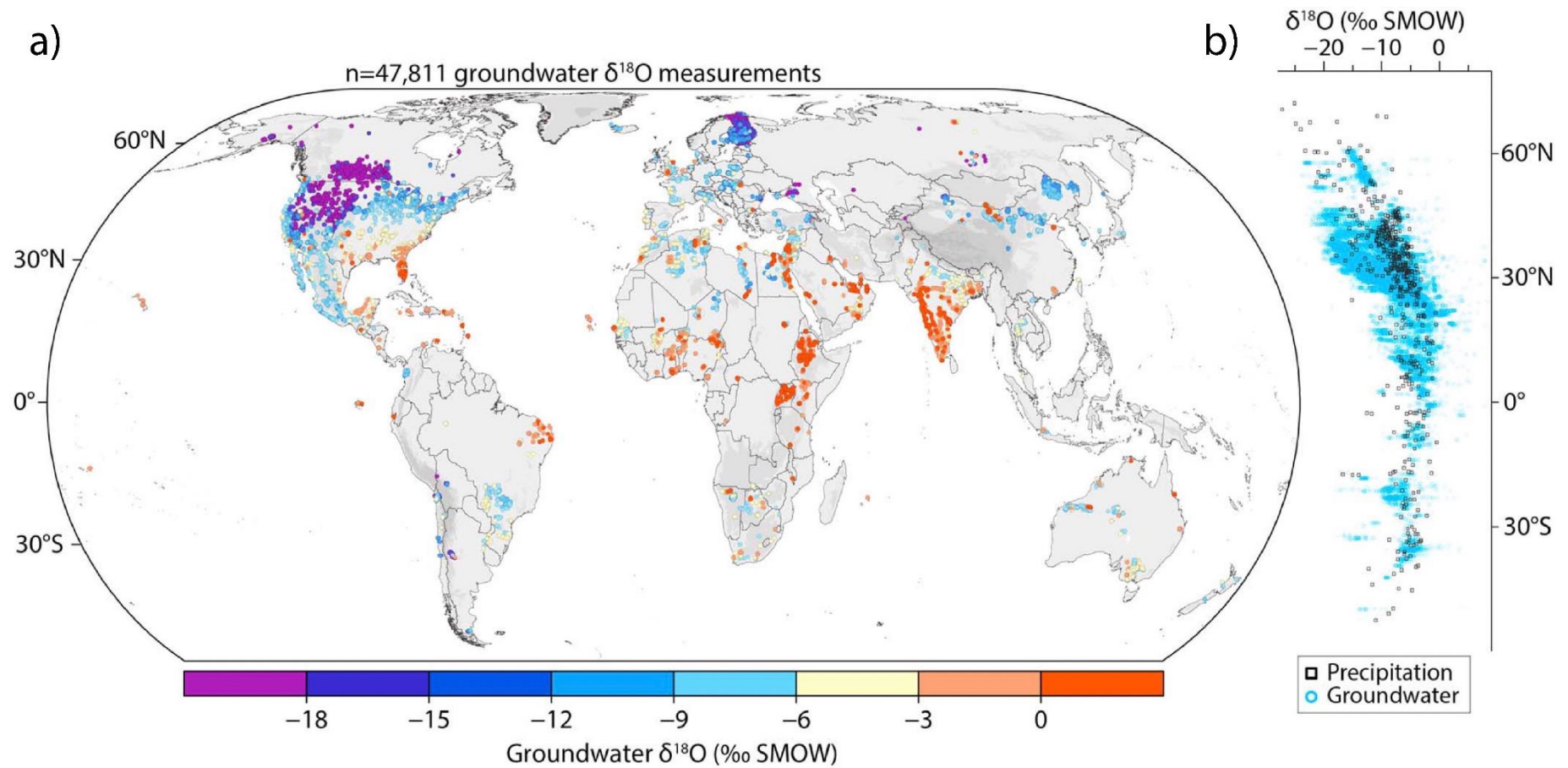


**Figure 15** - Global distribution of  $\delta^{18}\text{O}$  in groundwater: a) shows groundwater only; b) contains both groundwater and precipitation data. This graph summarizes nearly 48,000 measurements, from hundreds of publications over several decades. Image from Jasechko (2019).

## 6.1 Environmental Factors Affecting Water Isotopes (Isotope Effects)

### 6.1.1 The Temperature Effect

The temperature effect is the positive correlation between local air temperature and local precipitation stable isotope  $\delta$  values. Neither the temperature nor the stable isotopes are instantaneous values, but rather are the long-term (annual) means, to avoid sharp fluctuations that reflect only temporary factors related to a particular storm (cloud base elevation, precipitation intensity, and so on). The temperature effect results in water having more negative  $\delta$  values in areas with lower temperatures, and is due to several factors. First, evaporation from colder oceans, in mid-latitude (and polar) regions, is subject to a greater fractionation factor, because of the colder temperature, and produces vapor with more negative  $\delta$  values than those from warmer oceans. Second, condensation in colder clouds will produce more complete condensation of the vapor present, thereby incorporating more lighter isotopes. Third, the progressive rainout from low to high latitudes occurs in parallel to decreases in temperature, and so results in a higher correlation between  $T$  and  $\delta$ .

Araguás-Araguás and others (2000) noted this  $T$ - $\delta$  correlation for Vienna's precipitation, as shown in Figure 16. The correlation was improved by statistical smoothing and manipulation, mainly to remove the seasonal variation so that the interannual changes in  $T$  and  $\delta$  values could be displayed, and to show the change in  $T$  or  $\delta$  versus the average, rather than the absolute  $T$  or  $\delta$  values.

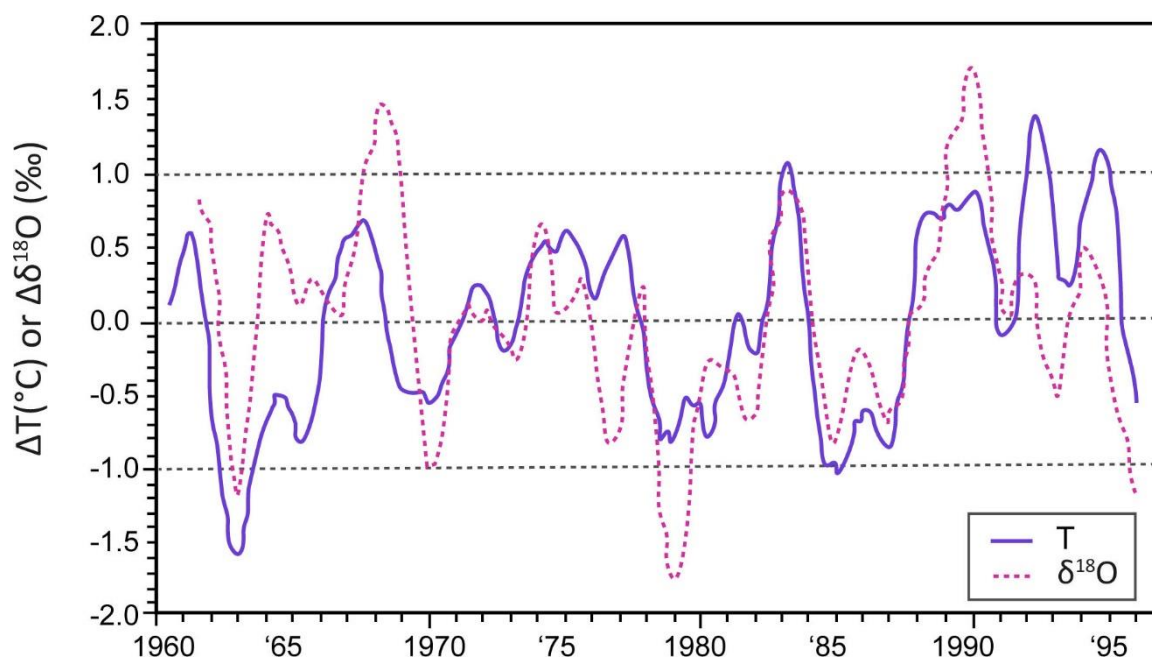


**Figure 16** - The relationship between surface air temperature and  $\delta^{18}\text{O}$  in Vienna from 1960-1996. Statistical removal of seasonality was accomplished by creating 12-month running means for  $T$  and  $\delta^{18}\text{O}$ , after which  $\Delta T$  and  $\Delta\delta^{18}\text{O}$  were calculated by subtracting the monthly running averages from the long-term means, and finally the curves were smoothed by reapplying a 12-month running mean (after Araguás et al., 2000).

The temperature effect manifests relatively well in high latitudes, but is not as strong in tropical regions, where the amount effect dominates (Jasecko, 2019; Rozanski et al., 1993; Yang et al., 2011).

### 6.1.2 The Latitude Effect

Most evaporation occurs over the tropical oceans (an estimated 65 percent as reported by Peixoto and Oort, 1983) because the higher temperature of the sea allows greater evaporation than in middle or high latitude ocean areas. Consequently, atmospheric moisture evolves isotopically as it moves away from the tropics. Condensation and rainout favor the removal of the heavier isotopes and so the precipitation at higher latitudes has more negative  $\delta$  values. Evaporation occurs from the mid-latitude oceans and because the temperatures are colder, the fractionation factors are greater, resulting in vapor relatively more depleted in the heavier isotopes than vapor forming above the tropical oceans.

The latitude effect is only easily perceptible over the continental to global scale, as the myriad local variations in moisture source, humidity, precipitation amount, altitude and so forth, create a large amount of "noise" when looking for the latitude- $\delta$  trend. As such, the latitude effect is mainly of interest in modeling global patterns of precipitation (Jasecko, 2019; Rozanski et al., 1993), but can be detected regionally in some cases (Laonamsai et al., 2020) as shown in Figure 17.

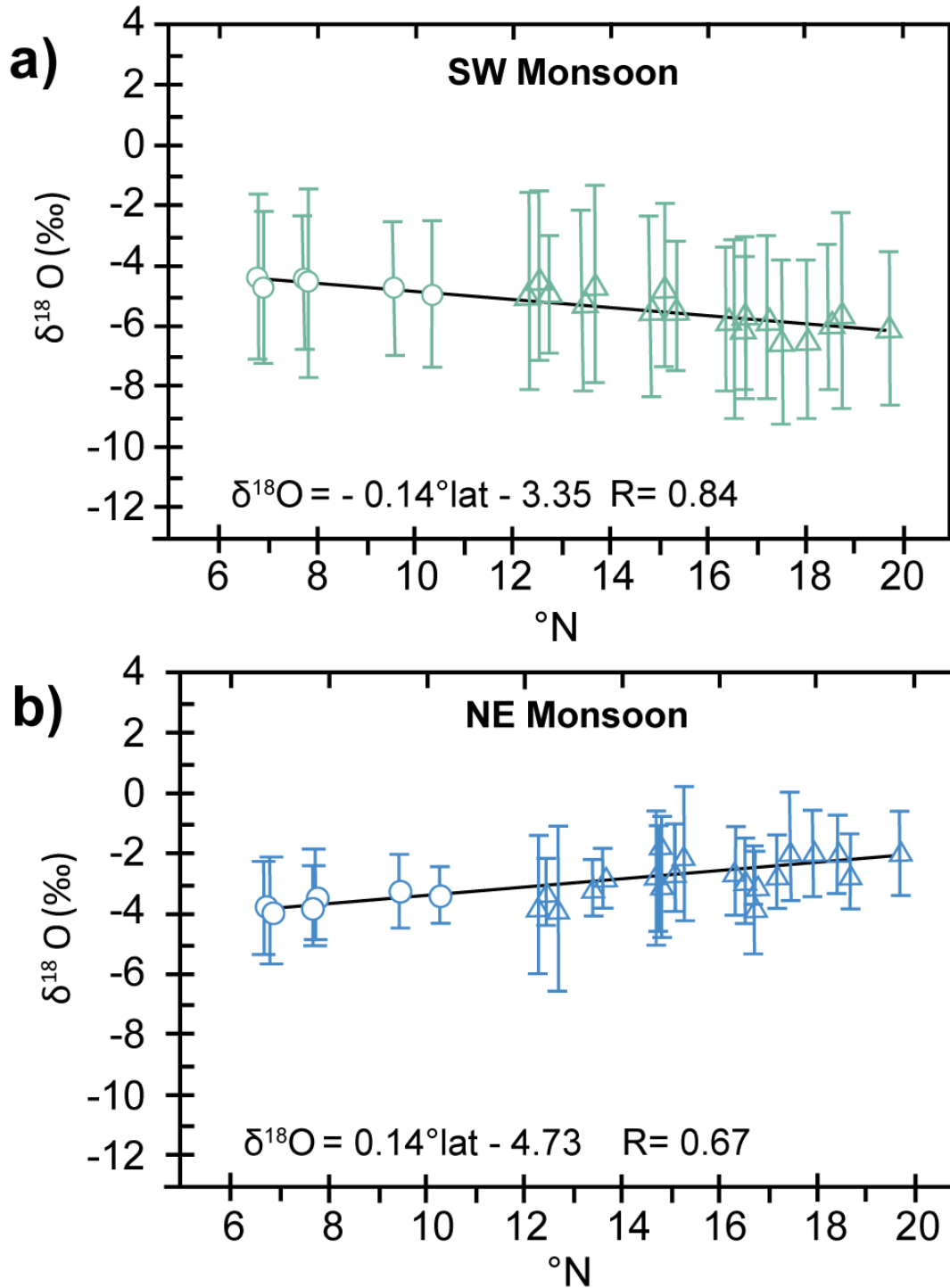


**Figure 17** - Stable oxygen isotopes for precipitation in Thailand based on monthly cumulative samples from 2013 to 2015. Rainout causes depletion of heavy isotopes with distance, which: a) in the case of the SW monsoon is the typical negative correlation with latitude; while b) in the case of the NE monsoon, is a positive correlation. During the NE monsoon, the weather systems move south-westward, or right to left in b), creating a continental effect where isotopic rainout over Vietnam and Laos lowers the delta values of rainfall with decreasing latitude (after Laonamsai et al., 2020).

### 6.1.3 The Continental Effect

Progressive rainout is the main cause of increasingly negative  $\delta$  values for precipitation that is further and further inland (Figure 18). The continental effect is seen as a decrease in delta values of precipitation with distance from the coast, as shown in Table 2.

In some cases, where winter precipitation occurs, cooler air inland may also reduce the amount of evaporation and isotopic change that occurs as rain drops fall through unsaturated air below the cloud. These colder inland temperatures will also increase the equilibrium fractionation factor that applies during condensation, thus removing heavier isotopes more effectively from the vapor and resulting in precipitation further inland being even lighter isotopically.

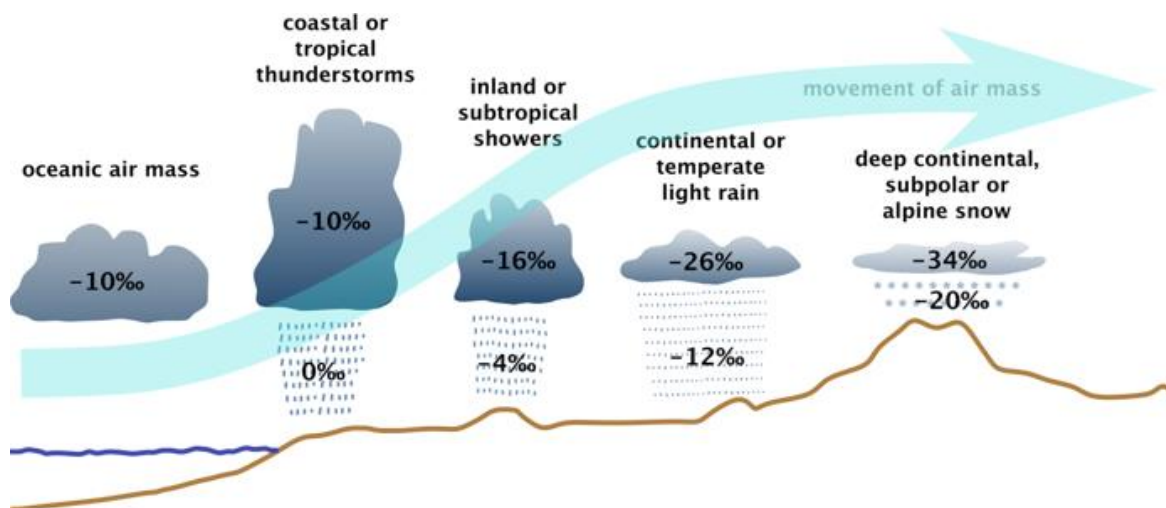


**Figure 18** - Schematic diagram illustrating both latitude and continental effects. Generalized values of  $\delta^{18}\text{O}$  are given, and these apply to both the evolution of moisture away from the tropics towards the poles (latitude effect) or evolution of moisture inland from the coast to the interior of a continent (continental effect). In both cases, progressive rainout (depletion of atmospheric moisture) is the key driver of the isotope composition.

In other cases, rainout can be so effective at removing the heavier isotopes that the temperature effect, due to seasonality, is overridden by the continental effect. For example, precipitation during summer (June to September) on the Tibetan Plateau is 6‰ ( $\delta^{18}\text{O}$ ) lighter than in winter when temperatures are 10° C colder (Araguás-Araguás et al., 1998). The continental effect is best observed over continental scales, but does operate at smaller, regional scales (Jasecko, 2019; Laonamsai et al., 2020).

**Table 2** - Some examples of the continental effect from around the world. The effect is given as a gradient, i.e., the change in mean  $\delta$  values of precipitation per 1000 km of distance.

Species	Gradient $\frac{\Delta\text{‰}}{1000\text{km}}$	Location	Reference
$\delta\text{D}$	-13	Europe: Belgium to Poland - summer	Rozanski et al., 1982
$\delta\text{D}$	-33	Europe: Belgium to Poland - winter	Rozanski et al., 1982
$\delta^{18}\text{O}$	-1.6	Europe: Poland to Russia	Rozanski et al., 1993
$\delta^{18}\text{O}$	-3.8	Europe: Poland to Russia	Rozanski et al., 1993
$\delta^{18}\text{O}$	-3 to -4	North America: Atlantic to Rockies	Clark and Fritz, 1997
$\delta^{18}\text{O}$	-10	Canada: Pacific to Prairies	Yonge et al., 1989
$\delta^{18}\text{O}$	-0.75	Amazon: Atlantic to Andes	Salati et al., 1979

### 6.1.4 The Altitude Effect

As with the continental effect, the altitude effect is caused mainly by rainout, in this case triggered by orographic uplift, as well as a decrease in temperature, resulting in greater fractionation factors, which will drive rainout of heavier isotopes and cause a faster shift to lighter isotopes with altitude. Also, rain falling at higher elevations will have less distance to travel to the ground and less chance for evaporative enrichment, in which the lighter isotopes preferentially evaporate. The altitude effect is shown as a decrease in  $\delta$  values per 100 m elevation gain in Table 3.

**Table 3** - Some examples of the altitude effect from around the world. The effect is given here as a gradient: the change in  $\delta$  values of precipitation per 100 m increase in elevation. The range of elevation over which the precipitation was sampled is also given.

Location	Country	$\delta^{18}\text{O}$ Gradient	Altitude masl	Reference
		$\frac{\Delta\text{‰}}{100\text{ m}}$		
Mount Cameroon	Cameroon	-0.16	0-4000	Gonfiantini et al., 2001
Eastern Andes	Bolivia	-0.24	200-5200	Gonfiantini et al., 2001
Hérault	France	-0.27	500-1800	Ladouche et al., 2009
Whole Island	Taiwan	-0.20	0-2500	Peng et al., 2010
Fuego Volcano	Guatemala	-0.67	800-1200	Mulligan et al., 2011
Table Mountain	South Africa	-0.075	100-1100	Diamond & Harris, 2019
Mount Shasta	California, USA	-0.21	1000-3100	Peters et al., 2018

The altitude effect for an area is derived by collecting precipitation in at least two locations close to each other, but at different elevations. If using only two locations, then several precipitation seasons (several years) of data should be collected so as to average out the differences between years or unusual years caused by climatic variability. It is important to collect all rain that falls, and to weight the data for each sample (be they daily or monthly precipitation samples) by precipitation amount, to get a representative average isotope composition. If more precipitation stations are used, then sampling can be undertaken over a shorter period, but ideally there should be several precipitation stations sampled over several rainy seasons, including climatically different years, for example El Niño and La Niña fluctuations.

The altitude effect creates large enough variations in stable isotope compositions to allow stable isotopes to be used as tracers over fairly small distances (kilometers to tens of kilometers). This is commonly used to delineate recharge locations for groundwater discharging at springs or boreholes at lower elevations (Blarasin et al., 2020; Diamond and Harris, 2019; Jasecko, 2019).

### 6.1.5 The Amount Effect

The amount effect also has a close relationship with rainout. The amount effect manifests as a shift to lighter isotope compositions for heavier precipitation events (Figure 19). First, heavy individual rainstorms will tend to remove more of the vapor and cloud droplets in the air, and so with increasing precipitation in one location, the isotopic

signature should become lighter. Second, the air below the cloud base will gradually become more saturated and colder, as rain and air from higher in the cloud descends (the downdraft), both of which will reduce evaporative enrichment of the later rain drops. The amount effect is known to be more pronounced in low latitudes (Dogramaci et al., 2012; Rozanski et al., 1993; Yang et al., 2011).

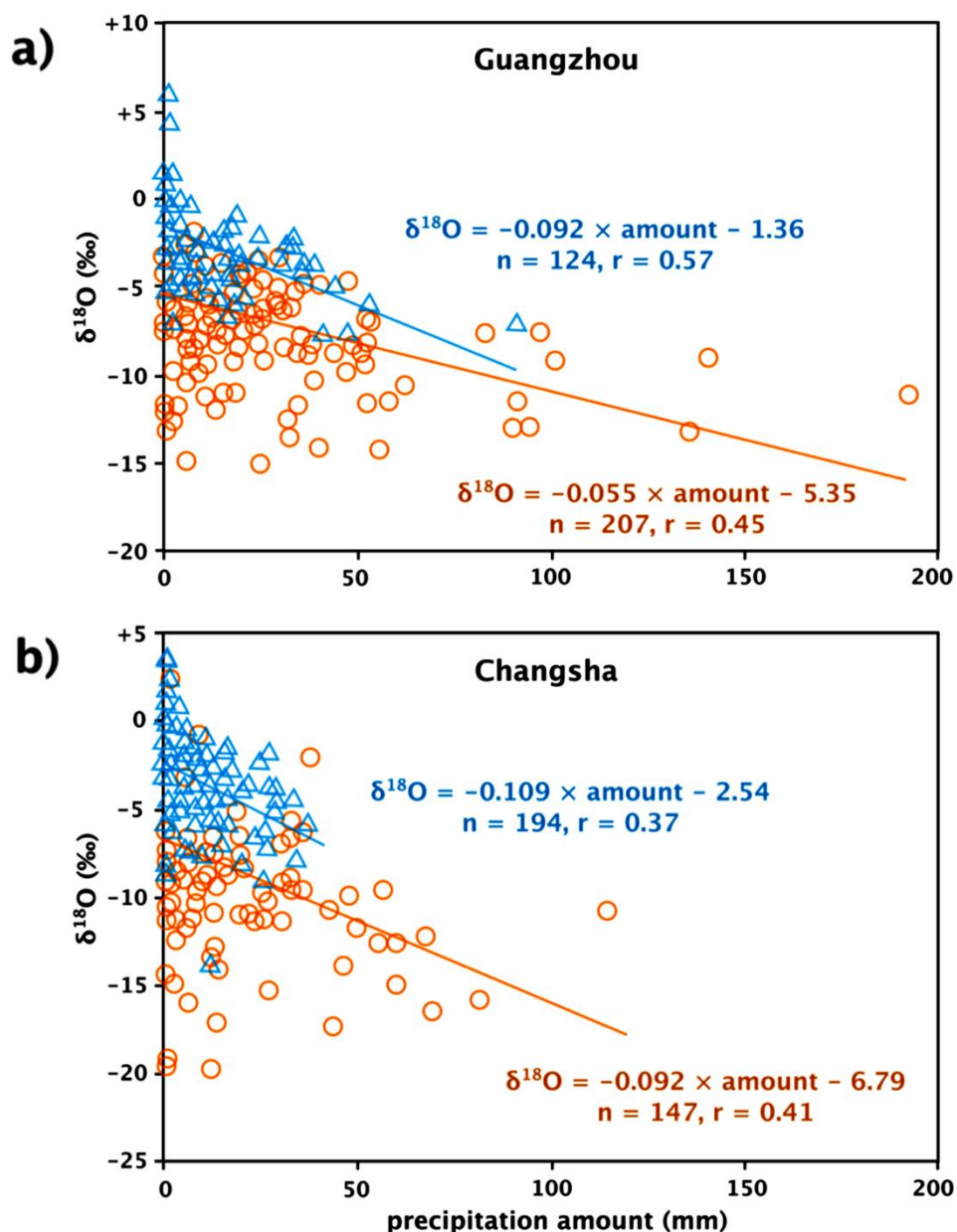


**Figure 19** - Oxygen isotopes of precipitation in winter (triangles) and summer (circles) for a) Guangzhou and b) Changsha from June 2006 to May 2009. The negative correlation with precipitation amount is apparent and has been quantified in the equations displayed on the graphs (from Yang et al., 2011).

Of the 5 isotope effects, temperature and rainout are the main underlying processes that drive the various 'effects'. It is important to note that all these effects and their underlying causes occur in a highly complex natural system where many variables contribute to the final isotopic composition of a rainwater sample. Other than temperature

and rainout, factors such as humidity, storm track, preceding atmospheric conditions and source region also modify the isotopic composition. Isotope content of rainwater varies by the minute in a rainstorm (Muller et al., 2015) and between rain events, as is typical of most meteorological phenomena (e.g., temperature, cloud formations, precipitation amount, storm duration). Averaging the isotope composition of precipitation over longer periods, such as a month, has been found to be the most useful way of understanding the variation in isotopic signatures in an area (Yurtsever and Gat, 1981).

## 6.2 The Deuterium Excess

Kinetic fractionation during evaporation from the ocean surface takes place because of diffusion of water vapor molecules from a saturated boundary layer at the sea surface and into the open atmosphere. The  $^1\text{H}^1\text{H}^{16}\text{O}$  isotopologue diffuses faster than all the others and so the vapor in the open atmosphere is depleted in the heavier isotopes. If the atmosphere was saturated, then isotope exchange would occur fully between the sea and water vapor in the air, resulting in isotopic equilibrium.

Importantly, there is a difference between the diffusion fractionation factors for  $^2\text{H}$ - $^1\text{H}$  and  $^{18}\text{O}$ - $^{16}\text{O}$  and so the relative depletion of  $^2\text{H}$  and of  $^{18}\text{O}$  is not the same. This difference between the rate of  $^2\text{H}$  depletion and  $^{18}\text{O}$  depletion changes with the degree of saturation, or relative humidity,  $h$ . In other words, at lower humidity,  $^2\text{H}$  is not affected by evaporation as much as  $^{18}\text{O}$ , which means vapor at lower humidity will be further from the GMWL. As  $h$  increases, more isotope exchange will occur and the fractionation the system will come closer to equilibrium (Clark and Fritz, 1997).

This means the position of a LMWL is partly a function of the relative humidity of the source region, where evaporation generated the vapor mass. Evaporation under low relative humidity will generate lines displaced further left of the GMWL. Figure 20 shows how evaporation from sea water under 85 percent relative humidity conditions and then condensation at equilibrium generates water with isotopic compositions that plot along the GMWL. At various values of relative humidity, vapor and the resulting water samples will be displaced from the GMWL to a greater or lesser degree and will have an intercept on the  $\delta^2\text{H}$  axis that is larger or smaller than 10. This intercept, known as the deuterium excess (D-excess, or  $d$ ) of a water sample is calculated with Equation 13.

$$\text{D-excess} = \delta^2\text{H} - 8\delta^{18}\text{O} \quad (13)$$

where:

$\delta^2\text{H}$  and  $\delta^{18}\text{O}$  = values for the water sample

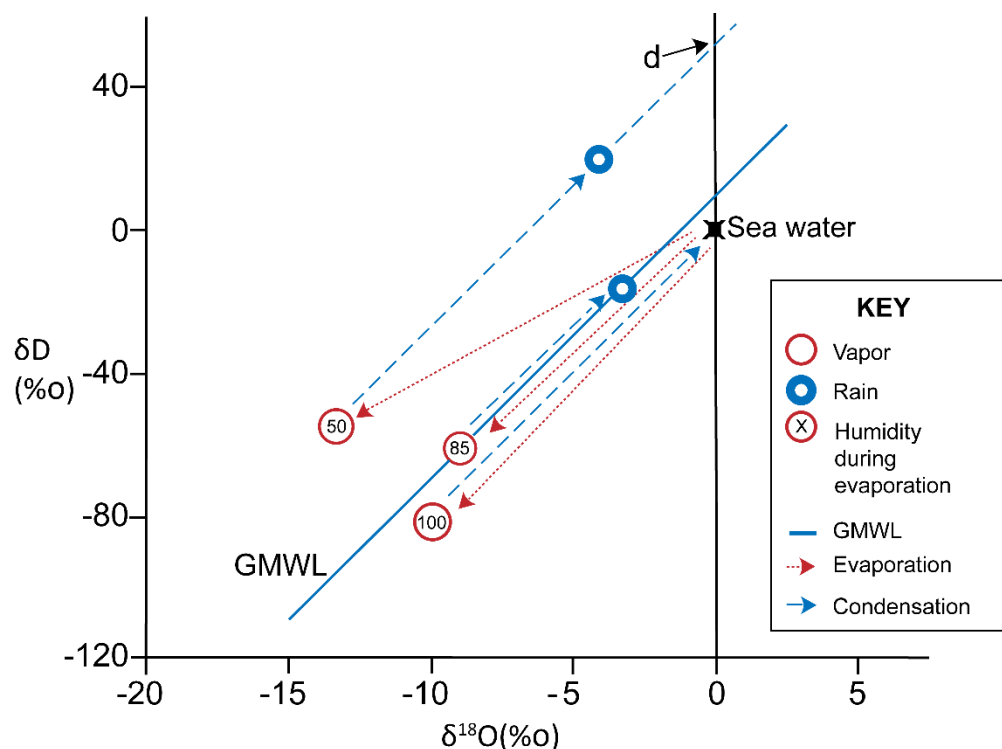


**Figure 20** - Different relative humidity in source regions during evaporation (red dotted lines) create moisture masses with different deuterium excess (*d*) values due to kinetic fractionation. Sea water lies at the 0,0 point on the graph. Evaporation of sea water at 100 percent humidity would produce vapor somewhere along the red dotted line pointing to 100 percent humidity, depending on the temperature. Higher temperatures would have lower fractionation factors and so the vapor would be closer to the sea water point. At lower humidity, kinetic fractionation affects evaporation, resulting in vapor plotting somewhere along the other red dotted lines, as shown for 85 percent and 50 percent humidity. The average global humidity at the sea surface is approximately 85 percent, so the GMWL intercepts the  $\delta^2\text{H}$  axis at a *d* value of 10. For a hypothetical region with evaporation occurring under 50 percent relative humidity conditions, *d* ~50 as indicated by the extrapolation of the dashed blue line to  $\delta^{18}\text{O} = 0$ . During condensation and precipitation, the *d* value remains similar for the vapor and the rain, even though rain or vapor samples will have very different  $\delta^2\text{H}$  and  $\delta^{18}\text{O}$  values along the blue dashed lines. This may not be the case for very low precipitation amounts and low humidity, for example in deserts (modified from Clark and Fritz, 1997).

The D-excess (*d*) is a proxy of the humidity of the source region, with lower humidity causing higher *d* values. An example of this is shown in Figure 21.

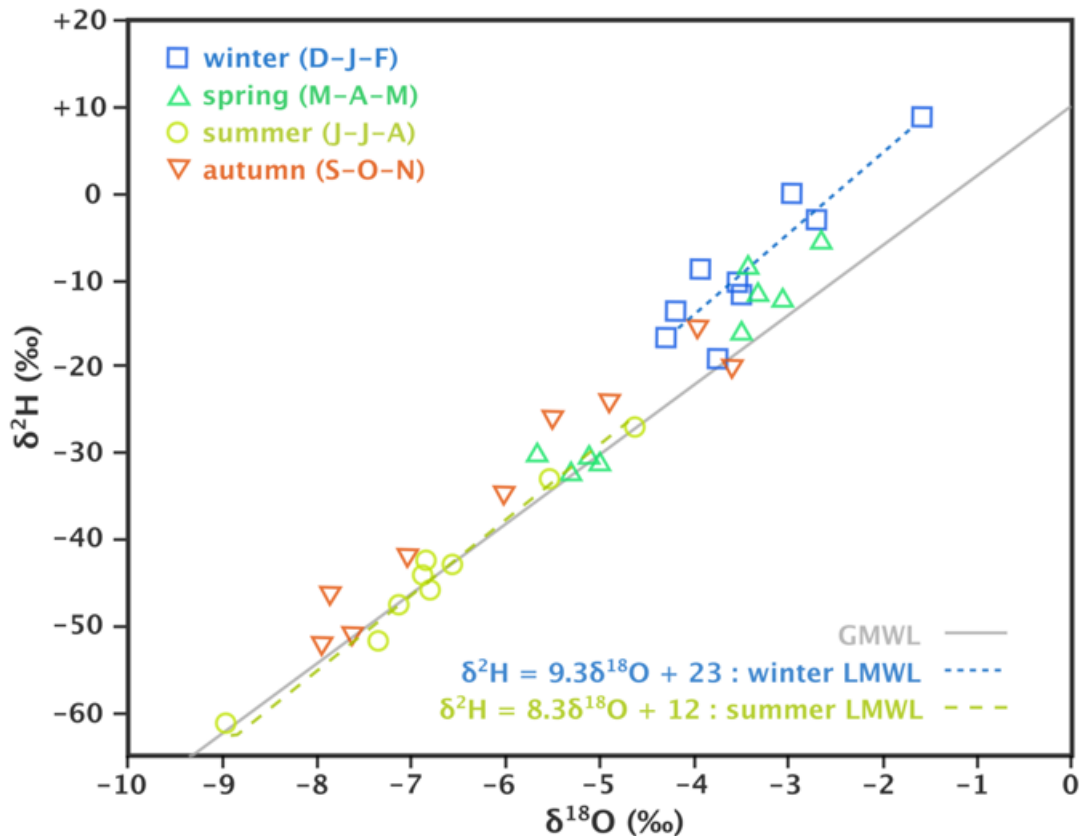


**Figure 21** - Hydrogen and oxygen isotopes for precipitation on Okinawa Island, south of Japan, from April 2008 to April 2011. The distinct separation of the winter precipitation from the rest of the year is shown by calculating a MWL for the winter precipitation only. The winter data has a higher d-excess than the rest of the year, suggesting less humid conditions during evaporation in the moisture source region, which was postulated to be due to local evaporation around the island into a relatively dry continental air mass, compared to the other precipitation that was sourced in the tropical western Pacific (from Uemura et al., 2012).

### 6.3 Event Variation

As stated in the introduction, knowledge of the whole hydrological cycle is often needed to unravel groundwater questions, and although the cycle has no end or beginning, the isotopic signature of precipitation is a good point to begin. This is particularly true for groundwater, as precipitation precedes recharge. Most hydrogeological studies make use of bulk isotope values for precipitation, typically monthly cumulative samples, as per the IAEA GNIP (International Atomic Energy Agency, Global Network for Isotopes in Precipitation) program, allowing calculation of a MWL, assessment of seasonality in isotope values, and generation of the mean annual isotope composition. This approach is sufficient for many groundwater applications.

However, some studies have analyzed the isotopic composition daily (Sanchez-Murillo et al., 2016), per event (Qu et al., 2014), within-event (Harris et al., 2010) and even down to 30 second increments (Munksgaard et al., 2012). The results show a tremendous variation in isotope composition of rain over short timeframes. From one location and a set of nine rain events totaling 15 days over 8 months, Munksgaard and others (2012) reported -140 to +13‰ in  $\delta^2\text{H}$  and -19.6 to +2.6‰ in  $\delta^{18}\text{O}$ , capturing as much

35

variation as the monthly cumulative samples across the whole continent of Australia over a period of 40 years.

Although the isotopic variation of a rain event is mostly dependent upon the type of event and its duration, typical variations are on the order of 10-50‰ for  $\delta^2\text{H}$  and 1-5‰ for  $\delta^{18}\text{O}$  (Han et al., 2020; Harris et al., 2010; Muller et al., 2015). Different studies have noted different trends. Harris and others (2010) found less  $\delta$  variation in a shorter (5 hour), heavier rain event associated with a cold front from the South Atlantic passing over Cape Town as opposed to a larger, more complex frontal system lasting more than a day. Qu and others (2014) similarly found more variation in  $\delta$  values during larger storms for the subtropical monsoon climate of eastern China, and Han and others (2020) saw variability decrease during an event (Figure 22).

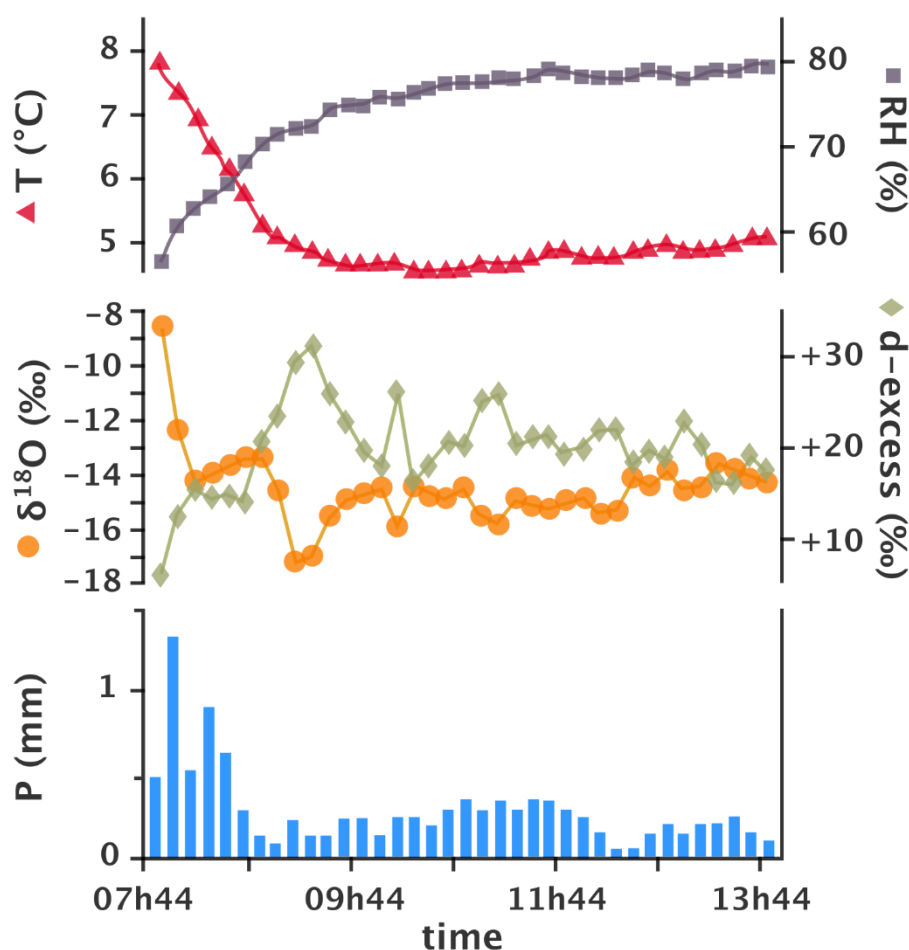


**Figure 22** - Variation of oxygen isotope composition with time, during a single rain event of several hours is revealed by analyzing 10-minute increment samples of the precipitation. This event exhibits an L-shaped trend in isotope composition, as well as stabilization of the variations with time (after Han et al., 2020).

From a review of previous work, Muller and others (2015) noted several intra-event patterns of change in isotope composition over time. These were increasing, decreasing, V-shaped, W-shaped, L-shaped and no-trend. The most common of these are the

increasing, decreasing, V-shaped and L-shaped. They also found a general relationship that  $\delta$  values are inversely proportional to rain rate, in other words, heavier rain is associated with lighter isotopes. This is not quite the same as the amount effect, where lighter isotopes are associated with larger total precipitation amounts (and not higher precipitation rate). For example, Sanchez-Murillo and others (2016), working in Costa Rica, where one would expect an amount effect due to its tropical latitude, took daily precipitation samples and found humidity and condensation levels to best correlate with isotope composition, and not precipitation amount. In contrast, Han and others (2020) found relative humidity to have no effect on isotope values, but saw that fresh input of an air mass into the weather system can renew the system with heavy isotopes and make the  $\delta$  values of the event increase. Adar and others (1998) hypothesized that rain from different parts of the storm system can also cause variations in the isotope composition of rain.

In understanding infiltration, runoff and other parts of the water cycle, a single sample for the total precipitation of a whole event is clearly going to obscure some of the detail. In a desert setting in Israel, Adar and others (1998) saw that some events of < 1 mm precipitation triggered runoff. If one wants to understand the detail on a site, high-frequency, sub-event rain monitoring may be needed, and if trying to understand a whole catchment, then sufficient spatial coverage may also be needed. Fortunately, the low cost and high speed of analysis with laser cavity instruments makes this type of science possible for researchers even on moderate budgets. The potential for application to understanding vadose zone processes, ecological issues, triggers for fracture flow, and other poorly understood aspects of hydrogeology, are tantalizing.

## 6.4 Mass Balance

The principle of mass balance can be applied widely across many disciplines, such as meteorology, oceanography and geochemistry. In essence it applies when a set of inputs merge perfectly and completely into a set of outputs. Quite often a system is simplified into only 2 or 3 inputs and a single output. For example, precipitation, groundwater and surface water could be the inputs to a river, which is the output. Assuming conservation of mass, in other words, no losses along the way, then the river quantity and quality must comprise the sum of the quantity multiplied by the quality, of all of the inputs.

For most calculations, the quantities can be flow rates in liters or cubic meters per unit time, or something similar. The use of moles is necessary when dealing with different compounds, but this is beyond the scope of this text and is seldom needed when dealing with water only. For isotope compositions, it is generally fine to represent them as delta values, but they are most accurately calculated using isotope ratios (Hayes, 2004). The errors introduced by using delta values are caused by rounding errors and mole fraction mixing, both of which are worse when there are large differences in delta values (personal communication from Robert Kalin 2022). These discrepancies are mostly below analytical

or other errors, and therefore probably only need to be considered when using high precision data (Steur et al., 2020).

Mass balance can be presented as an equation, here using stable isotopes ( $\delta$  values) as the quality parameter in Equation 14.

$$(Q_1 \times \delta_1) + (Q_2 \times \delta_2) + (Q_3 \times \delta_3) + \dots = Q_f \times \delta_f \quad (14)$$

where:

$Q$  = flow rate ( $MT^{-1}$ )

$\delta$  = delta value (as in Equations 1 and 2) of isotope species of interest (e.g.,  $^2H/^1H$ ) of each input (1, 2, 3, etc.)

1, 2, 3... = subscript for input streams

$f$  = subscript for output stream

It is important that the stable isotope compositions differ enough in the end-members for the method to work.

The simplest application of mass balance in stable isotope hydrology is to evaluate the groundwater contribution to surface water during precipitation events, often called storms. In this simple case, the mass balance equation is expressed by Equation 15.

$$(Q_g \times \delta_g) + (Q_p \times \delta_p) = Q_s \times \delta_s \quad (15)$$

where:

$g$  = subscript indicating groundwater

$p$  = subscript indicating precipitation

$s$  = subscript indicating resultant total stream flow

The isotopic composition of groundwater and pre-storm-event stream flow is assumed to be the same, as the river is assumed to be totally fed by baseflow, in other words,  $\delta_g = \text{pre-storm-}\delta_s$ . Note that these assumptions may often be close to the truth, but may be quite incorrect in other cases. The H and O isotope compositions for the precipitation ( $\delta_p$ ), groundwater ( $d_g$ ) and storm flow ( $\delta_s$ ) are measured, as is the total river flow during the storm or flood event ( $Q_s$ ). This leaves 2 unknowns,  $Q_g$  and  $Q_p$ , but these are related because they both add up to the streamflow. In equation form, this is as shown in Equation 16.

$$\begin{aligned} Q_g + Q_p &= Q_s \\ \therefore Q_p &= Q_s - Q_g \end{aligned} \quad (16)$$

Then, by substituting into the original mass balance equation (Equation 15) and rearranging the terms, results in Equation 17.

$$Q_g = Q_s(\delta_s - \delta_p) / (\delta_g - \delta_p) \quad (17)$$

In this way, with only one flow measurement (stream discharge), and three isotope values (precipitation, pre-storm streamflow and storm streamflow), we can calculate the baseflow and precipitation contributions to storm flow in a stream. In reality, due to the variability of isotope values in both precipitation and streamflow, multiple samples produce a more reliable result. For precipitation, instead of multiple samples, a single cumulative sample of all the precipitation during the storm can be taken, but this would most likely miss out on a lot of the finer detail and perhaps some critical changes in the contributions to flow that are known to occur (Xie et al., 2016).

This technique is suitable for small catchments with simple geology. Where groundwater contributions from the vadose and phreatic zones may differ, or where there is a large upstream catchment and the river flow may be expected to change stable isotope values during the storm due to varied isotope composition coming downstream, this method will need adjustment and more measurements will be required (Das et al., 2020).

Mass balance on a part of the Gariep River, the second largest river in southern Africa, after the Zambezi, was demonstrated by Diamond and Jack (2018) using only surface waters, as groundwater input was insignificant over short reaches. The stable isotopes were measured upstream on two tributaries and downstream after being well mixed at the location of a flow-gauging station. The contributions from the two tributaries were then calculated using the above equations.

## 6.5 Hydrograph Separation

Hydrographs are charts showing the amount of water flowing in a river over time. A hydrograph reflects the sum of the contributions to flow. Catchment water balance theory tells us the river flow at a point has a set of possible contributions, which, when there is no precipitation occurring and no flows provided by human activities, can only be groundwater, from both the phreatic and vadose zone, the latter sometimes called soil water or interflow. During a precipitation event or storm, the possible contributors also include direct precipitation (onto the river surface) and overland flow or runoff. In general, direct precipitation is negligible and interflow (from the vadose zone) is often assumed to be negligible, and so this leaves runoff and groundwater as the main sources of river flow during a storm as illustrated in Figure 23.

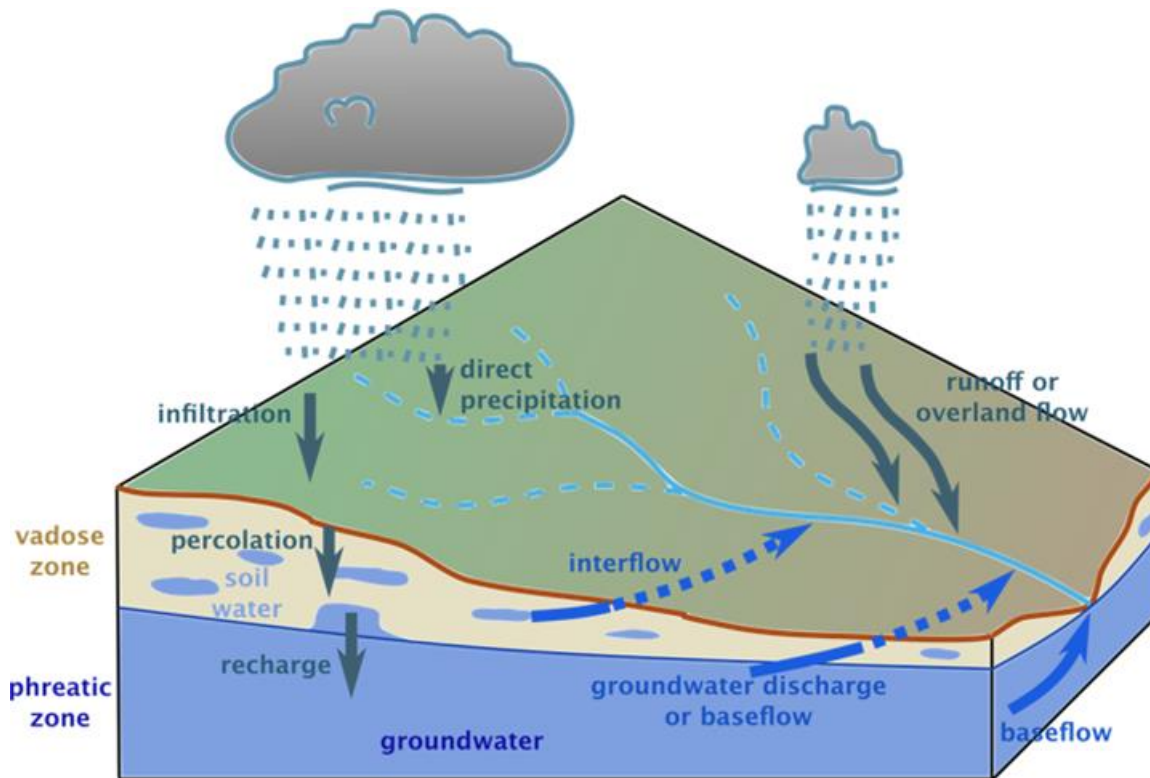


**Figure 23** - Schematic diagram of the main flows of water in a natural catchment. Inclusion or exclusion of each flow in a model depends on the degree of detail in the model, data availability and the catchment itself.

Hydrograph separation involves apportioning the river storm flow into components. In the past, this was done graphically by comparing the baseflow (fairly constant flow) and quick flow (rapidly rising and falling component of flow due to a storm) portions of the hydrograph and assuming that quick flow was mostly due to runoff. The assumption that the precipitation from a rain event is transferred to the stream via runoff was shown to be inaccurate in many parts of the world, especially after analysis of conservative tracers (e.g., H and O isotopes, Cl) in the water (Sklash and Farvolden, 1979; Hooper and Shoemaker, 1986). Although some hydrologists still use graphical methods to attempt hydrograph separation, many are of the opinion that this is as misleading as it is beneficial, with Beven (2001) stating "the best method of dealing with hydrograph separation is to avoid it altogether".

Natural tracers, such as dissolved ions and isotopes, both stable and radioactive, provide a different way of performing hydrograph separation. Each component or possible contributor to river flow can be characterized, such as groundwater and precipitation. For a 2-component system, the total river flow is then compared to these using a mixing line between the components and can provide an estimate of the proportions of groundwater and rainwater in the river. Isotopes in particular, due to their non-reactivity in aquifers, are ideal tracers, better than most dissolved species, as the latter often undergo various reactions and transitions. Certain conditions should be met to apply this method successfully, as stated by Sklash and Farvolden (1979).

- “(1) The isotopic content ( $^{18}\text{O}$ , D or T) of the event component is significantly different from that of the pre-event component.*
- (2) The event component maintains a constant isotopic content.*
- (3) The groundwater and vadose water are isotopically equivalent or vadose water contributions to runoff are negligible due to hydrogeologic constraints.*
- (4) Surface storage contributes minimally to the runoff event.”*

If these guidelines are applied (Laudon and Slaymaker, 1997), hydrograph separation using natural tracers may be reasonably successful. However, the study area may deliver complexities that cannot be easily resolved, or the study itself may be inadequate, rendering this simple approach less valuable (Klaus and McDonnell, 2013). To be more specific, Hooper and Shoemaker (1986) noted isotope compositions of various components to be indistinguishable at times and snowmelt contributions to vary over time, in a study in New Hampshire. The co-variation of  $\delta^2\text{H}$  and  $\delta^{18}\text{O}$  has been used to dismiss use of both of these tracers, however, Lyon and others (2009) find that each element gives a different result. Use of both is not as robust as two totally independent tracers, for example  $\delta^{18}\text{O}$  and  $\text{SiO}_2$ , but it is better than using only one. Also, as mentioned, the stable isotopes are least likely to undergo changes from reactions with the aquifer, other water types or the atmosphere.

One of the major challenges is estimating the isotopic compositions of the different components, also called end-members. Pu and others (2017) observed how sensitive their calculations were to their end-member estimates, and Penna and Van Meerveld (2019) used the observed variations in values for end-members from 148 studies to calculate the typical error due to natural variations of isotopes in groundwater, precipitation, streamflow and other components. They computed a value of 26 % for the variation, or error, in the estimates of final flow components. Another common issue is the number of components. In many cases flow originates from more than groundwater and precipitation. Snowmelt, glacier melt, surface storage (pre-existing water that becomes a flow component after precipitation) and vadose zone water may all contribute significant flows during an event. In these cases, a 3-component hydrograph separation is more likely to capture the main sources of flow (Klaus and McDonnell, 2013), such as groundwater, meltwater and runoff for a study on the Ganga River in the Himalaya (Maurya et al., 2011) or glacier melt, snowmelt and runoff at the Gangotri Glacier, also in the Himalaya (Rai et al., 2019). The latter study used a 2-component model on non-rainy days to determine that glacier melt and snowmelt were two distinguishable components, and therefore were able to apply the more complex 3-component model in rainy weather.

The results of isotopic hydrograph separation are therefore variable in accuracy, and often incorporate hydrochemical parameters, as does much other work in stable isotope hydrology. However, many studies have undertaken isotopic analysis of the

various hydrological flows in catchments in order to estimate the groundwater contribution to surface water flow (Jasecko, 2019). The results show that the ratio of groundwater to runoff as contributions to total river flow vary from catchment to catchment, and also within the same catchment, but under differing weather conditions (Camacho Suarez et al., 2015). Some studies, for example Iqbal (1998), continue to show that precipitation tends to recharge groundwater, driving an increase in baseflow, causing quick flow to have an isotopic composition closer to groundwater than event water, as shown in Figure 24.

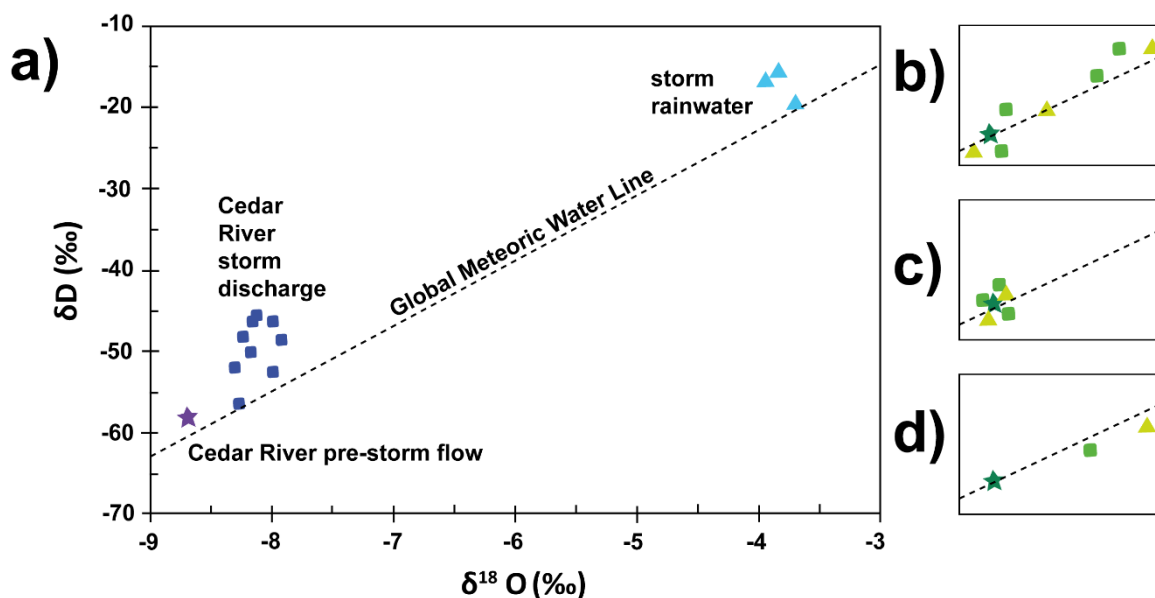


**Figure 24** - a) Stable isotopes for the Cedar River catchment, Iowa, USA (Iqbal, 1998). The final storm discharge in the river (blue squares) is assumed to comprise two components, namely groundwater discharge (purple star) and precipitation (turquoise triangles). The proportions that these two components contribute to the storm discharge can be calculated by measuring the graphed distances along a straight line between all 3 water types. In this case the distance between the pre-storm data point and the storm water discharge data points is about 0.15 of the total distance between the pre-storm and the rainwater data points, whereas the distance between the storm discharge and the rainwater data points is about 0.85 of the total distance, indicating the groundwater contributes roughly 85 percent of the storm discharge. The spread of data and number of samples in this case suggest this method is applicable. In contrast, scenarios where this method is not applicable are shown in the insets: b) too much scatter of the data resulting in high standard deviation of the estimate; c) too little variation of the data such that, statistically, their means that are not significantly different; and, d) too few samples producing statistically uncertain results.

Another study, shown in Figure 25, used data from a seasonal period to show that quick flow is mostly event water. It was theorized that this was due to steep slopes, poor aquifers and compaction of soils from agriculture in the basin (Tekleab et al., 2014).

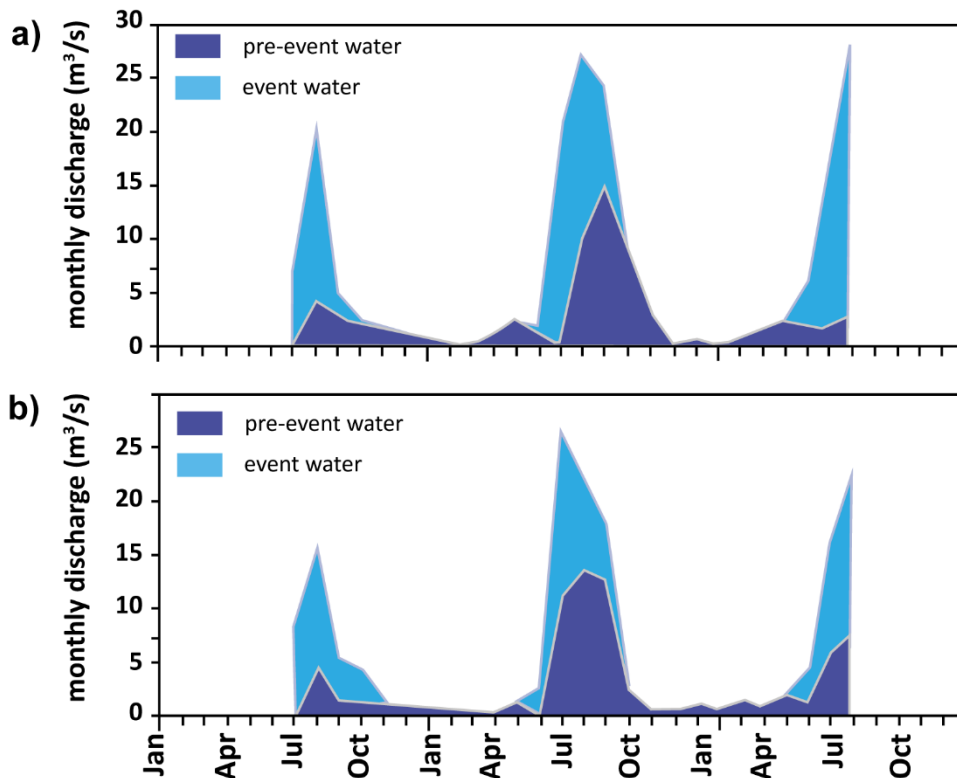


**Figure 25** - The results of a classic two-component hydrograph separation performed using  $\delta D$  and  $\delta^{18}O$  over a seasonal period for the a) Chemoga and b) Jedeb catchments in Ethiopia. The proportion of event water in the river flow was calculated to be an average of 71 percent and 64 percent in the two catchments respectively (from Tekleab et al., 2014).

Hydrograph separation is a worthy pursuit, and although some progress has been made in improving the procedure, more integration of physical, chemical and isotopic evidence is likely to bring greater understanding (Kirchner, 2003).

## 6.6 Geothermal Waters

Heated groundwater can be divided into two types, although there is a continuum between the two. The term thermal (or hot) springs usually applies to groundwater that is noticeably warmer than the mean annual temperature of an area, so the temperature definition varies with the local climate. For temperate climates, 15 °C is a typical threshold between shallow unheated groundwater and geothermally heated water. The threshold is closer to 20 °C for Mediterranean climates, around 25 °C in the tropics, and up to 35 °C in hot deserts. The depth to which groundwater must circulate in order to be heated again varies from region to region, depending on the geothermal gradient, which is influenced by the age and thickness of the crust and the degree of volcanic activity in the area. However, there is usually a clear distinction between relatively low geothermal gradients of around 10 to 30 °C/km in tectonically quiet areas (most of the earth's surface), versus the much higher geothermal gradients in volcanically active areas where boiling water and steam occur within tens to hundreds of meters of the surface. These latter areas are usually referred to as geothermal.

From an isotopic perspective, thermal springs are usually caused by deep circulation of meteoric water, usually at temperatures below those likely to cause isotope exchange with rocks. As such, studies evaluating recharge and flow paths, and other hydrogeologic issues, can be conducted using the stable isotopes, as they are conservative, for example as shown in Figure 26 (Chandrajith et al., 2012; Diamond and Harris, 2000; Durowoju et al., 2019). Most of the concepts in this book are applicable in these situations.

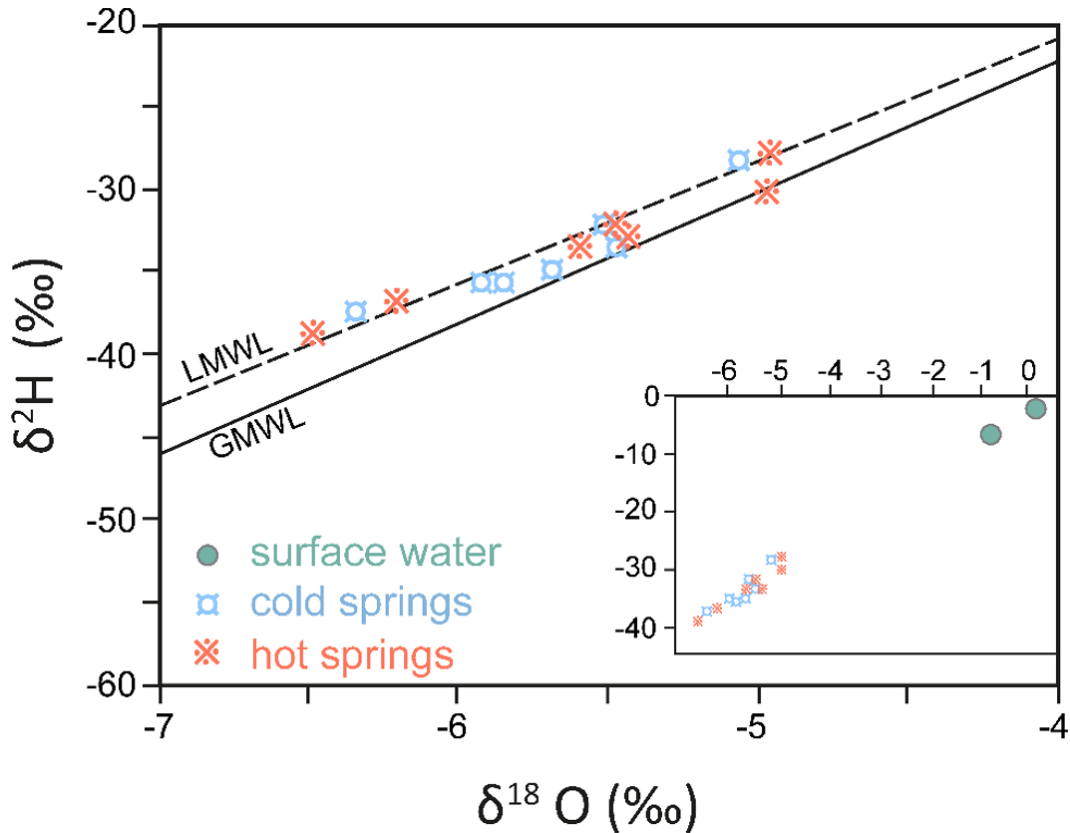


**Figure 26** - Stable isotope data for cold and hot springs (< 62 °C) in eastern Sri Lanka. The overlap of isotope compositions for hot and cold springs is typical for lower temperature thermal springs. Surface water typically has heavier isotope composition of the groundwater as displayed in the inset (after Chandrajith et al., 2012).

In contrast, geothermal waters usually experienced isotope exchange with the host rocks resulting in the isotope composition changes (Lelli et al., 2021). Figure 27 shows how isotope exchange, caused by the high temperatures of geothermal fields (> 100 °C), with silicates, which generally have positive δ<sup>18</sup>O values, is the cause of variation in isotope composition. If mixing with juvenile (magmatic) water was the cause, the δD values of the geothermal water would have changed and the mixing lines from the various geothermal fields would converge on the juvenile water type.

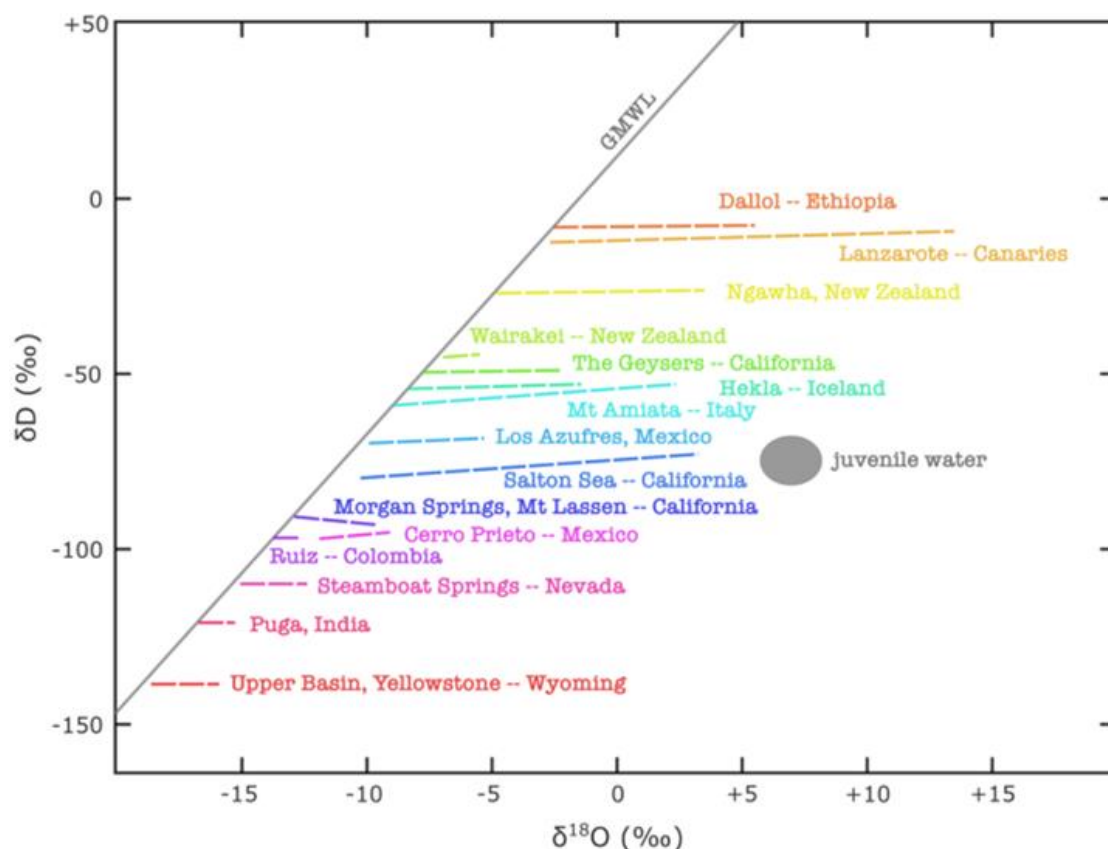


**Figure 27** - Stable isotope compositions for water and steam at geothermal locations around the world, in comparison to the GMWL (Global Meteoric Water Line). Mixing with juvenile (magmatic) water is not the cause of variation from meteoric water, but rather the variation is caused by isotope exchange with silicates. This is revealed by major changes in oxygen isotopes, while changes in hydrogen are negligible because of its lesser abundance in minerals (after Panichi and Gonfiantini, 1981; D'Amore and Panichi, 1985; Stewart, 1985).

In the case of Wairakei and some of the other fields, the shift in  $\delta^{18}\text{O}$  is not large. This likely occurs because the rocks already exchanged oxygen with the groundwater over many years and now the system is close to the equilibrium fractionation value with the meteoric water, so further exchange is minor. Extending this concept, the factors responsible for determining the degree of isotope exchange between water and rock are: original isotopic composition of the rocks, original isotopic composition of the meteoric water, quantity of rocks, quantity of water, temperature, water circulation path, the water/rock contact-surface area, and time (Panichi and Gonfiantini, 1981; Daniele et al., 2020).

Groundwater temperatures in geothermal fields are very high, so it is expected that, given the chance, significant evaporation will occur. This evaporation can either be at the surface, or in the subsurface, and there are ways to model both the amount of evaporation and the process. These processes include single-stage or continuous steam separation, the former being when steam is released only once the groundwater-steam mixture arrives at surface, the latter being where steam is continuously removed from the water as it boils underground. Work has been done monitoring the changes in hydrochemistry and isotopes

during exploitation of geothermal fields to provide estimates on the sustainability of the field (Prasetio et al., 2021).

Finally, stable isotopes of water and another compound, such as CH<sub>4</sub> or CO<sub>2</sub>, can be used to estimate the temperature underground. For example, if the hydrogen isotope composition of water and methane is measured at surface, and these are assumed to be in equilibrium, then the temperature of reaction can be estimated from the known change in fractionation factor with temperature. Several assumptions need to be fulfilled, but the method can be made more robust by using other geothermometers, such as oxygen isotopes in water and sulphate (Panichi and Gonfiantini, 1981).

## 6.7 Paleowaters

Paleowaters in groundwater include any water that was recharged under a different climate from the present one or formed under different environmental conditions to those now found at the site. For hydrogeologists, who are more concerned with circulating groundwater, waters involved with the genesis of rocks and minerals are generally of less interest as they are not an active part of the hydrological cycle and therefore do not represent a sustainable water resource. As such, connate water, formation water, juvenile water, interstitial water and crystallization water are excluded from the usual definition of paleowater.

Paleowater groundwater resources are called fossil aquifers and are sometimes used for water supply. An example is the Nubian Aquifer System of the eastern Sahara, shown in Figure 28. Roughly speaking, actively circulating groundwater is likely to be less than 10,000 years old, paleo groundwaters are in the range of tens to hundreds of thousands of years old, and connate, crystallization, formation, interstitial and juvenile waters are more likely to be millions to billions of years old.

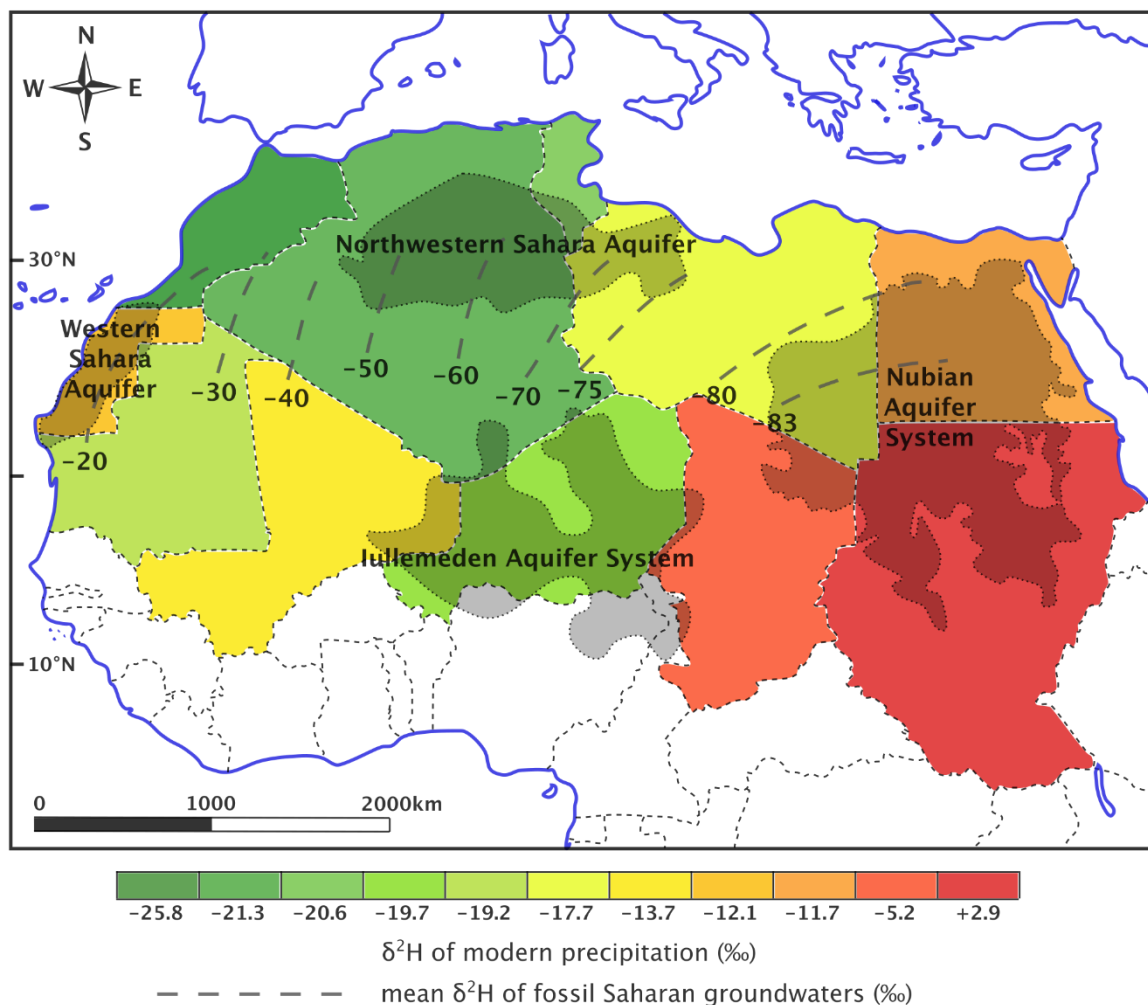


**Figure 28** - Contrast in isotope patterns for modern precipitation (shown by color-coded country outlines) versus paleowaters (shown by dashed contour lines) across the Sahara Desert. The west to east decrease in  $\delta^2\text{H}$  for paleowaters was used as evidence for an shift in westerly rain systems toward the equator during the last ice age (after Abouelmagd et al., 2012).

A common requirement for working on paleowaters is the ability to date the groundwater age. Tritium, although commonly used in young groundwater, is of no use in paleowaters as its half-life is too short (12.3 years). Carbon-14 (half-life 5730 years) is the most widely used dating method, but, as explained in another Groundwater Project book, *Introduction to Isotopes and Environmental Tracers as Indicators of Groundwater Flow* (Cook, 2020), this is far from simple. The quantity of  $^{14}\text{C}$  in the groundwater is given as pmc (percent modern carbon), from which the age can be calculated, however, there are complications which can cause this calculation give the wrong age. On the one hand the  $^{14}\text{C}$  can be removed by preferential precipitation or diluted by contributions of inorganic carbon dissolving out of the aquifer matrix, and on the other hand modern carbon can enter the system and mix with the old groundwater or contaminate the water during sampling. In general, therefore, although the analytical precision can theoretically date materials to 60,000 years, the uncertainties in the groundwater environment reduce this method's age maximum to around 30,000 years (Clark and Fritz, 1997; Fontes, 1981).

Other dating methods for paleowaters can also be used, for example  $^{36}\text{Cl}$  with a half-life of 301,000 years. This and other methods have advantages and disadvantages and have certain age ranges over which they may give reliable ages. Groundwater dating is a vast field and the reader is encouraged to consult other books on these topics, if they want to know more about it (Clark, 2015; Cook, 2020).

Although accurate groundwater dating is the surest way to know one is dealing with paleowater, discovering groundwater with a stable isotope composition different from groundwater known to be young, often alerts one to the presence of paleowater (Van Gelden et al., 2014). In most cases, the paleowater is in deeper, confined aquifers with little connection to unconfined aquifers with modern recharge (McIntosh et al., 2006), but there are instances where the geometry of aquifers and flow regime can result in the paleowater occurring at shallow depths (Malov and Tokarev, 2019).

Identifying the presence of paleowater from a difference in stable isotope composition with the young groundwater of the region is useful. One of its uses is to understand the sustainability of groundwater, because use of paleowater is generally assumed to be non-sustainable. This is because paleowaters were either recharged during a wetter climate and are not being recharged at all in the current climate, or are recharged very slowly, hence their great age, and therefore only sustainable at very low abstraction rates. Al-Charideh and Kattaa (2016) investigated groundwater in the regional, deep Cretaceous aquifer across western Syria, and were able to classify groundwater as renewable or semi-renewable when the stable isotope composition was similar to modern precipitation ( $\delta^{18}\text{O}$  of  $-7.0$  to  $-7.2\text{‰}$ ), or as non-renewable when the stable isotope composition was significantly more negative, suggesting recharge during a previous climate ( $\delta^{18}\text{O}$  of  $-8.0\text{‰}$ ). Additionally,  $^{14}\text{C}$  values for the latter groundwater were  $< 15$  pmc, confirming this as older groundwater.

A study by Smith and others (2002) in the Great Basin region (centered on Nevada, USA) identified locations where  $\delta^2\text{H}$  of groundwater was more than  $10\text{‰}$  lighter than winter precipitation. They proceeded to rule out sites adjacent to mountains, where the altitude effect could be the cause of the isotopically lighter groundwater values, and then classified areas as having possible paleowater ( $10$ - $19\text{‰}$  lighter) and probable paleowater ( $>20\text{‰}$  lighter), recharged during the Pleistocene.

In previously glaciated parts of the world where meltwater from receding glaciers recharged groundwater as the previous glacial period ended, differences in paleowater and modern groundwater isotope compositions can be large. However, in some cases the paleowater in far northern latitudes are not from glacial meltwater and can therefore have differences to modern waters that are similar to those in mid-latitudes or tropical areas. For example, in Germany, Van Gelden and others (2014) noted the similarity of modern precipitation ( $-9.8\text{‰}$  and  $-66\text{‰}$ ) and the shallow, unconfined aquifer ( $-9.6$  to  $-8.9\text{‰}$  and  $-68$  to  $-65\text{‰}$ ) compared to the confined Benkersandstein ( $-10.6\text{‰}$  and  $-74\text{‰}$ ) giving roughly a

1‰ and 10‰ difference in  $\delta^{18}\text{O}$  and  $\delta^2\text{H}$  respectively, between modern (shallow groundwater or precipitation) and paleowater. In contrast, in the Great Lakes region of North America, McIntosh and others (2006) found current precipitation and surficial aquifers to have  $\delta^{18}\text{O}$  of -7 to -4.5‰ in northern Indiana and Ohio, and -11 to -8‰ in northern Michigan, whereas the Silurian-Devonian carbonate aquifers were in the -13 to -15‰ range, exhibiting a difference of 5-10‰ in  $\delta^{18}\text{O}$ , as shown in **Figure 29**.

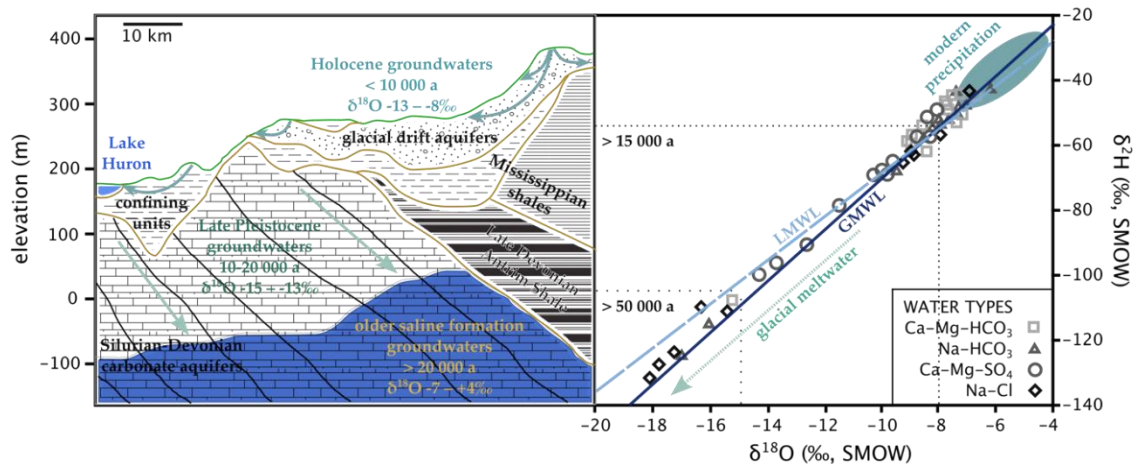


**Figure 29** - Groundwater regime and stable isotope systematics for northern Ohio and Indiana states in the USA, south of the Great Lakes. Various groundwater samples are plotted on the  $\delta^2\text{H} - \delta^{18}\text{O}$  graph according to their dominant dissolved ions. The estimated isotope composition for glacial meltwater ranges from -25 to -11‰ for  $\delta^{18}\text{O}$ . Stable isotope ranges for paleoprecipitation are shown as dotted boxes with associated ages. The  $\text{CaMgHCO}_3$  waters are associated with the shallow, unconfined glacial drift aquifers and tend to have stable isotope values somewhat more negative than modern precipitation, but plotting close to the LMWL and GMWL. The other water types are found in confined aquifers, at depth, and their chemistry is influenced by rock dissolution and mixing with formation brines. The existence of isotopically very negative groundwater at shallow depths in the Silurian-Devonian carbonate aquifer suggests this groundwater was recharged by melting glaciers at the end of the last ice age and is largely isolated from modern recharge by aquitards (after McIntosh et al., 2006).

In much of the southern interior of Canada and parts of the northern plains of the USA, there is abundant paleowater within the Quaternary deposits overlying bedrock. As the Pleistocene glaciers were melting (about 10,000 to 20,000 years before present), run-off from these glaciers formed lakes with deposits rich in silt and clay across broad plains. These deposits have exceptionally low permeability (with thicknesses from 5 to 40 m) and function as aquitards with the water table positioned near the ground surface. Studies of these aquitards show that where the thickness is greater than ~20 m, the groundwater is comprised mostly or entirely of water derived from the Pleistocene glaciers (**Figure 29**). This conclusion is based on stable isotopes indicated by cold weather isotopic signatures.

One of the most extensive deposits of these glacial lake sediments occurs in Manitoba, Canada, and extends southward into North Dakota, USA. A uniform oxygen isotope value of -25‰ was obtained at depths of 20 to 30 m in a thick deposit of clay found in the southernmost part of the glacial Lake Agassiz plain (Remenda et al., 1994). The lake occupied parts of North Dakota and southern Manitoba at the end of the last glacial

maximum and received water from the ice margin and the interior plains region of Canada. The value of  $-25\text{‰}$  is characteristic of meltwater impounded in the southern basin of Lake Agassiz. This value corresponds to an estimated mean air temperature of  $-16\text{ °C}$ , compared with the modern mean air temperature of  $0\text{ °C}$  for this area.

Groundwater from thick, late Pleistocene-age clay deposits elsewhere in Canada shows the same uniform oxygen isotope value at similar depths, including a glacial till in southern Saskatchewan and a glaciolacustrine deposit in northern Ontario. These aquitards are at about  $50\text{ °N}$  latitude, span a distance of 2000 kilometers, and like the Lake Agassiz sites, have a groundwater velocity of less than a few millimeters per year. Hence, there is a substantial volume of this paleowater in the southern interior regions of Canada, but almost all of this water occurs in aquitards where flow rates are minimal, rather than in aquifers. This is because water of glacial origin, that initially filled the aquifers, has flushed out since the glaciers disappeared. An exception is the regional aquifer beneath the lake sediments in southwestern Ontario where the aquitard is an effective cap, impeding the flow of paleowater (Husain et al., 2004). The glacial age of these paleowater occurrences has been confirmed by carbon dating. However, given the characteristically negative stable isotope values for the paleowater in this region, the most cost-effective method for dating paleowater is through the use of stable isotopes.

The differences in stable isotope composition for modern water and paleowater may be known in a region. Sultan and others (2000) applied such regional knowledge to the unconsolidated aquifers close to the Nile River, south of Cairo, near Wadi El Tarfa. These aquifers had  $\delta^{18}\text{O}$  of  $-2$  to  $+5.2\text{‰}$  and  $\delta^2\text{H}$  of  $-10$  to  $+34\text{‰}$ , which ruled out upwards leakage from the Nubian Aquifer, known to have mean values of  $-11\text{‰}$  and  $-80\text{‰}$ , respectively (Figure 30). They concluded that recharge of the shallow aquifers was from flash flood events with rare, but appreciable recharge into coarse sediments and fractured rock underlying alluvial channels. As such, these aquifers can be sustainably used, if the frequency and magnitude of recharge from these events is known.

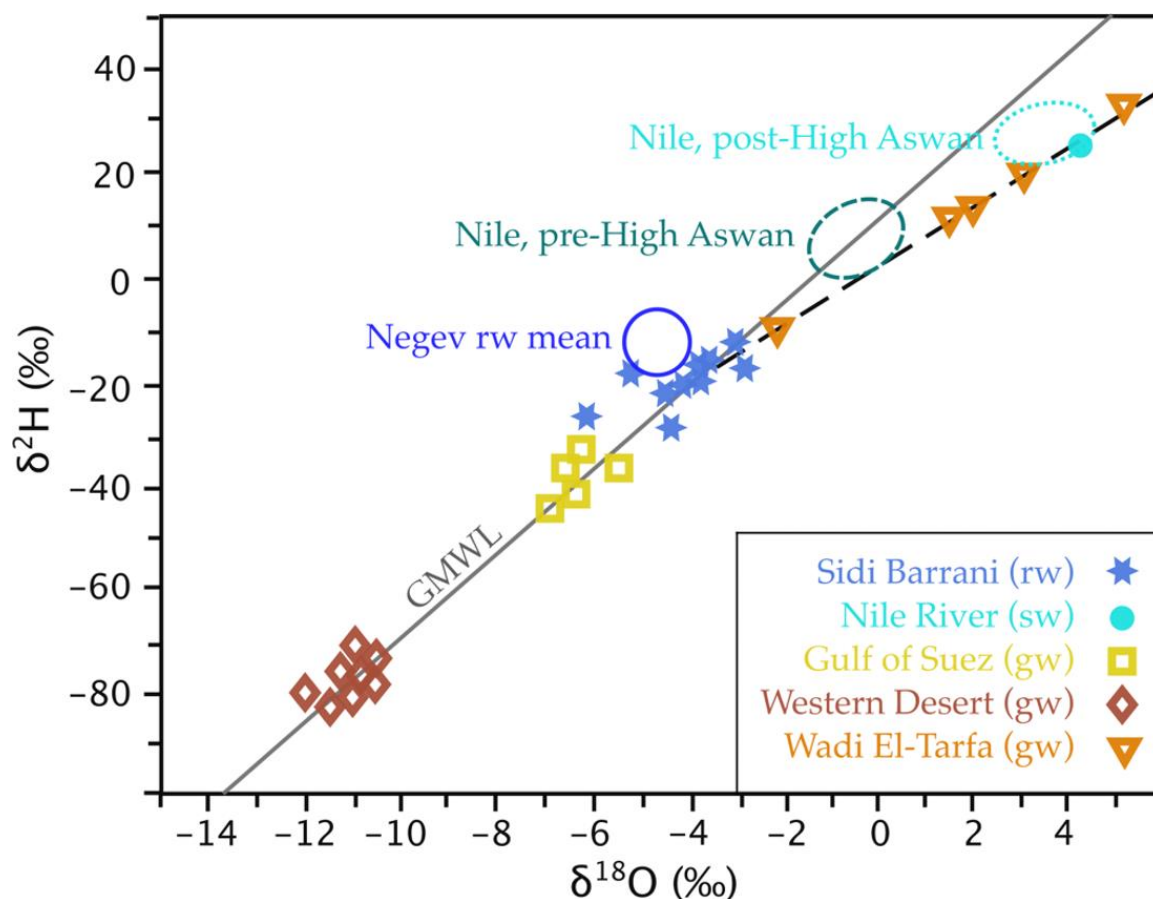


**Figure 30** - Stable isotope analyses of various waters in Egypt and rain from the Negev Desert in Israel, with the GMWL and a trend line for Wadi El-Tarfa groundwater, in order to determine the likely source of Wadi El-Tarfa groundwater. Upwards leakage of paleowater from the Nubian Sandstone Aquifer of the Western Desert was ruled out due to its lighter isotope composition. The position of the Wadi El-Tarfa samples below the GMWL is suggestive of evaporation. The dashed trendline has a gradient of 5.7, indicating evaporation from an open water body, such as a temporary pond after heavy rain. The extrapolation of the trendline into the cluster of Sidi Barrani rain water suggests evaporated modern rainfall recharges the Wadi El-Tarfa groundwater, meaning abstraction is potentially sustainable at a rate similar to the recharge (after Sultan et al., 2000).

In nearby Libya, Al Faitouri and Sandford (2015) conducted a survey of three sandstone aquifers within the Nubian Aquifer System, to establish paleoclimatic and recharge dynamics. However, the stable isotope characteristics of these three aquifers can also be used to detect leakage or mixing of groundwater, by monitoring the pumped groundwater for changes in stable isotope composition over time. Initial results suggest that younger groundwater is being incorporated into the deeper aquifers as the potentiometric head of the deeper aquifers has been lowered and therefore flow induced from the shallower, younger groundwater.

Work on the Nubian Aquifer System, as well as other paleowaters in the Saharan region, has extended to paleoclimatic reconstruction. Using d-excess values calculated by Sonntag and others (1979) for 20,000-year old groundwater beneath the Sahara, Merlivat and Jouzel (1979) were able to, with the aid of an isotopic precipitation model, calculate the humidity under which evaporation took place over the ancient ocean, finding a result of 90 percent as compared to 80 percent for the current climate. Abouelmagd and others (2012)

showed how the average modern precipitation can get isotopically heavier from west to east (W to E), but the paleowater gets isotopically lighter from W to E (Figure 28). However, some modern rain events show isotopic depletion from W to E, matching the fossil groundwater. These were produced with westerly winds and so it was inferred that the paleoclimatic recharge was due to the westerlies (mid-latitude cyclones or frontal depressions) shifting toward the equator during the previous ice age.

In contrast to the findings in the Sahara, Plummer and others (2012) found high D-excess values for paleowater in the vicinity of Chesapeake Bay, USA, indicating lower relative humidity during moisture formation (Figure 31). This is consistent with the colder temperatures and icy conditions expected over mid-latitudes during glacial periods. The higher humidity detected for paleowater recharge conditions over the Sahara and the lower humidity over the American mid-latitudes agree with the general model that current polar conditions (cold and dry) occupied mid-latitudes and current temperate conditions (wet and rainy) occupied low latitudes during the previous ice age.

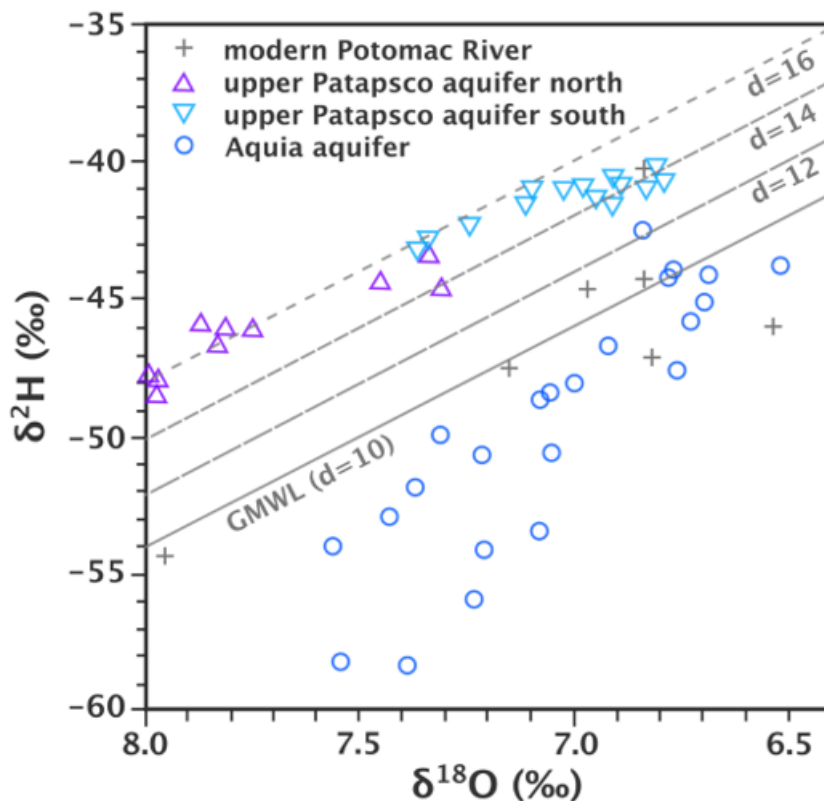


**Figure 31** - Stable isotope values for groundwater from various aquifers in the Chesapeake Bay region. Distinct groups are apparent for the various aquifers, reflecting differences in climate, and particularly the  $d$  values, which is an indicator of the humidity level in the region that provided the moisture source. Higher  $d$  values indicate lower humidity in the moisture source region (after Plummer et al., 2012).

Stable isotopes of groundwater may also be used indirectly in paleoclimatic and other reconstructions. Andrews (2006) provides a review of the use of groundwater-fed riverine tufas (carbonate deposits) for these purposes. The method used the  $\delta^{18}\text{O}$  of the

carbonates, corrected for fractionation at the temperature of precipitation from water, to determine the  $\delta^{18}\text{O}$  of the groundwater at recharge. High resolution sampling of tufas (sub annual scale) tends to provide more information on the temperature of precipitation (precipitation), whereas decadal scale sampling gives more information on the groundwater isotope composition, and is susceptible to the well-known isotope effects of continentality, amount and temperature. These allow some inference regarding the types of events responsible for groundwater recharge. For north-western Europe, tufas revealed centennial scale cooling prior to the end of the last ice age, reaching a minimum temperature around 8200 years before present. Tufas are therefore a good alternative or complement to paleoclimatic methods using speleothems.

Canavan and others (2014) performed analyses of the  $\delta^2\text{H}$  of volcanic glass in the central Andes. Primary volcanic glass has only 0.1-0.3 weight percent  $\text{H}_2\text{O}$ , whereas after hydration (thousands of years) the glass contains about 5 weight percent  $\text{H}_2\text{O}$ , and the hydration seals in the isotopic content of the hydration water with a layer of "silica gel". This means the hydrogen is largely sourced from meteoric water and the original  $\delta^2\text{H}$  of hydrating water can be calculated after applying the fractionation factor for glass- $\text{H}_2\text{O}$ . With this paleowater  $\delta^2\text{H}$  signature, and applying known altitude isotope gradients, the elevation at the time of eruption (given that hydration is achieved shortly thereafter) can be calculated. This in turn can be used to infer uplift rates and continental geodynamics of a region.

It should be apparent that stable isotopes of paleowater, and associated materials (e.g., speleothems, tufas, volcanic glasses) are a mine of potential information. However, the corrections and complexities require attention, to avoid misinterpretation. Geological dating, in particular, is very useful in this area, but attention to fractionation, mixing, dilution and other factors is necessary. As is often the case, use of hydrochemistry or other isotope systems can assist in painting a fuller picture.

## 6.8 Plant Waters

Plants use water in their leaves, (and sometimes stems and other parts) for photosynthesis to create simple sugars and in turn all the compounds in their structure. They obtain this water, and a mixture of nutrients dissolved in the water, from the soil by absorption into their roots (Dawson et al., 2002). Describing this as use of soil water is an oversimplification. In fact, water for plant use is available from many sources, including surface water (e.g., as used by rice, mangroves, riparian plants), water in the vadose zone (e.g., water adhered to soil particles, gravitational water, and capillary water), as well as groundwater in the phreatic zone. This is further complicated by the fact that, with time, these sources may merge, separate or dry up.

Stable isotopes of H and O provide a way to discover which pools of water are being used by plants, and have the added advantage of being fairly inexpensive to analyze (especially with laser cavity instruments) and requiring small samples, therefore causing less disturbance to the soil and plants (Ehleringer and Dawson, 1992).

Caution is necessary with the use of the IRIS (isotope ratio infra-red spectroscopy) or laser instruments, as trace quantities of organic compounds in plant waters may distort the analysis and produce errors of more than 10‰ for both  $\delta^2\text{H}$  and  $\delta^{18}\text{O}$ . Adequate filtration to remove organic contaminants is necessary (West et al., 2010).

The basic principle of the method is to measure the isotope compositions of plant waters and potential source waters then compare the  $\delta$  values to determine which pool of water the plant is using. Although this approach may work in simple situations, research over the last 40 years has shown there are many complications that may require unravelling. For example, most earlier studies assumed there was no fractionation during water uptake at the roots (Dawson and Ehleringer, 1991; Ehleringer and Dawson, 1992), although Alison and Hughes (1983) noticed fractionation and ascribed it to a 2-stage process of soil water evaporation followed by root uptake of the vapor with its evaporated isotope signature, leaving isotopically heavier water in the soil. More recent studies, have shown there is appreciable fractionation, up to 10‰ for  $\delta^2\text{H}$  (Ellsworth and Williams, 2007), correlated with the strength of the halophytic character of a species, or the magnitude of salt stress experienced by an individual plant (Gat et al., 2007). Non-halophytic plants may also display fractionation during water uptake, but this is dependent upon soil type and, again, the drier the soil, the more fractionation (Vargas et al., 2017). It is fairly clear that fractionation between the soil and the plant is mainly a concern in dry or salty environments, typical of deserts or in areas that experience seasonal droughts.

Large variation has also been noted in the isotope composition in different parts of the plant. This is to be expected, especially near the leaves, where transpiration causes large fractionation effects. The degree of fractionation is correlated with the transpiration rate, which is in turn influenced by higher temperature and precipitation (Pan et al., 2020) and lower relative humidity or dry conditions (Yakir et al., 1990; Bodé et al., 2019). As a result, there will be a variation in isotope composition between the water in a plant's leaves and elsewhere in the plant, with a range of  $\delta$  values occurring as water in the stems mixes with the fractionated leaf water. Also, over time, as transpiration varies, the degree of fractionation in the leaves will vary, and therefore any part of the plant exposed to fractionated water in the leaves will also vary. For example, Goldsmith and others (2018) found the variation in  $\delta$  values within one tree to be similar to that between different trees.

Because of these complexities, a simple 2-point model with soil water and groundwater at each end, and one value for plant water which hopefully sits on the mixing line between the 2 source waters, is often not applicable. Instead, models have been developed to incorporate this complexity, whether it be calculation of soil water  $\delta$  values

(Goldsmith et al., 2018), incorporation of species-specific traits (Yakir et al., 1990), transpiration and leaf- and soil-water potentials (Cook and O'Grady, 2006) (Figure 32) or tree-water deficit, fine root distribution and soil water potentials (Nehemy et al., 2020). The choice of model then becomes a factor to consider in this kind of work (Wang et al., 2019).

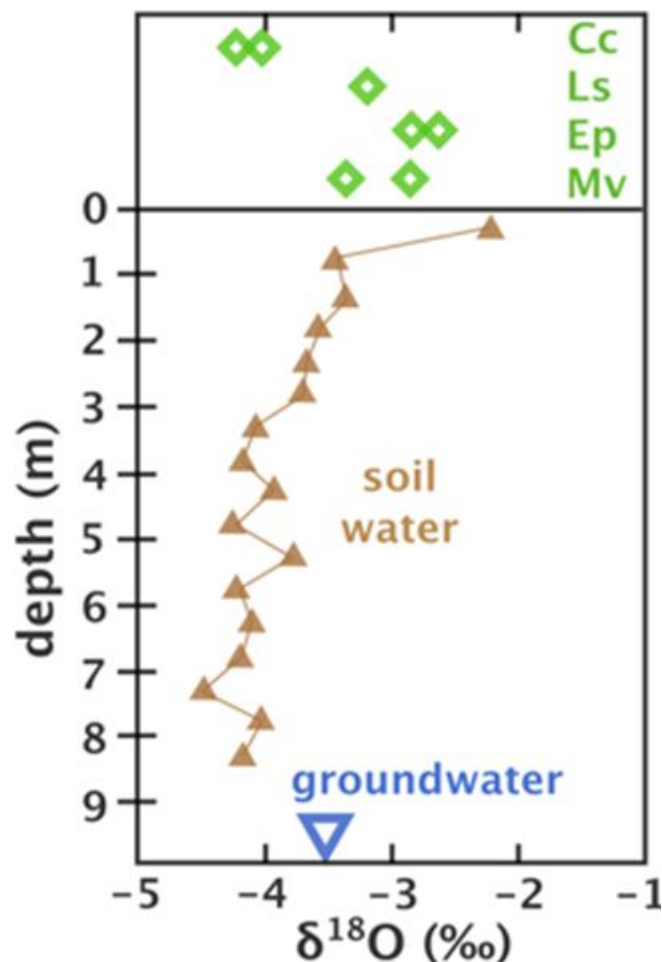


**Figure 32** - Stable isotope values for groundwater, soil water and leaf water in 4 species of tree in northern Queensland, Australia. Cc = *Corymbia clarksoniana*, Ls = *Lophostemon suavolens*, Ep = *Eucalyptus platyphylla*, Mv = *Melaleuca viridiflora*. The stable isotope values were used in conjunction with transpiration rates, leaf and soil water pressure potentials to estimate the proportions of soil water and groundwater used by the 4 species (after Cook and O'Grady, 2006).

In spite of these challenges, stable isotope studies of plants have wide application in agriculture and forestry (Penna et al., 2020) and have produced some important findings, such as the proportions of groundwater versus soil water use (Dawson and Ehleringer, 1991; Cook and O'Grady, 2006), surface water versus soil water use in rice (Mahindawansa et al., 2018). They have also made it obvious that much care needs to be taken when using  $\delta^{18}\text{O}$  values in old or fossilized plant material to determine paleoclimates (Gat et al., 2007).

## 7 Case Studies

Some examples of the application of stable isotopes to groundwater are included here. Most of these examples include work with precipitation and surface water, emphasizing how, in most cases, groundwater work involves aspects of the rest of the water cycle. The excerpts from these studies are brief, merely to illustrate the concept. Before implementing these methods, it is important to read more widely about the topic, including reading of the full article used for the example.

### 7.1 Moisture Source Region

Uemura and others (2012) monitored precipitation weekly on Okinawa Island, to the south of Japan. They found a negative correlation between air temperature and  $\delta^2\text{H}$  and  $\delta^{18}\text{O}$  values, which is the converse of the usual positive correlation where temperature and  $\delta$  values decrease in concert (Figure 33). The reason for this negative correlation was related to the source regions for precipitation, which had a greater effect on the isotope composition than temperature at the precipitation site. In summer, precipitation has lower  $\delta$  values than in winter. When considering atmospheric circulation, they noticed that summer precipitation is sourced from a distant oceanic location, allowing greater rainout and therefore more negative  $\delta$  values. Winter precipitation is sourced by local evaporation from the warm Kuroshio Current into dry Asian continental air, allowing little rainout prior to precipitation at the site. The higher D-excess values for winter are also typical for evaporation into drier air. The finding that precipitation on Okinawa has different sources in winter and summer may be important when predicting how climate change may affect precipitation and therefore water resources on the island.

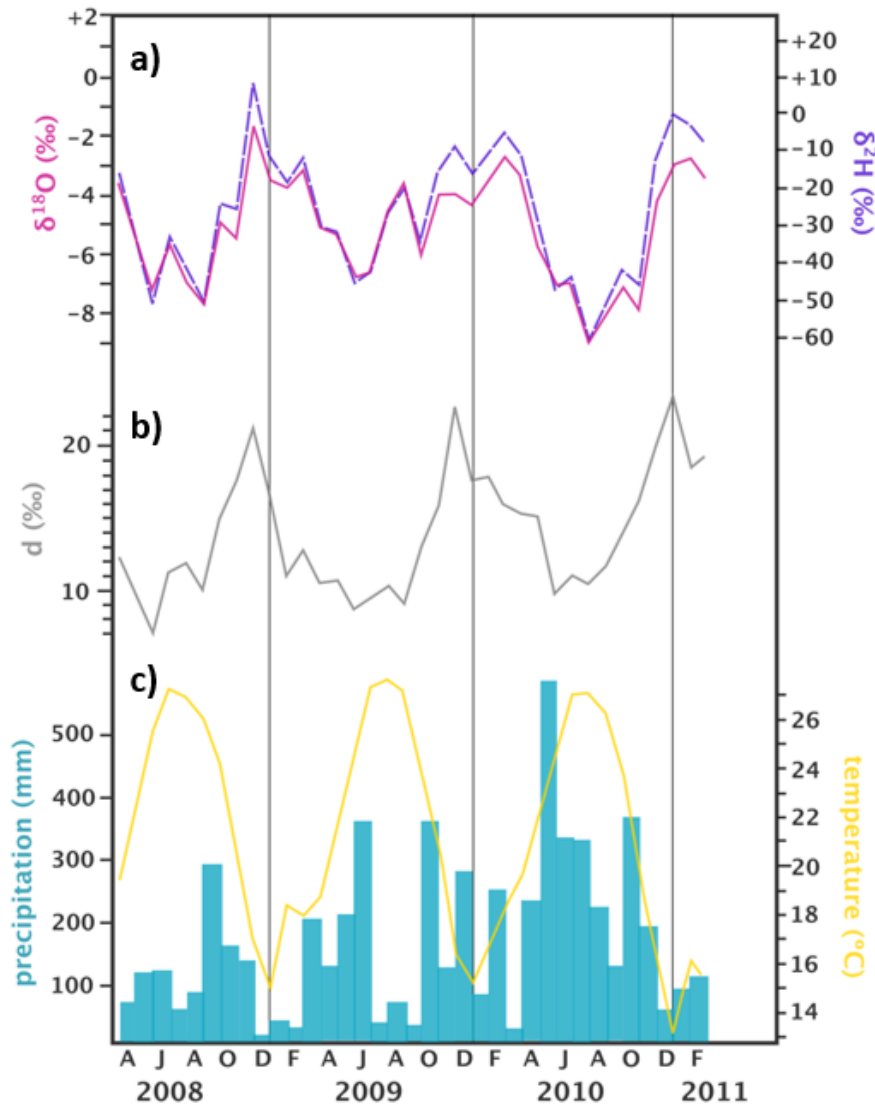


**Figure 33** - Graphs of a)  $\delta^2\text{H}$  and  $\delta^{18}\text{O}$ , b) d-excess and c) precipitation and temperature over a 3-year period on Okinawa Island. The negative correlation between T and  $\delta$  values is caused by differences in moisture source region for summer and winter, and the degree of rainout as moisture travels from those different regions to the island (after Uemura et al., 2012).

## 7.2 Recharge Area

Diamond and Harris (2000) made a study of the hot springs (Figure 34) in Western Cape, South Africa, including collection of precipitation near springs. They found the stable isotope values of the springs to be significantly more negative than the rain falling on the ground near each spring (Figure 35). Isotope exchange with rocks was ruled out due to the relatively low temperature of the spring water (the maximum being 64 °C), thus a deep, long flow path through the fractured quartzites of the Table Mountain Group was postulated. The flow paths for each spring included recharge at high altitude (up to 2000 m), which could explain the relatively negative isotope compositions, caused by the altitude effect. The postulated high elevation of recharge was consistent with a high head required to drive a long flow path with deep circulation that could heat meteoric water to

the spring water temperatures. The existence of long groundwater flow paths is important for protecting recharge areas because any impact on the water source may not be observed at the discharge location until many years later.



**Figure 34** - The Citrusdal hot spring (43 °C) in the Cape Fold Belt of South Africa. Groundwater flows through the Cape Supergroup in fractures and in some cases circulates deeply enough for water to be heated. This photograph shows one of the discharge points of the spring - several other fractures within a few meters of this point also discharge hot water.

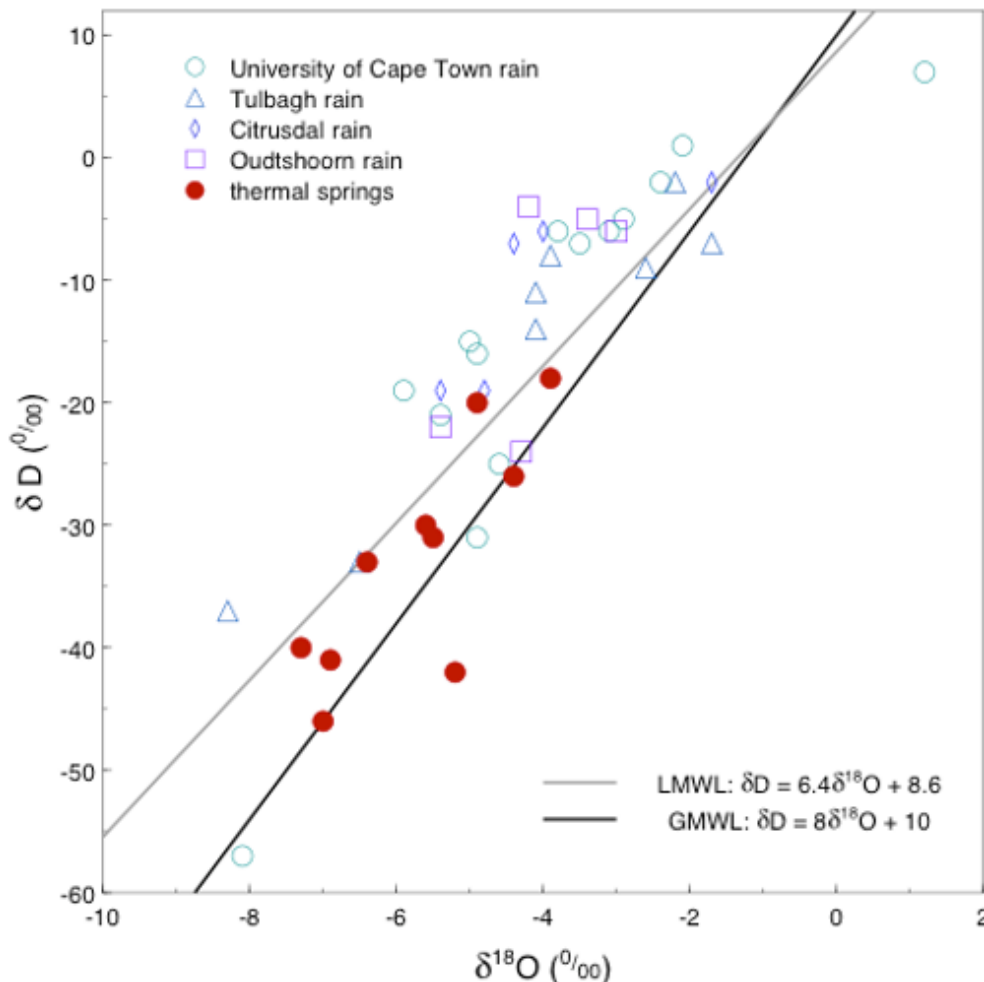


**Figure 35** - Stable isotope compositions of cumulative monthly precipitation samples from 4 precipitation stations and single samples or averages of monthly samples from the thermal springs of the Cape Fold Belt in South Africa. The tendency of the spring water to have lighter isotopic composition suggests recharge at higher altitude, made possible by deep groundwater circulation through large fold structures, which have wavelengths of many kilometers. Data from Diamond and Harris (2000), LMWL from Harris and others (2010) and GMWL from Craig (1961).

### 7.3 Selective Recharge of Heavy Rains

Vogel and Van Urk (1975) sampled groundwater and precipitation in the semi-arid interior of southern Africa. They found stable isotopes in precipitation were highly variable, whereas stable isotopes in groundwater of each region was quite consistent. Further, the groundwater tended to be more isotopically negative than precipitation, indicating that recharge took place during precipitation events with more negative  $\delta$  values, which are typically the larger rainfall events (as per the amount effect). Similar findings have been made by many workers, for example Dogramaci and others (2012) for another semi-arid region, the Pilbara in Western Australia (Figure 36) and Li (2018) near Beijing in China. Gat (1996) termed this phenomenon "selection".

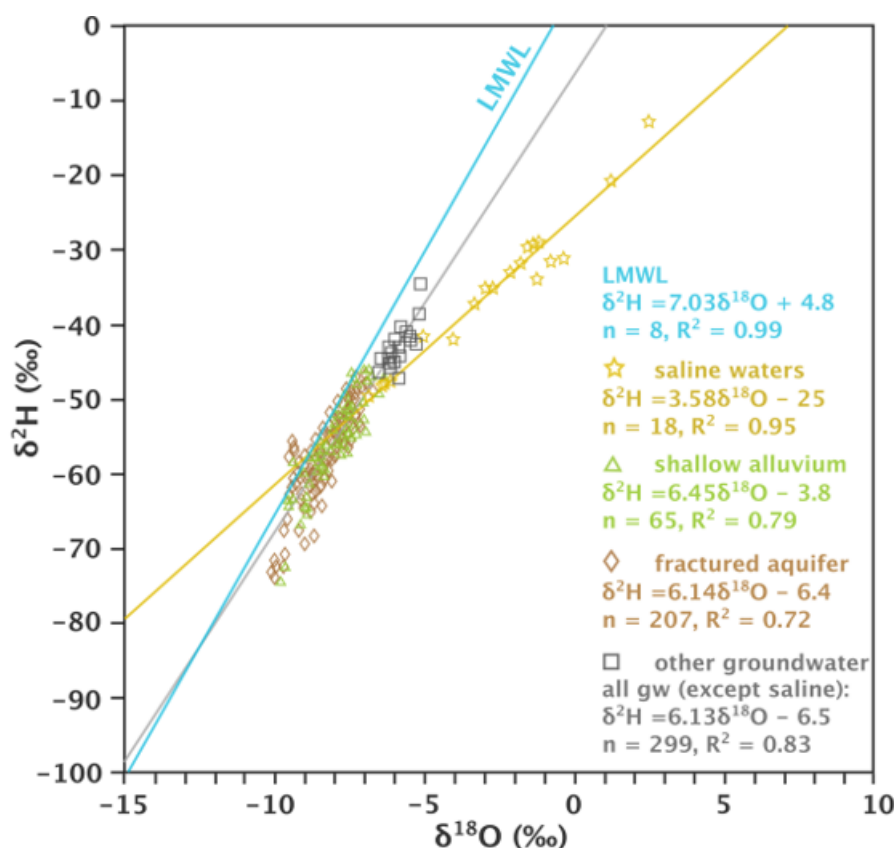


**Figure 36** - Stable isotope data for the Hamersley Basin in Western Australia. The LMWL was calculated for only larger rainfall events (> 20 mm). The near coincidence of this line with the data from shallow alluvium and fractured rock aquifers suggests recharge for these aquifers is during large precipitation events. The low gradient of the saline waters line is evidence for substantial evaporation of these waters, providing evidence that the salinity is from concentration of salts resulting from the evaporation process. The ultimate source of the salts, from rock weathering or marine aerosol, would have to be proven by evaluating the balance of salts, such as dominance of bicarbonate over chloride, or magnesium over sodium (after Dogramaci et al., 2012).

## 7.4 Recharge Estimation

Yidana and others (2016) evaluated water fluxes through the vadose zone in the Nabogo catchment of the White Volta Basin, Ghana. They sampled rain, surface water, pore water (vadose zone) and groundwater (phreatic zone) and analyzed these samples for their stable isotope composition and chloride content (Figure 37). They used Cl mass balance to estimate the fraction of infiltrating water remaining at each sampling interval and therefore estimate evapotranspiration (ET). The Cl content was still changing at their maximum sampling depth of 3 m, suggesting there is more ET taking place at greater depths. Their estimated recharge was 13 to 20 percent of precipitation. They also used differences in the stable isotope composition of phreatic zone groundwater, vadose zone porewater and precipitation to estimate evaporation, according to the Craig-Gordon model (1965) as outlined by Dogramaci and others (2015), which was found to be about 40 percent of precipitation. This suggested that transpiration makes up 40 to 47 percent of the water losses prior to recharge (i.e., with 13 to 20 percent of precipitation recharged and 40 percent

evaporated, then the remainder (40 to 47 percent) is transpired by plants). The use of Cl mass balance is sufficient to estimate total ET and hence recharge, but when combined with an evaporation-only estimate based on stable isotopes, transpiration can also be calculated.

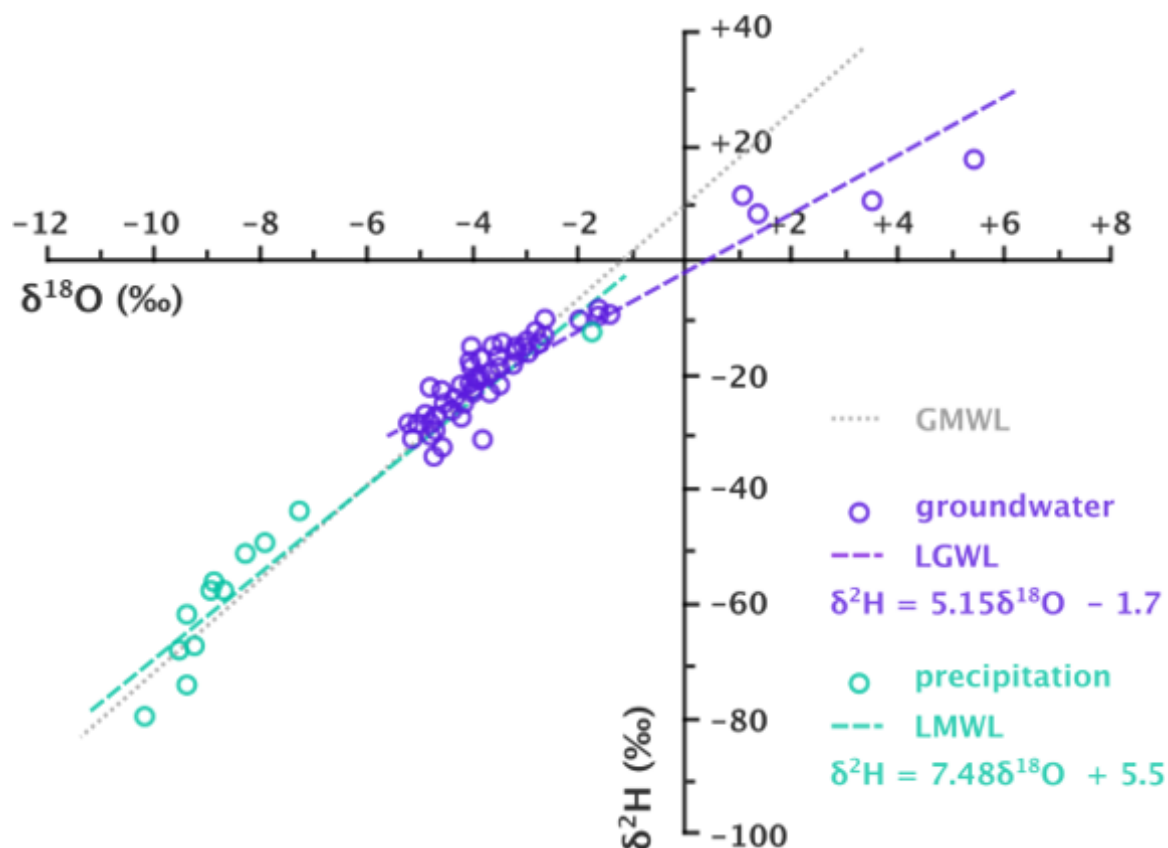


**Figure 37** - Stable isotope values from the Nabogo catchment in the White Volta Basin of Ghana. Distinct clustering of the precipitation and groundwater, and the low gradient of the groundwater trendline (LGWL) is strong evidence for evaporation of precipitation prior to recharge of groundwater (after Yidana et al., 2016).

### 7.5 Piston Flow of Groundwater During a Storm

Midgley and Scott (1994) conducted a study of streams in the Jonkershoek area near Cape Town, South Africa, where they collected stream water and precipitation samples simultaneously. Interestingly, they found that although the streamflow rose as the rain event proceeded, the stable isotope composition of the stream water did not match that of the rain (Figure 38).

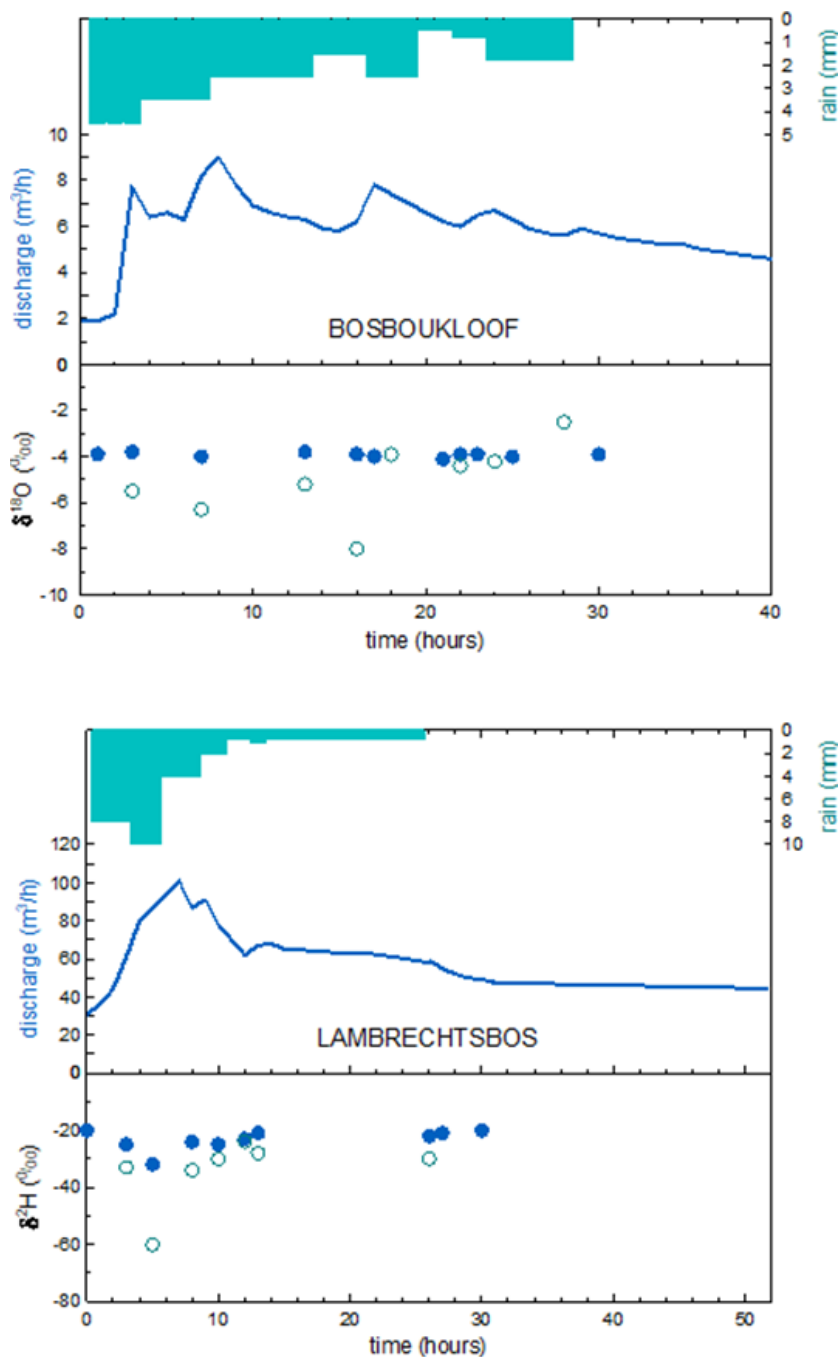


**Figure 38** - Stable isotope data for stream water (solid circles) and precipitation (open circles) in relation to a precipitation event and associated streamflow. The lack of correspondence of the streamflow isotope composition to the precipitation suggests groundwater as the source of streamflow, especially at Bosbukloof where the stream discharge isotope composition is steady. Lambrechtsbos stream water shows some change in isotope composition toward the isotopic composition of the precipitation early in the precipitation event, suggesting either runoff or recent interflow is contributing to the total streamflow during that period (after Midgley and Scott, 1994).

Using the stable isotope compositions and a mass balance approach, they determined that < 5 percent of the streamflow was direct precipitation runoff. They did not take groundwater samples, but rather assumed that the streamflow prior to the rain event was purely baseflow and therefore representative of the groundwater. As discussed in

Section 6.5 “Hydrograph Separation”, this assumption is not always valid. Nonetheless, they concluded groundwater was being driven, in a piston flow fashion, by the recharging precipitation, towards the stream and discharging at increased rates during the precipitation event (Figure 39).

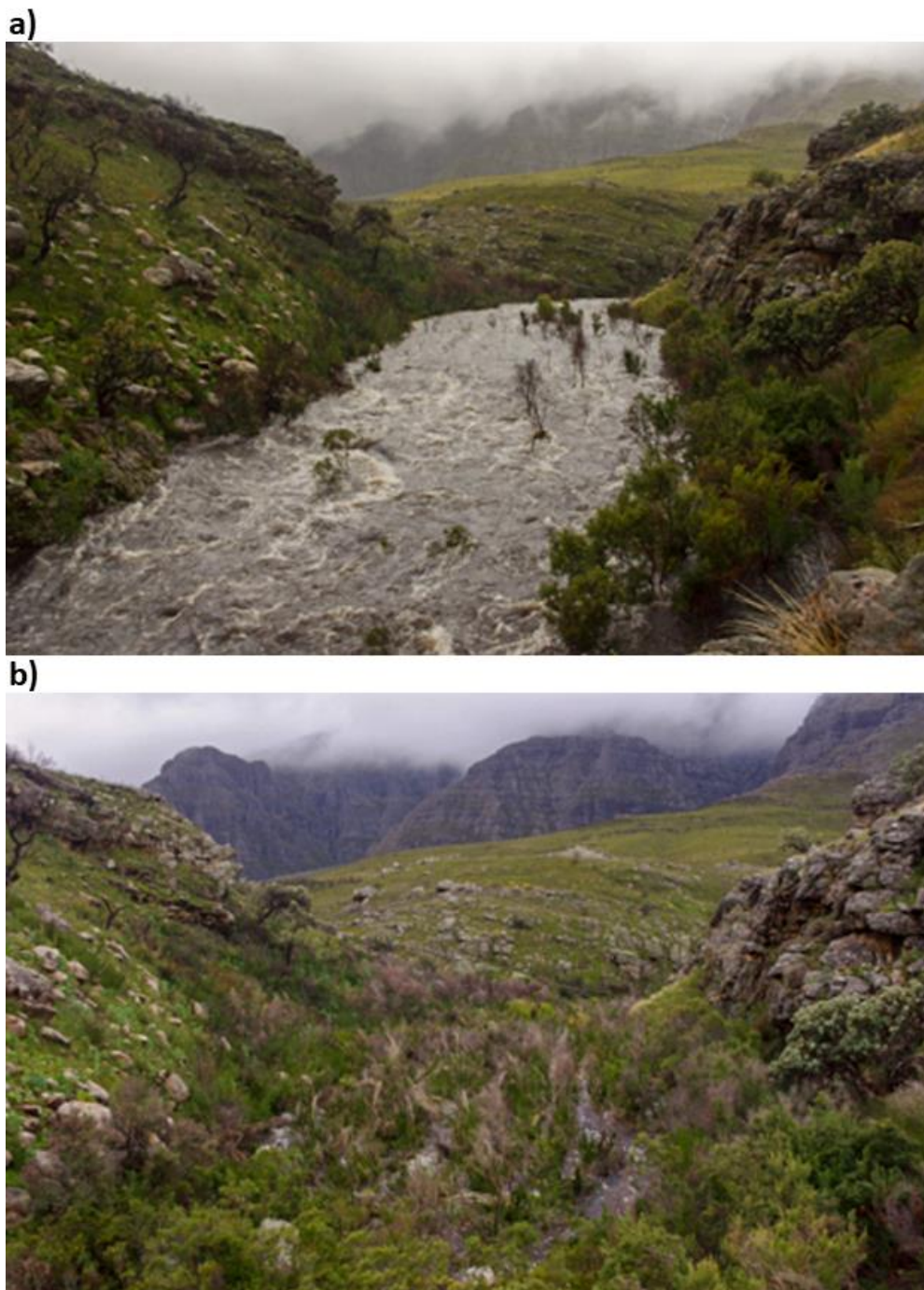


**Figure 39** - The Elandspad River, Western Cape, during a) and after b) the passage of a cold front of the South Atlantic Ocean in July 2012. The two pictures were taken 16 hours apart. In the nearby Jonkershoek catchment, Midgley and Scott (1994) found stable isotopes of the flood flow matched that of groundwater and not precipitation, suggesting that rapid increase of baseflow from fractures in the quartzite of the Table Mountain Group were largely responsible for the flood peak.

## 7.6 Groundwater Circulation and Age

Yin and others (2011) measured stable isotope ratios in groundwater and lake water in the Habor Lake Basin of the Ordos Plateau in north-central China. Their results for the groundwater hydrochemistry revealed a range of ionic compositions, but no clear separation between aquifers. The stable isotope values, however, varied according to depth, with the deepest samples (up to 300 m) showing the most negative isotope values (Figure 40). Shallow Cretaceous aquifer groundwater and Quaternary aquifer groundwater have values between modern precipitation and modern lake water. This suggests substantial evaporation prior to recharge, as the lake water represents a highly evaporated isotope composition. The deep Cretaceous aquifer groundwater was probably recharged during the wetter climate of the glacial period at the end of the Pleistocene, during which the precipitation would have been isotopically lighter than the present, and evaporation would have been less during recharge, because of the cooler, more humid conditions than today.

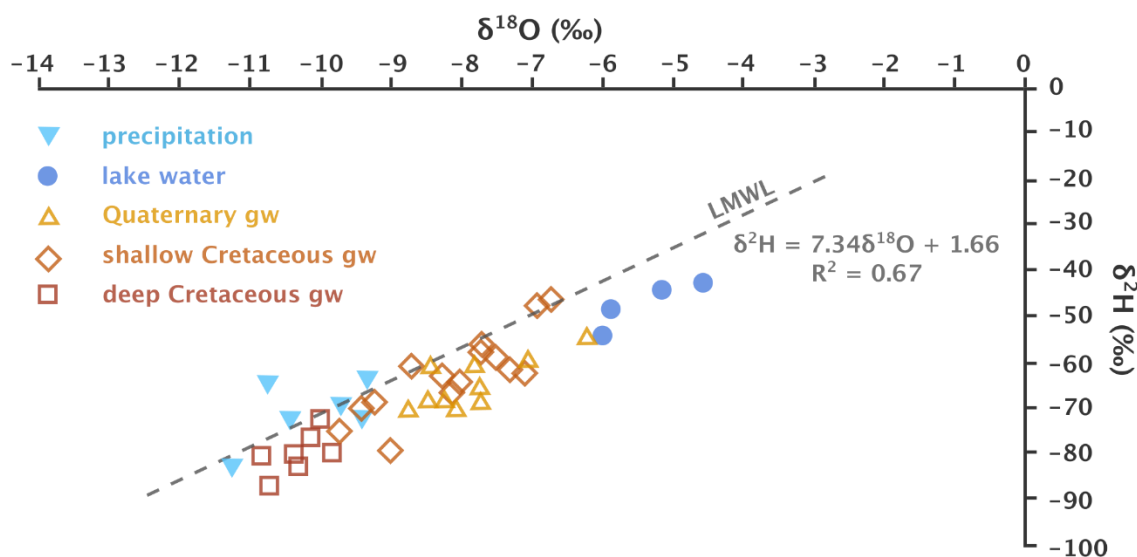


**Figure 40** -  $\delta^2\text{H}$  -  $\delta^{18}\text{O}$  diagram for water samples from the Lake Habor area in north-central China. Differences in the stable isotope composition of shallow and deep groundwater, and comparison with precipitation and lake water allow inferences to be made about the age and recharge conditions of the various groundwaters as explained in the text of Section 7.6 (after Yin et al., 2011).

## 7.7 Detecting Surface Water in Groundwater

Grimmeisen and others (2017) conducted a multi-tracer study, using chemical parameters (especially  $\text{Cl}^-$  and  $\text{NO}_3^-$ ) and the stable isotopes of H, N and O, in and around the city of As-Salt in Jordan (Figure 41). The stable water isotopes alone provided good evidence for leakage from various possible "surface water" sources, in this case human sources such as water mains and sewers. The distinctive isotope composition of these urban water sources is due to the city's water supply being the King Abdullah Canal, fed largely from highly evaporated surface water in Lake Tiberias and the Yarmouk River, with only

a portion from the Mukheiba wells. Mixing with local groundwater is apparent in some of the boreholes that were monitored, with a seasonal fluctuation in locations where leakage from urban water sources affects some of the local groundwater more in the dry summer (May to November) and less in the wetter winter. The mixing line allows estimation of the proportion of leakage water comprising local groundwater, which the authors calculated as up to 70 percent.

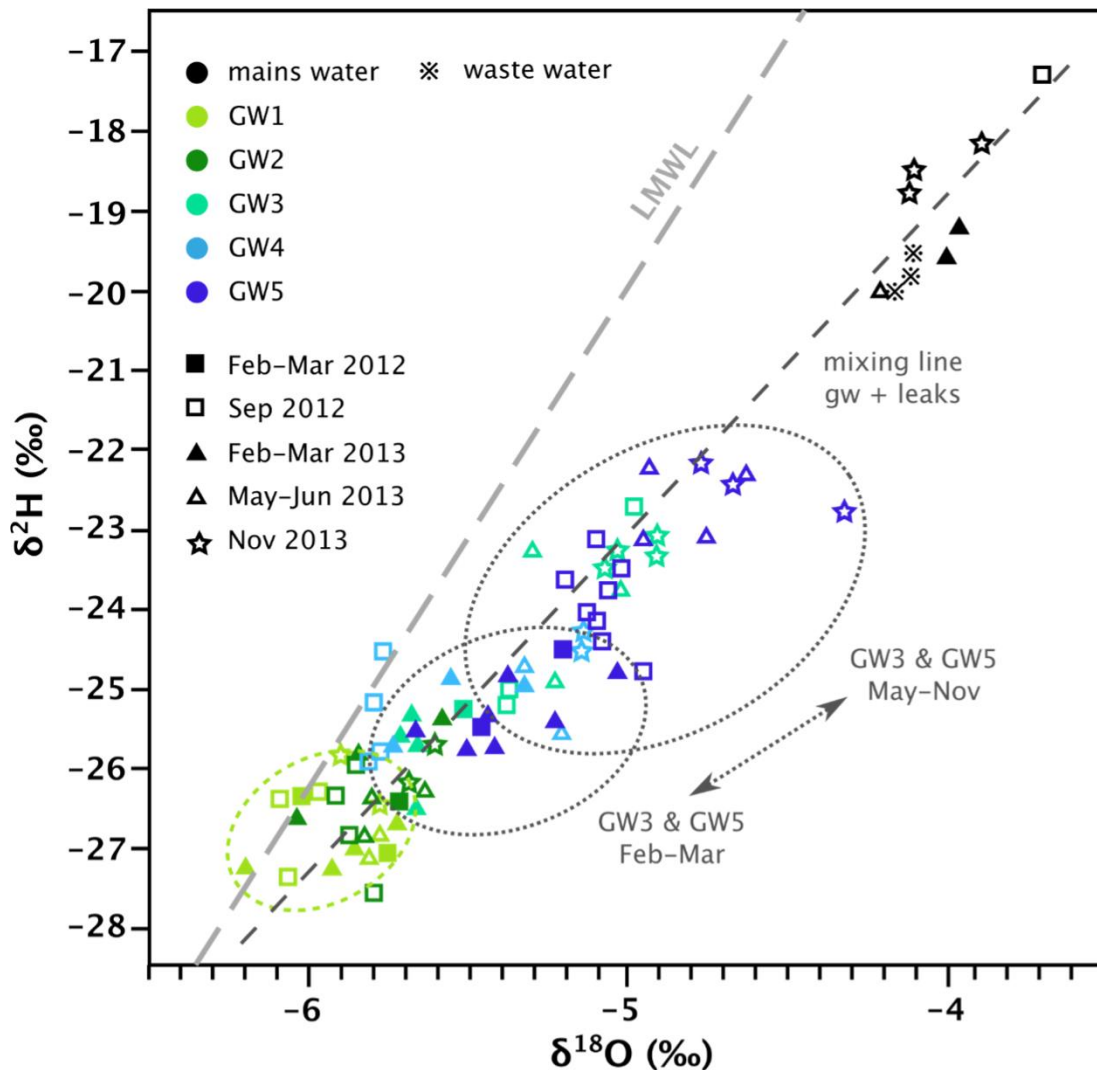


**Figure 41** - Isotope composition of various groundwater sources (GW1-5) and the urban water (clean water and waste water) over several seasons at As-Salt, Jordan. The changes in groundwater from unmixed/fresh (GW1-2) to the most mixed/polluted (GW3 & GW5 in May-Nov) is revealed by the change in stable isotope composition, which can be used to estimate leakage (after Grimmeisen et al., 2017).

Sunguro and others (2000) undertook a study of groundwater in the dolomites of the Mcheka Formation of the Palaeoproterozoic Lomagundi Belt in northern Zimbabwe, known informally as the Lomagundi dolomites. Spring water had relatively negative  $\delta$  values, compared to precipitation, indicating recharge during heavy precipitation events (as discussed in Section 7.3 "Selective Recharge"), whereas boreholes, particularly those in

areas of active irrigation, tended to have water with more positive  $\delta$  values, suggestive of evaporative isotope enrichment and therefore irrigation return flows to the aquifer. This further highlights the vulnerability of the aquifer to pollution by agricultural waters.

## 7.8 Detecting Groundwater in Surface Water

Camacho Suarez and others (2015) used stable isotopes in combination with hydrochemistry to compare water types and discharge rates in the Kaap catchment, Mpumalanga, South Africa. They made use of multi-component hydrograph separations with steady-state mass balance equations, as per Uhlenbrook and others (2002). The results of their two-component hydrograph separation yielded runoff contributions of 5 to 36 percent of direct runoff as a proportion of streamflow for 4 different rain events. In addition to this, they conducted a principal component analysis (PCA) and found  $\delta^2\text{D}$  and K to be poorly correlated (i.e., to vary independently) and were thus able to use these two parameters to conduct a three-component separation, as shown in Figure 42. This revealed a large difference in relative contributions of shallow versus deep groundwater to streamflow. In particular, for events where prior precipitation has wetted the catchment, the shallow groundwater and runoff contributions are greater than for events occurring after a dry period.

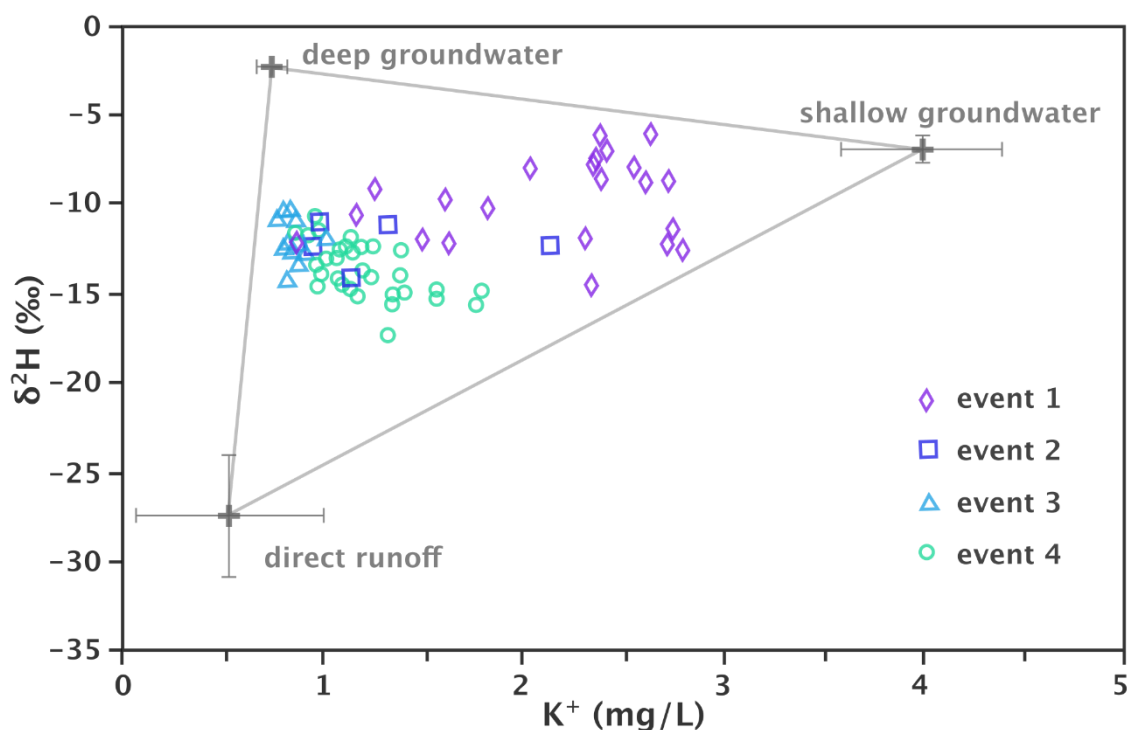


**Figure 42** - Three-point hydrograph separation based on  $\delta^2\text{H}$  and K values for 4 rain events in the Kaap catchment, Mpumalanga, South Africa. Different events revealed different proportions of groundwater and runoff in the streamflow, depending on the weather and ground conditions before and during each event (after Camacho Suarez et al., 2015).

## 7.9 Residence Time

Paulsson and Widerland (2020) investigated 4 pit lakes (waterbodies in abandoned open pit mines) in central Sweden, including measuring stable isotope compositions for snow, rain, groundwater and the pit lakes (Figure 43). Their study was complicated by the fact that the lakes are stratified, and that for 6 months of the year, the lake surface is frozen. Nonetheless, they applied the *hydrocalculator* (<http://hydrocalculator.gskrzypek.com>) method of Skrzypek and others (2015), which is based on the Craig-Gordon evaporation model (Craig and Gordon, 1965). The *hydrocalculator* uses measured, calculated and estimated values for the initial and final isotope compositions, relative humidity, temperature, as well as equilibrium and kinetic fractionation factors and enrichment and adjustment factors (Biggs et al., 2015; Dogramaci et al., 2015) to estimate the amount of evaporation that occurred from the lake surface, based on the change in  $\delta^2\text{H}$  and  $\delta^{18}\text{O}$  values. With adjustments for the lake stratification and the volume of water in each pit lake, they used the estimated evaporation value to calculate the residence time of water in each lake. The residence times varied from 3 to 14 years as the lakes are quite different in size and shape. These values can easily have a factor of 2 error, due to natural variability and complexity, and the assumptions in the models, but these results are useful to help quantify the broad differences between the hydrological systems of each pit lake.

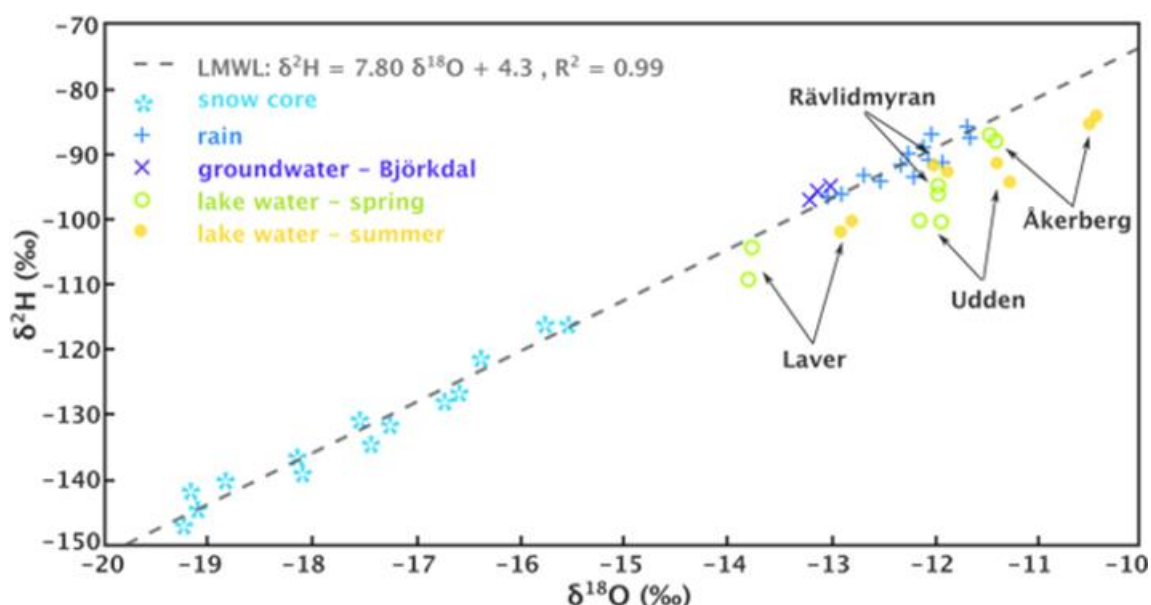


**Figure 43** - Stable isotope data for snow, rain, groundwater and pit lakes (named) in central Sweden. The distinct isotope compositions of rain and snow, and of each of the pit lakes allow calculation of residence time of water in the pit lakes (from Paulsson and Widerland, 2020). The large negative isotope compositions are due to the high latitude of the study area.

## 8 Water Sampling for Stable Isotope Analysis

### 8.1 Practical Considerations

Stable isotopes of water have a major advantage over many other water analytes, in that they comprise virtually all of the sample, rather than being a minor or trace constituent, such as  $\text{Cl}^-$  or  $^3\text{H}$ . This means that contamination is less of a concern during sampling and storage. However, stable isotopes are sensitive to evaporation, so ensuring the sample is well sealed is essential.

Sample bottles need not be specialized. They can be glass or plastic, but must seal completely. Sample volumes required for IRMS or CRDS are only a few milliliters, so any bottle more than 50 ml will suffice. Duplicates are useful if loss or breakage may occur. Duplicates that are labeled so it is not obvious that they are duplicates (e.g., given a fake sample number) are useful as a check of the laboratory's precision.

Answering hydrogeological questions almost always requires knowledge of the whole water cycle, so it is usually necessary to sample precipitation and surface water, in addition to groundwater (Orlowski et al., 2016).

### 8.2 Precipitation

From a hydrogeological perspective, the main reason to sample precipitation is to better understand recharge. The isotope composition of precipitation provides an input value for water cycle or catchment related studies. The isotope composition of recharge may differ from that of precipitation, primarily due to evaporation during infiltration, however, knowing the original precipitation value is useful for many applications.

#### 8.2.1 Spatial and Temporal Variation in Precipitation

Precipitation varies isotopically over time and space. Spatial variation increases with the size of the study area, the climatic complexity (erratic precipitation or multiple types of weather systems) and terrain complexity (mainly altitude change). It is the responsibility of the investigator to ensure capture of such variation. Temporal variation occurs by the minute in rain events (Muller et al., 2015) as well as over many years (Diamond and Harris, 2019). The more completely that all of the rain is captured and the longer the period of sampling (years to decades), the more accurate the average isotope composition. Over decades of sampling, climate change is likely to have an impact so long-term averages may reflect rising or falling trends, rather than steady means.

Sampling of precipitation can be challenging. The ultimate goal is to capture all precipitation that would otherwise have fallen on the ground and to measure how much fell, according to local or internationally accepted measurement methods (Bosman, 1981). Challenges arise due to many possible factors, including strong winds that can blow over precipitation collectors or blow the precipitation past the opening, heavy rain that can fill

the collector in under 24 hours, low precipitation in hot and dry climates that can evaporate from the collector, snow and ice that can block openings, and so forth. Wildlife can also pose hazards, such as insects clogging tubes or drinking the captured water, birds defecating into the collector, lizards falling in the collector and dying, monkeys breaking parts of the equipment or a rhinoceros inadvertently having a scratch against the collector and totally destroying it without noticing! Fortunately, interference by organisms tends to be uncommon or to not affect the isotope ratios. The last possible issue is human tampering, which is a very real concern in some places.

### 8.2.2 Standard Daily or Cumulative Monthly Collectors

Standard rain gauges tend to be designed to be emptied at 08h00 daily, with a typical maximum volume that represents 100 mm precipitation. Using a manned precipitation collection site where this happens, typically at a weather station that records other parameters, is ideal, as any problems will be noticed and can be rectified soon. However, often precipitation is monitored in possible groundwater recharge areas which can be remote mountain tops or upper valley slopes, where no personnel are available. Such settings require a cumulative collector that is emptied monthly. The cumulative collector needs to achieve two main goals: 1) to capture all the rain that falls; and, 2) to prevent evaporation from occurring. For the first goal, the tank of the collector needs to be large enough to contain all the precipitation for the wettest month of the wettest year. For the second goal, the simplest method is to use a narrow tube of approximately 4 mm internal diameter to connect the collection funnel with the storage tank (Gröning et al., 2012). This is wide enough to let water flow down freely but narrow enough to prevent moisture from easily moving back to the atmosphere (Figure 44). Other methods include using oil to cover the water but this generally becomes messy, not only in the field, but also in sample bottles and even back at the laboratory. The evaporation effect by using a narrow tube was shown to be less than use of oil (Gröning et al., 2012). Shielding the storage tank from the sun will also help prevent moisture loss.

Sampling at frequencies less than monthly (more than one month's rain per sample) is not recommended. Too many things can go wrong and the loss of one sample result in the loss of data for a greater period of time and could considerably derail research.

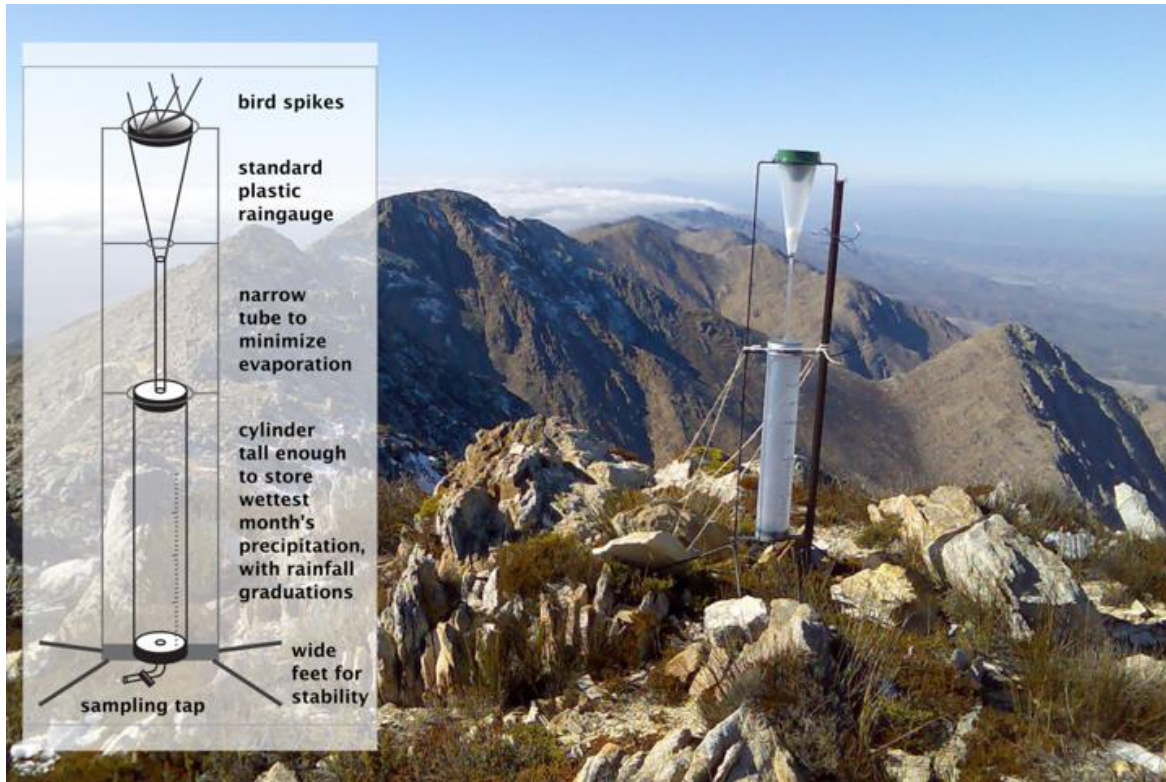


**Figure 44** - A cumulative precipitation collector, designed to be emptied monthly. These are ideal for remote locations, such as this mountain top, Blesberg in the Groot Swartberg Mountains, Eastern Cape, South Africa.

### 8.3 Surface Water

Stable isotopes in surface water bodies may vary spatially and temporally, and capturing this variation is important to generate a meaningful average, as well as to understand seasonality, stratification, inflow sources and other hydrologically important variations. From a hydrogeological perspective, the isotopic variations in a surface water body may help determine the degree or nature of surface water-groundwater interaction.

Temporal changes in surface water isotope composition are not as sudden as with precipitation, which changes by the minute, but it is equally important to capture them because these isotopic changes are often associated with large changes in flow. A flood may only last a few hours in a small catchment, but may be a substantial percentage of the mean annual runoff. This is particularly true for arid environments where watercourses may not flow much during most of the year such that the mean annual runoff may occur in a single event. In more temperate catchments where the mean annual runoff is the result of many storms throughout the year, temporal changes are important because seasonal, and other changes, in weather or land use affect flow dynamics and water quality. Increasingly erratic and stormy weather is predicted due to global climate change and this will require a preparedness to capture such variations in order to obtain representative samples (IPCC, 2014).

The extent of spatial variation of isotopes in surface water bodies depends largely on the water body type. Rivers tend to be fairly well mixed, so the spatial variations are

restricted to upstream and downstream as influenced by inputs and outputs. Lakes are more complex because they may be stratified and may vary temporally between net inflow or net outflow. Reservoirs (man-made) have similar properties to lakes. Wetlands are even more complex in that they may be seasonal or episodic, having no surface water in dry periods that may last months to years. The role of groundwater is usually very important in wetlands.

The degree to which a study needs to capture the temporal and spatial variations in surface water is dependent on the goals of the study. Researchers must be aware that having only one sample from a single location is not as reliable as having multiple samples. The value of one sample for representing the larger system, depends on the system.

## 8.4 Groundwater

### 8.4.1 Natural Groundwater Sources: Springs and Seeps

Natural sampling points for groundwater are most easily sampled. If totally natural, then the water is taken directly from the source (Figure 45). For springs (particularly hot springs) that have been capped or developed into resorts, it is best to sample as close to the source as possible. This may require finding the inlet to a hot pool, which is often an enjoyable sampling experience!



**Figure 45** - Sibusiso Mbonani sampling gas from a CO<sub>2</sub>-rich cold-water spring near the uMtamvuna River on the Bongwana Fault, kwaZulu-Natal, South Africa. The water is sampled easily, but the gas is collected by first filling the sample bottle with water, then inverting it and capturing enough gas to fully displace all water and then sealing the bottle whilst still underwater. Stable isotopes of the CO<sub>2</sub> suggest dissolution of carbonate rocks at depth as the source of CO<sub>2</sub> (Harris et al., 1997), but more work remains to be done on the groundwater source and flow path.

## 8.4.2 Artificial Groundwater Sampling Points: Wells, Boreholes and Piezometers

### Purging

Depending on the borehole construction and groundwater flow regime, groundwater may pass through the borehole casing and be relatively fresh, or it may not be part of the active flow system and become stagnant. If this condition is known, sampling procedures can be adjusted, but in many cases, the flow regime and in particular, the borehole construction, are not known. It is therefore advisable, to always purge a borehole before sampling.

Borehole purging requires removing enough water from the borehole to provide a fresh sample of water from the aquifer, which is representative of the natural groundwater. The rule of thumb is to purge 3 times the borehole volume before sampling. Calculating this value requires knowledge of the borehole diameter (this is usually the same as that seen at surface but may decrease with depth) and the height of the water column in the borehole. This height is the difference between the water level and the bottom of the borehole. Unfortunately, in many cases the depth of the borehole is not known. If this is the case, and the bottom cannot be sounded, then a rough guess can be made based on nearby boreholes in the aquifer being targeted to estimate the number of liters stored in the borehole and therefore, how much purging must be done.

In other cases, boreholes are equipped with pumps and the owner refuses to move these, and one has little idea of the water level and borehole depth. In this case, again, it is best to estimate values to calculate the volume to be purged. On the other hand, in many of these equipped boreholes, the groundwater is being pumped frequently and so a full purge is not as essential as in a research borehole that may have been standing unpumped for months or years.

If one has a thermometer, or other field probes, then these can also be used to determine when fresh aquifer water is being pumped because such readings should stabilize after sufficient purging. With temperature probes, it is useful to be aware of the difference between the air temperature (at which the probe will start reading) and the groundwater temperature. It may seem the groundwater is changing temperature rapidly at first, but that is the probe adjusting to the groundwater temperature.

### Groundwater Heterogeneity

Groundwater is often assumed to be well mixed such that one sample will be representative of an aquifer. This is not always the case, and various investigations have discovered heterogeneity on a scale from centimeters upwards. Pollutants are well known to be heterogeneously distributed due to point source releases, accumulation near the water table, or other factors (Lasagna and De Luca, 2016; Ronen et al., 1987), but natural water quality parameters also vary substantially, even when the aquifer matrix appears relatively homogenous (Baloyi and Diamond, 2019; Petrella and Celico, 2012). The causes of these

differences are complex and beyond the discussion here. However, it is important to understand how well a sample, or set of samples, represents the aquifer, bearing in mind issues such as heterogeneity. For example, a single sample may contain water that is not representative because of the variation from place to place, including materials and conditions between boreholes, or vertically within one borehole. This sample is not representative of the aquifer because it only characterizes one of the various water types present. On the other hand, the process of sampling, especially pumping at high rates from a borehole open to, or screened in, a large interval of the aquifer, can mix water from different levels that may have quite distinct compositions. This sample is not representative because it averages some or all of the water types present. For some investigations, often for regional studies, these sampling errors may not be an issue, but for others, such as characterizing contamination at a site, isolating discrete intervals and sampling them to preserve the natural heterogeneity is important. Technology to sample discrete horizons has been developed in more recent years (Cherry et al., 2007).

From a stable isotope perspective, many of the variations in water chemistry may not be accompanied by related changes in stable isotope composition. However, some hydrochemical changes may be associated with stable isotope changes, such as evaporation prior to recharge causing an increase in salinity, and an associated increase in  $\delta$  values. Leaking water mains (or sewers) with hydrochemistry (or pollution levels) different from that of the local groundwater, may or may not reflect in the stable isotopes, depending on the source of municipal water relative to the source of local groundwater. Petrella and Celico (2012) mapped stable isotopes from the water table downward in a carbonate aquifer in Italy and found the upper 12 m or so to contain varied compositions, while below that the groundwater was better mixed. They concluded the level at which mixing is achieved depends upon the physical nature of the aquifer as well as the hydraulic conditions, for example the precipitation history and water level fluctuations.

## 9 Further Reading

For me, the materials listed in this section serve as substantial resources of information about stable isotope behavior, data analysis, interpretation and presentation, and will be useful in any aspirant stable isotope hydrologist's library, real or digital. I list them in chronological order to preserve the natural development of ideas.

*Isotopic Variations in Meteoric Waters* by Harmon Craig. *Science*, volume 133, pages 1702-1703, **1961**, <https://www.science.org/doi/10.1126/science.133.3465.1702>.

*Stable isotopes in precipitation* by Willi Dansgaard. *Tellus*, volume 16, pages 436-468, **1964**, <https://www.tandfonline.com/doi/abs/10.3402/tellusa.v16i4.8993>.

*Stable Isotope Hydrology - Deuterium and Oxygen-18 in the Water Cycle* by Joel Gat and Roberto Gonfiantini (editors). International Atomic Energy Agency, Technical Reports Series #210, 339 pages, **1981**, [https://inis.iaea.org/search/search.aspx?orig\\_q=RN:13677657](https://inis.iaea.org/search/search.aspx?orig_q=RN:13677657).

*Isotopic Patterns in Modern Global Precipitation* by Kazimierz Rozanski, Luis Araguás-Araguás and Roberto Gonfiantini. In: *Climate Change in Continental Isotopic Records*, Swart PK, Lohmann KC, McKenzie J and Savin S (editors), Geophysical Monograph 78, American Geophysical Union, pages 1-36, **1993**, <https://agupubs.onlinelibrary.wiley.com/doi/abs/10.1029/GM078p0001>.

*Oxygen and hydrogen isotopes in the hydrologic cycle* by Joel Gat. *Annual Reviews in Earth & Planetary Sciences*, volume 24, pages 225-262, **1996**, <https://www.annualreviews.org/doi/abs/10.1146/annurev.earth.24.1.225>.

*Stable Isotopes in Plant Ecology*. Todd Dawson, Stefania Mambelli, Agneta Plamboeck, Pamela Templer and Kevin Tu. *Annual Review of Ecology and Systematics*, volume 33, pages 507-559, **2002**, <https://www.annualreviews.org/doi/abs/10.1146/annurev.ecolsys.33.020602.095451>.

*Hydrograph separation using stable isotopes: Review and evaluation* by Julian Klaus and Jeffrey McDonnell. *Journal of Hydrology*, volume 505, pages 47-64, **2013**, [https://water.usask.ca/hillslope/documents/pdfs/2013/13-08%20Klaus2013JOH\\_505\\_47-64.pdf](https://water.usask.ca/hillslope/documents/pdfs/2013/13-08%20Klaus2013JOH_505_47-64.pdf).

*Groundwater Geochemistry and Isotopes* by Ian Clark. CRC Press, Boca Raton, 438 pages, **2015**, <https://www.taylorfrancis.com/books/mono/10.1201/b18347/groundwater-geochemistry-isotopes-ian-clark>.

*Global Isotope Hydrogeology -- Review* by Scott Jasecko. *Reviews of Geophysics*, volume 57, pages 835-965, **2019**, <https://agupubs.onlinelibrary.wiley.com/doi/full/10.1029/2018RG000627>.

## 10 Wrap-up

Research using the stable isotopes of water was originally focused on the major flows of water in the hydrological cycle. This included evaporation from the oceans, condensation from vapor to cloud, and precipitation in different environments across the globe. It was during this time that the effects of temperature, latitude, altitude, continentality, precipitation amount, source region, humidity and other parameters on isotope composition of precipitation became known. Once these global patterns of isotope composition were fairly well understood in the oceans, lakes, rivers and groundwater, researchers started more detailed regional and local investigations. These focused works provided insight regarding transpiration, recharge, groundwater flow, hydrograph separation, mixing of water masses and other processes.

By the late 20<sup>th</sup> century, stable isotope studies were integrating information from geology, hydrochemistry, other isotope systems (both stable and radioactive) as well as biological work. Topics being addressed included geothermal studies, paleowaters, paleoclimatic interpretation, and plant water sources.

Moving into the 21<sup>st</sup> century, the arrival of laser cavity instruments reduced the time and cost of isotope analysis, previously only done by mass spectrometer. Oxygen and hydrogen isotopes in water could now be routinely analyzed by mining companies, agricultural interests and local government, generating huge datasets that could be used to monitor for leaking canals or pipes, movement of pollution plumes and determination of the sustainability of groundwater abstraction (Figure 46). Isotope hydrology had become a mature science, used by researchers at universities while being applied by natural resource managers.



**Figure 46** - Artesian flow from a future production borehole on the Coega Fault, tapping the Table Mountain Group, Eastern Cape, South Africa. Stable isotope information can help manage such large, deep groundwater reserves sustainably.

The forefront of stable isotope hydrology now includes analysis of global datasets to quantify changes in groundwater storage, applications to urban water issues and use of triple oxygen isotopes ( $^{16}\text{O}$ ,  $^{17}\text{O}$  and  $^{18}\text{O}$ ) to re-evaluate the existing meteoric water lines and kinetic fractionation effects. At the same time, the greater accessibility to information via the internet and the lower cost of isotopic analysis has allowed the benefits of this science to penetrate less-wealthy parts of the world and assist in understanding developing world issues, such as community water supply, sanitation, environmental protection and sustainability.

Isotope hydrology is poised to continue expanding, both in research settings and for application to day-to-day water management. This book was written to educate and motivate the next generation of isotope hydrologists, so they can advance the science and tackle the swathe of environmental challenges that need to be addressed for humanity to continue to inhabit a healthy and beautiful planet.

# 11 Exercises

## Exercise 1 - Meteoric Water Line Calculations

Meteoric water lines are not essential for every stable isotope study, but they are needed frequently, particularly when comparing surface water or groundwater to precipitation. The calculation of a meteoric water line was covered theoretically in this book, but this exercise provides readers with the opportunity to develop a MWL.

Precipitation and stable isotope data for the University of Cape Town for 2010 are given in the table below. Using the data:

1. Calculate the local meteoric water line using the RMA (reduced major axis) regression method and calculate the Pearson's  $r$  correlation coefficient; and,
2. Calculate the precipitation-weighted RMA regression line and its Pearson's  $r$ .

Stable isotope data for UCT precipitation				
Location	Date	Precipitation mm	$\delta^{18}\text{O}$ ‰	$\delta\text{D}$ ‰
UCT	Jan 2010	9	+0.75	+9.7
UCT	Feb 2010	12	-0.54	-5.8
UCT	Mar 2010	7	-0.83	+0.4
UCT	Apr 2010	44	-2.25	-12.1
UCT	May 2010	277	-2.78	-8.4
UCT	Jun 2010	222	-3.31	-17.0
UCT	Jul 2010	166	-3.69	-15.0
UCT	Aug 2010	121	-1.74	-4.9
UCT	Sep 2010	100	-2.24	-3.3
UCT	Oct 2010	102	-2.15	-3.3
UCT	Nov 2010	73	-2.39	-6.2
UCT	Dec 2010	17	-5.06	-39.9

[Click for solution to Exercise 1](#) ↴

## Exercise 2 - Calculation of Recharge Altitude

Determine the recharge altitude of the Kirstenbosch spring, which is 160 masl, by working through the 4 items listed here.

1. Calculate the mean isotopic composition of the spring water based on the measurements provided in this table.

<b>Stable isotope data for the Kirstenbosch spring</b>		
<b>date</b>	<b><math>\delta\text{D}</math></b> $\Delta\text{‰}$	<b><math>\delta^{18}\text{O}</math></b> $\Delta\text{‰}$
March 2010	-13.7	-3.01
November 2010	-9.4	-3.03
May 2011	-12.4	-3.71
October 2011	-12.9	-3.04
May 2012	-10.2	-3.48
September 2012	-10.1	-2.37

2. Calculate the weighted mean stable isotope compositions (ignore missing values) for the University of Cape Town (135 masl) and the Table Mountain Cableway (1074 masl) using the 3-year dataset provided in the table on the following page.
3. Use the weighted means calculated in item 2 to calculate an altitude effect for Table Mountain.
4. Calculate the recharge altitude of the Kirstenbosch spring.

**Stable isotope data for precipitation at UCT and the Table Mountain Upper Cableway Station.**

	UCT			TMC		
	$\delta D$ ‰	$\delta^{18}O$ ‰	Precipitation mm	$\delta D$ ‰	$\delta^{18}O$ ‰	Precipitation mm
J	+9.7	+0.75	9			
F	-5.8	-0.54	13			
M	+0.4	-0.83	7			
A	-12.1	-2.25	45			
M	-8.4	-2.78	275	-15.0	-3.14	280
J	-17.0	-3.31	201	-24.4	-4.35	170
J	-15.0	-3.69	166			200
A	-4.9	-1.74	121			150
S	-3.3	-2.24	101			100
O	-3.3	-2.15	103	-16.3	-3.04	120
N	-6.2	-2.39	73	-13.1	-2.65	90
D	-39.9	-5.06	17	-16.0	-2.35	60
<hr/>						
J	-5.2	-0.15	16	-1.2	-0.75	30
F	13.9	+3.19	3			20
M	-23.6	-4.12	16			50
A	-5.8	-2.73	111	-14.8	-4.61	90
M	-12.3	-3.69	145	-14.7	-4.17	142
J	-18.3	-4.82	191	-16.9	-4.85	150
J	-14.6	-4.68	49	-11.6	-4.71	70
A	-3.8	-2.63	209	-14.4	-4.64	165
S	-0.1	-1.51	141	-9.2	-3.51	115
O	-17.0	-3.48	41	-13.6	-3.84	100
N	-12.0	-3.21	72	-17.4	-4.64	100
D	-1.6	-2.05	62	-9.6	-3.51	90
<hr/>						
J	+5.4	+0.78	46	-4.7	-2.93	130
F	-2.5	-0.68	21	-1.0	-2.05	80
M	-11.9	-3.07	69	-12.9	-3.91	110
A	-9.8	-3.12	133	-13.7	-4.34	130
M	-10.4	-3.08	143			155
J	-6.4	-4.15	230	-8.7	-2.32	200
J	-8.8	-2.67	300	-7.6	-2.93	240
A	-13.5	-3.25	214	-20.8	-4.82	145
S	-10.8	-2.36	172	-22.4	-5.75	215
O	-7.1	-3.16	44			123
N	+0.1	-1.08	60			44
D	+6.9	-0.17	10			20

[Click for solution to Exercise 2](#)

## Exercise 3 - Hydrograph Separation

In the most simplified case, the surface water flow from a catchment may comprise only baseflow (groundwater discharge to the river). One notch of added complexity is that the surface water may comprise a mixture of baseflow and precipitation. For this scenario in Yongan watershed in Zhejiang, eastern China, estimate the fractions of groundwater and precipitation contributing to surface water flow using the data from Hu and others (2020) provided in the table below. Comment on the significance of the errors (as shown in the table) to the estimated proportions.

<b>Stable isotope data for key flows in Yongan, Zhejiang, China</b>		
<b>Sample Type</b>	<b><math>\delta^2\text{H}</math> (‰)</b>	<b><math>\delta^{18}\text{O}</math> (‰)</b>
Precipitation	$-33.9 \pm 24.1$	$-6.4 \pm 2.9$
River water	$-42.8 \pm 6.1$	$-6.9 \pm 1.1$
Groundwater	$-44.7 \pm 3.3$	$-7.2 \pm 0.9$

[Click for solution to Exercise 3](#) ↴

## 12 References

- Abouelmagd, A., M. Sultan, A. Milewski, A.E. Kehew, N.C. Sturchio, F. Soliman, R.V. Krishnamurthy, and E. Cutrim, 2012, Toward a better understanding of palaeoclimatic regimes that recharged the fossil aquifers in North Africa: Inferences from stable isotopes and remote sensing data. *Palaeogeography, Palaeoclimatology, Palaeoecology*, volume 329-330, 13 pages, [doi:10.1016/j.palaeo.2012.02.024](https://doi.org/10.1016/j.palaeo.2012.02.024).
- Adar, E.M., A. Dody, M.A. Geyh, A. Yair, A. Yakirevich, and A.S. Issar, 1998, Distribution of stable isotopes in arid storms I. Relation between the distribution of isotopic composition in rainfall and in consequent runoff. *Hydrogeology Journal*, volume 6, 16 pages, [doi:10.1007/s100400050133](https://doi.org/10.1007/s100400050133).
- Al-Charideh, A. and B. Kattaa, 2016, Isotope hydrology of deep groundwater in Syria: renewable and non-renewable groundwater and paleoclimate impact. *Hydrogeology Journal*, volume 24, 20 pages, [doi:10.1007/s10040-015-1324-4](https://doi.org/10.1007/s10040-015-1324-4).
- Al Faitouri, M. and W.E. Sanford, 2015, Stable and radio-isotope analysis to determine recharge timing and paleoclimate of sandstone aquifers in central and southeast Libya. *Hydrogeology Journal*, volume 23, 11 pages, [doi:10.1007/s10040-015-1232-7](https://doi.org/10.1007/s10040-015-1232-7).
- Alison, G.B. and M.W. Hughes, 1983, The use of natural tracers as indicators of soil-water movement in a temperate semi-arid region. *Journal of Hydrology*, volume 60, 17 pages, [doi:10.1016/0022-1694\(83\)90019-7](https://doi.org/10.1016/0022-1694(83)90019-7).
- Andrews, J.E., 2006, Palaeoclimatic records from stable isotopes in riverine tufas: Synthesis and reviews. *Earth Science Reviews*, volume 75, 20 pages, [doi:10.1016/j.earscirev.2005.08.002](https://doi.org/10.1016/j.earscirev.2005.08.002).
- Antunes, P., D.F. Boutt, and F.C. Rodrigues, 2019, Orographic distillation and spatio-temporal variations of stable isotopes in precipitation in the North Atlantic. *Hydrological Processes*, volume 33, 19 pages, [doi:10.1002/hyp.13362](https://doi.org/10.1002/hyp.13362).
- Araguás-Araguás, L., K. Froehlich, and K. Rozanski, 1998, Stable isotope composition of precipitation over southeast Asia. *Journal of Geophysical Research*, volume 103, number D22, 22 pages, [doi:10.1029/98JD02582](https://doi.org/10.1029/98JD02582).
- Araguás-Araguás, L., K. Froehlich, and K. Rozanski, 2000, Deuterium and oxygen-18 isotope composition of precipitation and atmospheric moisture. *Hydrological Processes*, volume 14, 15 pages, [doi:10.1002/1099-1085\(20000615\)14:8<1341::AID-HYP983>3.0.CO;2-Z](https://doi.org/10.1002/1099-1085(20000615)14:8<1341::AID-HYP983>3.0.CO;2-Z).
- Baloyi, R.S. and R.E. Diamond, 2019, Variable water quality of domestic wells emphasizes the need for groundwater quality monitoring and protection: Stinkwater, Hammanskraal, Gauteng. *Water SA*, volume 45, 9 pages, [doi:10.4314/wsa.v45i2.08](https://doi.org/10.4314/wsa.v45i2.08).
- Beven, K.J., 2001, *Rainfall-Runoff Modelling - The Primer*. John Wiley and Sons, Ltd., New York, 488 pages.
- Biggs, T.W., C.T. Lai, P. Chandan, R.M. Lee, A. Messina, R.S. Leshner, and N. Khatoon, 2015, Evaporative fractions and elevation effects on stable isotopes of high elevation

- lakes and streams in arid western Himalaya. *Journal of Hydrology*, volume 522, 11 pages, [doi:10.1016/j.jhydrol.2014.12.023](https://doi.org/10.1016/j.jhydrol.2014.12.023).
- Blarasin, M., A. Cabrera, I. Matiatos, V. Lutri, L. Maldonado, D. Giacobone, E. Matteoda, F.B. Quinodoz, J.G. Albo, C.E. Felizzia, and J. Felizzia, 2020, Application of isotope techniques to enhance the conceptual hydrogeological model and to assess groundwater sustainability in the Pampean Plain in Cordoba, Argentina. *Isotopes in Environmental and Health Studies*, volume 56, 16 pages, [doi:10.1080/10256016.2020.1796658](https://doi.org/10.1080/10256016.2020.1796658).
- Bodé, S., L. de Wispelaere, A. Hemp, D. Verschuren, and P. Boeckx, 2019, Water-isotope ecohydrology of Mount Kilimanjaro. *Ecohydrology*, volume 13, issue 1, 19 pages, [doi:10.1002/eco.2171](https://doi.org/10.1002/eco.2171).
- Boschetti, T., J. Cifuentes, P. Iacumin, and E. Selmo, 2019, Local meteoric water line of northern Chile (18-30°S): An application of error-in-variables regression to the oxygen and hydrogen stable isotope ratio of precipitation. *Water*, volume 11, issue 4, 791 pages, [doi:10.3390/w11040791](https://doi.org/10.3390/w11040791).
- Bosman, H.H., 1981, Raingauges: Quality pays. *Water SA*, volume 7, 2 pages.
- Camacho Suarez, V.V., A.M. Saraiva Okello, J.W. Wenninger, and S. Uhlenbrook, 2015, Understanding runoff processes in a semi-arid environment through isotope and hydrochemical hydrograph separations. *Hydrology and Earth System Sciences*, volume 19, 17 pages, [doi:10.5194/hess-19-4183-2015](https://doi.org/10.5194/hess-19-4183-2015).
- Canavan, R.R., B. Carrapa, M.T. Clementz, J. Quade, P.G. DeCelles, and L.M. Schoenbohm, 2014, Early Cenozoic uplift of the Puna Plateau, Central Andes, based on stable isotope paleoaltimetry of hydrated volcanic glass. *Geology*, volume 42, 4 pages, [doi:10.1130/G35239.1](https://doi.org/10.1130/G35239.1).
- Chacko, T., D.R. Cole, and J. Horita, 2001, Equilibrium oxygen, hydrogen and carbon isotope fractionation factors applicable to geological systems, editors, Valley J.W. and D.R. Cole, *Stable Isotope Geochemistry, Reviews in Mineralogy and Geochemistry*, volume 43, 81 pages, [doi:10.2138/gsrmg.43.1.1](https://doi.org/10.2138/gsrmg.43.1.1).
- Chandrajith, R., J.A. Barth, N.D. Subasinghe, D. Merten, and C.B. Dissanayake, 2012, Geochemical and isotope characterisation of geothermal spring waters in Sri Lanka: Evidence for steeper than expected geothermal gradients. *Journal of Hydrology*, volume 476, 10 pages, [doi:10.1016/j.jhydrol.2012.11.004](https://doi.org/10.1016/j.jhydrol.2012.11.004).
- Cherry, J.A., B.L. Parker, and C. Keller, 2007, A new depth-discrete multilevel monitoring approach for fractured rock. *Groundwater Monitoring and Remediation*, volume 27, 14 pages, [doi:10.1111/j.1745-6592.2007.00137.x](https://doi.org/10.1111/j.1745-6592.2007.00137.x).
- Clark, I., 2015, *Groundwater Geochemistry and Isotopes*, CRC Press, Boca Raton, 456 pages, [doi:10.1201/b18347](https://doi.org/10.1201/b18347).
- Clark, I.D. and P. Fritz, 1997, *Environmental Isotopes in Hydrogeology*, CRC Press, Boca Raton, 342 pages, [doi:10.1201/9781482242911](https://doi.org/10.1201/9781482242911).

- Cook, P., 2020, Introduction to isotopes and environmental tracers as indicators of groundwater flow. The Groundwater Project, Guelph, Ontario, Canada, 74 pages, <https://gw-project.org/books/introduction-to-isotopes-and-environmental-tracers-as-indicators-of-groundwater-flow/>.
- Cook, P.G. and A.P. O'Grady, 2006, Determining soil and groundwater use of vegetation from heat pulse, water potential and stable isotope data. *Oecologia*, volume 148, 11 pages, [doi:10.1007/s00442-005-0353-4](https://doi.org/10.1007/s00442-005-0353-4).
- Craig, H., 1961, Isotopic variations in meteoric waters. *Science*, volume 133, 2 pages, [doi:10.1126/science.133.3465.1702](https://doi.org/10.1126/science.133.3465.1702).
- Craig, H. and L.I. Gordon, 1965, Deuterium and oxygen 18 variations in the ocean and the marine atmosphere, editor, Tongiorgi, E., *Stable Isotopes in Oceanographic Studies and Palaeotemperatures*. Proceedings of the Spoleto Conferences in Nuclear Geology, Pisa, 122 pages.
- D'Amore, F. and C. Panichi, 1985, Geochemistry in geothermal exploration. *Energy Research*, volume 9, 22 pages, [doi:10.1002/er.4440090307](https://doi.org/10.1002/er.4440090307).
- Daniele, L., M. Taucare, B. Viguier, G. Arancibia, D. Aravena, T. Roquer, J. Sepúlveda, E. Molina, A. Delgado, M. Muñoz, and D. Morata, 2020, Exploring the shallow geothermal resources in the Chilean Southern Volcanic Zone: Insight from the Liqueñe thermal springs. *Journal of Geochemical Exploration*, volume 218, 15 pages, [doi:10.1016/j.gexplo.2020.106611](https://doi.org/10.1016/j.gexplo.2020.106611).
- Dansgaard, W., 1964, Stable Isotopes in Precipitation. *Tellus*, volume 16, 33 pages, [doi:10.3402/tellusa.v16i4.8993](https://doi.org/10.3402/tellusa.v16i4.8993).
- Das, P., A. Mukherjee, S.A. Hussain, M.S. Jamal, K. Das, A. Shaw, M.K. Layek, and P. Sengupta, 2020, Stable isotope dynamics of groundwater interactions with Ganges River. *Hydrological Processes* 2021, volume 35, issue 1, 15 pages, [doi:10.1002/hyp.14002](https://doi.org/10.1002/hyp.14002).
- Dawson, T.E. and J.R. Ehleringer, 1991, Streamside trees that do not use stream water. *Nature*, volume 350, 3 pages, [doi:10.1038/350335a0](https://doi.org/10.1038/350335a0).
- Dawson, T.E., S. Mambelli, A.H. Plamboeck, P.H. Templer, and K.P. Tu, 2002, Stable isotopes in plant ecology. *Annual Review of Ecology and Systematics*, volume 33, 53 pages, [doi:10.1146/annurev.ecolsys.33.020602.095451](https://doi.org/10.1146/annurev.ecolsys.33.020602.095451).
- Diamond, R.E. and C. Harris, 1997, Oxygen and hydrogen isotope composition of Western Cape meteoric water. *South African Journal of Science*, volume 93, 4 pages, [https://hdl.handle.net/10520/AJA00382353\\_74](https://hdl.handle.net/10520/AJA00382353_74).
- Diamond, R.E. and C. Harris, 2000, Oxygen and hydrogen isotope geochemistry of thermal springs of the Western Cape, South Africa: recharge at high altitude?. *Journal of African Earth Sciences*, volume 31, 15 pages, [doi:10.1016/S0899-5362\(00\)80002-0](https://doi.org/10.1016/S0899-5362(00)80002-0).
- Diamond, R.E. and C. Harris, 2019, Annual shifts in O- and H-isotope composition as measures of recharge: the case of the Table Mountain Springs, Cape Town, South Africa. *Hydrogeology Journal*, volume 27, 16 pages, [doi:10.1007/s10040-019-02045-5](https://doi.org/10.1007/s10040-019-02045-5).

- Diamond, R.E. and S. Jack, 2018, Evaporation and abstraction determined from stable isotopes during normal flow on the Gariep River, South Africa. *Journal of Hydrology*, volume 559, 16 pages, [doi:10.1016/j.jhydrol.2018.02.059](https://doi.org/10.1016/j.jhydrol.2018.02.059).
- Dogramaci, S., G. Skrzypek, W. Dodson, and P.F. Grierson, 2012, Stable isotope and hydrochemical evolution of groundwater in the semi-arid Hamersley Basin of subtropical northwest Australia. *Journal of Hydrology*, volume 475, 13 pages, [doi:10.1016/j.jhydrol.2012.10.004](https://doi.org/10.1016/j.jhydrol.2012.10.004).
- Dogramaci, S., G. Firmani, P. Hedley, G. Skrzypek, and P.F. Grierson, 2015, Evaluating recharge to an ephemeral dryland stream using a hydraulic model and water, chloride and isotope mass balance. *Journal of Hydrology*, volume 521, 13 pages, [doi:10.1016/j.jhydrol.2014.12.017](https://doi.org/10.1016/j.jhydrol.2014.12.017).
- Druhan, J.L. and K. Maher, 2017, The influence of mixing on stable isotope ratios in porous media: A revised Rayleigh model. *Water Resources Research*, volume 53, 24 pages, [doi:10.1002/2016WR019666](https://doi.org/10.1002/2016WR019666).
- Durowoju, O.S., M. Butler, G.E. Ekosse, and J.O. Odiyo, 2019, Hydrochemical processes and isotopic study of geothermal springs within Soutpansberg, Limpopo Province, South Africa. *Applied Sciences*, volume 9, issue 8, 18 pages, [doi:10.3390/app9081688](https://doi.org/10.3390/app9081688).
- Ehleringer, J.R. and T.E. Dawson, 1992, Water uptake by plants: perspectives from stable isotope composition. *Plant, Cell and Environment*, volume 15, 10 pages, [doi:10.1111/j.1365-3040.1992.tb01657.x](https://doi.org/10.1111/j.1365-3040.1992.tb01657.x).
- Ellsworth, P.Z. and D.G. Williams, 2007, Hydrogen isotope fractionation during water uptake by woody xerophytes. *Plant Soil*, volume 291, 15 pages, [doi:10.1007/s11104-006-9177-1](https://doi.org/10.1007/s11104-006-9177-1).
- Emiliani, C., 1987, *Dictionary of the Physical Sciences*. Oxford University Press, New York.
- Epstein, S. and T. Mayeda, 1953, Variation of  $^{18}\text{O}$  content of waters from natural sources. *Geochimica et Cosmochimica Acta*, volume 4, 12 pages, [doi:10.1016/0016-7037\(53\)90051-9](https://doi.org/10.1016/0016-7037(53)90051-9).
- Fontes, J.Ch., 1981, *Palaeowaters*, editors, Gat J.R. and R. Gonfiantini, *Stable Isotope Hydrology*, Technical Reports Series 210, International Atomic Energy Agency, Vienna, 30 pages, <http://www-naweb.iaea.org/napc/ih/documents/IAEA%20Monographs/TRS%20210%20Stable%20Isotope%20Hydrology1981.pdf>.
- Friedman, I., 1953, Deuterium content of natural waters and other substances. *Geochimica et Cosmochimica Acta*, volume 4, 15 pages, [doi:10.1016/0016-7037\(53\)90066-0](https://doi.org/10.1016/0016-7037(53)90066-0).
- Gat, J.R., 1981, *Historical Introduction*, editors, Gat J.R. and R. Gonfiantini, *Stable Isotope Hydrology*, Technical Reports Series 210, International Atomic Energy Agency, Vienna, 6 pages,

- <http://www-naweb.iaea.org/naweb/ih/documents/IAEA%20Monographs/TRS%20210%20Stable%20Isotope%20Hydrology1981.pdf>.
- Gat, J.R., 1996, Oxygen and hydrogen isotopes in the hydrological cycle. Annual Reviews in Earth and Planetary Sciences, volume 24, 38 pages, [doi:10.1146/annurev.earth.24.1.225](https://doi.org/10.1146/annurev.earth.24.1.225).
- Gat, J.R. and E. Matsui, 1991, Atmospheric water balance in the Amazon Basin: an isotopic evapotranspiration model. Journal of Geophysical Research, volume 96, issue D7, 10 pages, [doi:10.1029/91JD00054](https://doi.org/10.1029/91JD00054).
- Gat, J.R., D. Yakir, G. Goodfriend, P. Fritz, P. Trimborn, J. Lipp, I. Gev, E. Adar, and Y. Waisel, 2007, Stable isotope composition of water in desert plants. Plant Soil, volume 298, 15 pages, [doi:10.1007/s11104-007-9321-6](https://doi.org/10.1007/s11104-007-9321-6).
- Gillespie, J., S.T. Nelson, A.L. Mayo, and D.G. Tingey, 2012, Why conceptual groundwater flow models matter: a trans-boundary example from the arid Great Basin, western USA. Hydrogeology Journal, volume 20, 15 pages, [doi:10.1007/s10040-012-0848-0](https://doi.org/10.1007/s10040-012-0848-0).
- Goldsmith, G.R., S.T. Allen, S. Braun, N. Engbersen, C.R. González-Quijano, J.R. Kirchner, and R.T. Siegwolf, 2018, Spatial variation in throughfall, soil, and plant water isotopes in a temperate forest. Ecohydrology, volume 12, 11 pages, [doi:10.1002/eco.2059](https://doi.org/10.1002/eco.2059).
- Gonfiantini, R., 1981, The  $\delta$  notation and the mass-spectrometric measurement techniques, editors, Gat J.R. and R. Gonfiantini, Stable Isotope Hydrology, International Atomic Energy Agency, Technical Reports Series #210, Vienna. Chapter 4, 50 pages, <https://inis.iaea.org/collection/NCLCollectionStore/Public/13/677/13677657.pdf?r=1>.
- Gonfiantini, R., M.A. Roche, J.C. Olivry, J.C. Fontes, and G.M. Zuppi, 2001, The altitude effect on the isotopic composition of tropical rains. Chemical Geology, volume 181, 21 pages, [doi:10.1016/S0009-2541\(01\)00279-0](https://doi.org/10.1016/S0009-2541(01)00279-0).
- Grimmeisen, F., M.F. Lehmann, T. Liesch, N. Goeppert, J. Klinger, J. Zopfi, and N. Goldscheider, 2017, Isotopic constraints on water source mixing, network leakage and contamination in an urban groundwater system. Science of the Total Environment, volume 583, 12 pages, [doi:10.1016/j.scitotenv.2017.01.054](https://doi.org/10.1016/j.scitotenv.2017.01.054).
- Gröning, M., H.O. Lutz, Z. Roller-Lutz, M. Kralik, L. Gourcy, and L. Pölsenstein, 2012, A simple rain collector preventing water re-evaporation dedicated for delta O-18 and delta H-2 analysis of cumulative precipitation samples. Journal of Hydrology, volume 448, 6 pages, [doi:10.1016/j.jhydrol.2012.04.041](https://doi.org/10.1016/j.jhydrol.2012.04.041).
- Han, T., M. Zhang, S. Wang, D. Qu, and Q. Du, 2020, Sub-hourly variability of stable isotopes in precipitation in the marginal zone of East Asian monsoon. Water, volume 12, issue 8, 14 pages, [doi:10.3390/w12082145](https://doi.org/10.3390/w12082145).
- Harris, C., C. Burgers, J. Miller, and F. Rawoat, 2010, O- and H-isotope record of Cape Town rainfall from 1996 to 2008, and its application to recharge studies of Table Mountain groundwater, South Africa. South African Journal of Geology, volume 113, 24 pages, [doi:10.2113/gssajg.113.1.33](https://doi.org/10.2113/gssajg.113.1.33).

- Harris, C., W.D. Stock, and J. Lanham, 1997, Stable isotope constraints on the origin of CO<sub>2</sub> gas exhalations at Bongwan, Natal. *South African Journal of Geology*, volume 100, 6 pages, <https://journals.co.za/doi/pdf/10.10520/EJC-92945afa1>.
- Hayes, J.M., 2004, *An Introduction to Isotopic Calculations*. Woods Hole Oceanographic Institution, Woods Hole, Massachusetts, USA, 10 pages, [https://www.whoi.edu/cms/files/jhayes/2005/9/IsoCalcs30Sept04\\_5183.pdf](https://www.whoi.edu/cms/files/jhayes/2005/9/IsoCalcs30Sept04_5183.pdf).
- Hooper, R.P. and C.A. Shoemaker, 1986, A comparison of chemical and isotopic hydrograph separation. *Water Resources Research*, volume 22, 11 pages.
- Horibe, Y. and M. Kobayakawa, 1960, Deuterium abundance of natural waters. *Geochimica et Cosmochimica Acta*, volume 20, 11 pages, [doi:10.1016/0016-7037\(60\)90078-8](https://doi.org/10.1016/0016-7037(60)90078-8).
- Hu, M., Y. Zhang, K. Wu, H. Shen, M. Yao, R.A. Dahlgren, and D. Chen, 2020, Assessment of streamflow components and hydrologic transit times using stable isotopes of oxygen and hydrogen in waters of a subtropical watershed in eastern China. *Journal of Hydrology*, volume 589, 11 pages, [doi:10.1016/j.jhydrol.2020.125363](https://doi.org/10.1016/j.jhydrol.2020.125363).
- Hughes, C.E. and J. Crawford, 2012, A new precipitation weighted method for determining meteoric water line for hydrological applications demonstrated using Australia and global GNIP data. *Journal of Hydrology*, volume 465, 8 pages, [doi:10.1016/j.jhydrol.2012.07.029](https://doi.org/10.1016/j.jhydrol.2012.07.029).
- Husain, M.M., J.A. Cherry, and S.K. Frape, 2004, The persistence of a large stagnation zone in a developed regional aquifer, southwestern Ontario. *Canadian Geotechnical Journal*, volume 41, 16 pages, [doi:10.1139/t04-040](https://doi.org/10.1139/t04-040).
- IPCC, 2014, Intergovernmental Panel on Climate Change, *Climate Change 2014: Synthesis Report. Contribution of Working Groups I, II and III to the Fifth Assessment Report of the Intergovernmental Panel on Climate Change* [Core Writing Team, editors, Pachauri R.K. and L.A. Meyer]. IPCC, Geneva, Switzerland, 151 pages, [https://archive.ipcc.ch/pdf/assessment-report/ar5/syr/SYR\\_AR5\\_FINAL\\_full\\_wcover.pdf](https://archive.ipcc.ch/pdf/assessment-report/ar5/syr/SYR_AR5_FINAL_full_wcover.pdf).
- Iqbal, M.Z., 1998, Application of environmental isotopes in storm-discharge analysis of two contrasting stream channels in a watershed. *Water Research*, volume 32, 10 pages, [doi:10.1016/S0043-1354\(98\)00070-0](https://doi.org/10.1016/S0043-1354(98)00070-0).
- Jasecko, S., 2019, Global Isotope Hydrogeology - Review. *Reviews of Geophysics*, volume 57, 101 pages, [doi:10.1029/2018RG000627](https://doi.org/10.1029/2018RG000627).
- Jasecko, S., Z.D. Sharp, J.J. Gibson, S.J. Birks, Y. Yi, and P.J. Fawcett, 2013, Terrestrial water fluxes dominated by transpiration. *Nature*, volume 496, 4 pages, [doi:10.1038/nature11983](https://doi.org/10.1038/nature11983).
- Kirchner, J.W., 2003, A double paradox in catchment hydrology and geochemistry. *Hydrological Processes*, volume 17, 4 pages, [doi:10.1002/hyp.5108](https://doi.org/10.1002/hyp.5108).

- Klaus, J. and J.J. McDonnell, 2013, Hydrograph separation using stable isotopes: Review and evaluation. *Journal of Hydrology*, volume 505, 18 pages, [doi:10.1016/j.jhydrol.2013.09.006](https://doi.org/10.1016/j.jhydrol.2013.09.006).
- Ladouche, B., A. Luc, and D. Nathalie, 2009, Chemical and isotopic investigation of rainwater in southern France (1996-2002): Potential use as input signal for karst functioning investigation. *Journal of Hydrology*, volume 367, 15 pages, [doi:10.1016/j.jhydrol.2009.01.012](https://doi.org/10.1016/j.jhydrol.2009.01.012).
- Laonamsai, J., K. Ichiyanagi, K. Kamdee, A. Putthividhya, and M. Tanoue, 2020, Spatial and temporal distributions of stable isotopes in precipitation over Thailand. *Hydrological Processes*, volume 35, 15 pages, [doi:10.1002/hyp.13995](https://doi.org/10.1002/hyp.13995).
- Lasagna, M. and D.A. De Luca, 2016, The use of multilevel sampling techniques for determining shallow aquifer nitrate profiles. *Environmental Science Pollution Research*, volume 23, 18 pages, [doi:10.1007/s11356-016-7264-2](https://doi.org/10.1007/s11356-016-7264-2).
- Laudon, H. and O. Slaymaker, 1997, Hydrograph separation using stable isotopes, silica and electrical conductivity: an alpine example. *Journal of Hydrology*, volume 201, 20 pages, [doi:10.1016/S0022-1694\(97\)00030-9](https://doi.org/10.1016/S0022-1694(97)00030-9).
- Lelli, M., T.G. Kretzschmar, J. Cabassi, M. Doveri, J.I. Sanchez-Avila, F. Gherardi, G. Magro, and F. Norelli, 2021, Fluid geochemistry of the Los Humeros geothermal field (LHGF - Puebla, Mexico): New constraints for the conceptual model. *Geothermics*, volume 90, 17 pages, [doi:10.1016/j.geothermics.2020.101983](https://doi.org/10.1016/j.geothermics.2020.101983).
- Li, J., Z. Pang, Y. Kong, S. Wang, G. Bai, H. Zhao, D. Zhou, F. Sun, and Z. Yang, 2018, Groundwater isotopes biased toward heavy rainfall events and implications on the local meteoric water line. *Journal of Geophysical Research: Atmospheres*, volume 123, 8 pages, [doi:10.1029/2018JD028413](https://doi.org/10.1029/2018JD028413).
- Los Gatos Research, 2020, Off-Axis Integrated Cavity Output Spectroscopy, <http://www.lgrinc.com/advantages>.
- Lyon, S.W., S.L. Desilets, and P.A. Troch, 2009, A tale of two isotopes: differences in hydrograph separation for a runoff event when using  $\delta D$  and  $\delta^{18}O$ . *Hydrological Processes*, volume 23, 7 pages, [doi:10.1002/hyp.7326](https://doi.org/10.1002/hyp.7326).
- Ma, Y.Z., 2019, *Quantitative Geosciences: Data Analytics, Geostatistics, Reservoir Characterization and Modeling*. Springer, Cham, Switzerland, 401 pages, [doi:10.1007/978-3-030-17860-4](https://doi.org/10.1007/978-3-030-17860-4).
- Mahindawansa, A., N. Orłowski, P. Kraft, Y. Rothfuss, H. Racela, and L. Breuer, 2018, Quantification of plant water uptake by water stable isotopes in rice paddy systems. *Plant Soil*, volume 429, 22 pages, [doi:10.1007/s11104-018-3693-7](https://doi.org/10.1007/s11104-018-3693-7).
- Malov, A.I. and I.V. Tokarev, 2019, Using stable isotopes to characterize the conditions of groundwater formation on the eastern slope of the Baltic Shield (NW Russia). *Journal of Hydrology*, volume 578, 10 pages, [doi:10.1016/j.jhydrol.2019.124130](https://doi.org/10.1016/j.jhydrol.2019.124130).
- Maurya, A.S., M. Shah, R.D. Deshpande, R.M. Bhardwaj, A. Prasad, and S.K. Gupta, 2011, Hydrograph separation and precipitation source identification using stable water

- isotopes and conductivity: River Ganga at Himalayan foothills. *Hydrological Processes*, volume 25, 10 pages, [doi:10.1002/hyp.7912](https://doi.org/10.1002/hyp.7912).
- McIntosh, J.C. and L.M. Walter, 2006, Paleowaters in Silurian-Devonian carbonate aquifers: Geochemical evolution of groundwater in the Great Lakes region since the Late Pleistocene. *Geochimica et Cosmochimica Acta*, volume 70, 26 pages, [doi:10.1016/j.gca.2006.02.002](https://doi.org/10.1016/j.gca.2006.02.002).
- Merlivat, L. and J. Jouzel, 1979, Global climatic interpretation of the deuterium-oxygen 18 relationship from precipitation. *Journal of Geophysical Research*, volume 84, C8, 5 pages, [doi:10.1029/JC084iC08p05029](https://doi.org/10.1029/JC084iC08p05029).
- Midgley, J.J. and D.F. Scott, 1994, The use of stable isotopes of water (D and  $^{18}\text{O}$ ) in hydrological studies in the Jonkershoek Valley. *WaterSA*, volume 20, 4 pages, [https://researchspace.csir.co.za/dspace/bitstream/handle/10204/805/Midgley\\_1994.pdf?sequence=1&isAllowed=y](https://researchspace.csir.co.za/dspace/bitstream/handle/10204/805/Midgley_1994.pdf?sequence=1&isAllowed=y).
- Mix, H.T., S.P. Reilly, A. Martin, and G. Cornwell, 2019, Evaluating the roles of rainout and post-condensation processes in a landfalling atmospheric river with stable isotopes in precipitation and water vapor. *Atmosphere*, volume 10, issue 2, 86 pages, [doi:10.3390/atmos10020086](https://doi.org/10.3390/atmos10020086).
- Muller, C.L., A. Baker, I.J. Fairchild, C. Kidd, and I. Boomer, 2015. Intra-event trends in stable isotopes: Exploring midlatitude precipitation using a vertically pointing micro rain radar. *Journal of Hydrometeorology*, volume 16, 20 pages, [doi:10.1175/JHM-D-14-0038.1](https://doi.org/10.1175/JHM-D-14-0038.1).
- Mulligan, B.M., M.C. Ryan, and T.P. Cámara, 2011, Delineating volcanic aquifer recharge areas using geochemical and isotopic tools. *Hydrogeology Journal*, volume 19, 13 pages, [doi:10.1007/s10040-011-0766-6](https://doi.org/10.1007/s10040-011-0766-6).
- Munksgaard, N.C., C.M. Wurster, A. Bass, and M.I. Bird, 2012, Extreme short-term stable isotope variability revealed by continuous rainwater analysis. *Hydrological Processes*, volume 26, 5 pages, [doi:10.1002/hyp.9505](https://doi.org/10.1002/hyp.9505).
- Nehemy, M.F., P. Benettin, M. Asadollahi, D. Pratt, A. Rinaldo, and J.J. McDonnell, 2020, Tree water deficit and dynamic source water partitioning. *Hydrological Processes*, volume 35, 22 pages, [doi:10.1002/hyp.14004](https://doi.org/10.1002/hyp.14004).
- O'Keefe, A. and D. Deacon, 1988, Cavity ringdown optical spectrometer for absorption measurements using pulsed laser sources. *Review of Scientific Instruments*, volume 59, 8 pages, [doi:10.1063/1.1139895](https://doi.org/10.1063/1.1139895).
- Orlowski, N., P. Kraft, J. Pferdmenges, and L. Breuer, 2016, Exploring water cycle dynamics by sampling multiple water isotope pools in a developed landscape in Germany. *Hydrology and Earth System Sciences*, volume 20, 22 pages, [doi:10.5194/hess-20-3873-2016](https://doi.org/10.5194/hess-20-3873-2016).
- Pan, Y-X., X-P. Wang, X-Z. Ma, Y-F. Zhang, and R. Hu, 2020, The stable isotopic composition variation characteristics of desert plants and water sources in an

- artificial revegetation ecosystem in northwest China. *Catena*, volume 189, 10 pages, [doi:10.1016/j.catena.2020.104499](https://doi.org/10.1016/j.catena.2020.104499).
- Panichi, C. and R. Gonfiantini, 1981, *Geothermal Waters*, editors, Gat J.R. and R. Gonfiantini, Stable Isotope Hydrology, Technical Reports Series No 210, International Atomic Energy Agency, Vienna, 32 pages, <http://www-naweb.iaea.org/naweb/ih/documents/IAEA%20Monographs/TRS%20210%20Stable%20Isotope%20Hydrology1981.pdf>.
- Paul, D., G. Skrzypek, and I. Fórizs, 2007, Normalization of measured stable isotopic compositions to isotope reference scales - a review. *Rapid Communications in Mass Spectrometry*, volume 21, 9 pages, [doi:10.1002/rcm.3185](https://doi.org/10.1002/rcm.3185).
- Paulsson and Widerland, 2020, Pit lake oxygen and hydrogen isotopic composition in subarctic Sweden: A comparison to the local meteoric water line. *Applied Geochemistry*, volume 118, 10 pages, [doi:10.1016/j.apgeochem.2020.104611](https://doi.org/10.1016/j.apgeochem.2020.104611).
- Peixoto, J.P. and A.H. Oort, 1983, The atmospheric branch of the hydrological cycle and climate. In: *Variations in the Global Water Budget*, Street-Perrott, et al (editors), D Reidel Publishing Company, 61 pages, [doi:10.1007/978-94-009-6954-4\\_2](https://doi.org/10.1007/978-94-009-6954-4_2).
- Penna, D., J. Geris, L. Hopp, and F. Scandellari, 2020, Water sources for root water uptake: using stable isotopes of hydrogen and oxygen as a research tool in agricultural and agroforestry systems. *Agriculture, Ecosystems and Environment*, volume 291, 6 pages, [doi:10.1016/j.agee.2019.106790](https://doi.org/10.1016/j.agee.2019.106790).
- Penna, D. and H.J. van Meerveld, 2019, Spatial variability in the isotopic composition of water in small catchments and its effect on hydrograph separation. *Wiley Reviews Water*, volume 6, 33 pages, [doi:10.1002/wat2.1367](https://doi.org/10.1002/wat2.1367).
- Peng, T.R., C.H. Wang, C.C. Huang, L.Y. Fei, C.T. Chen, and J.L. Hwong, 2010, Stable isotope characteristics of Taiwan's precipitation: A case study of western Pacific monsoon region. *Earth and Planetary Science Letters*, volume 289, 10 pages, [doi:10.1016/j.epsl.2009.11.024](https://doi.org/10.1016/j.epsl.2009.11.024).
- Peters, E., A. Visser, B.K. Esser, and J.E. Moran, 2018, Tracers reveal recharge elevations, groundwater flow paths and travel times on Mount Shasta, California. *Water*, volume 10, 22 pages, [doi:10.3390/w10020097](https://doi.org/10.3390/w10020097).
- Petrella, E. and F. Celico, 2012, Mixing of water in a carbonate aquifer, southern Italy, analysed through stable isotope investigations. *International Journal of Speleology*, volume 42, 9 pages, [doi:10.5038/1827-806X.42.1.4](https://doi.org/10.5038/1827-806X.42.1.4).
- Plummer, L.N., J.R. Eggleston, D.C. Andreasen, J.P. Raffensperger, A.G. Hunt, and G.C. Casile, 2012, Old groundwater in parts of the upper Patapsco aquifer, Atlantic Coastal Plain, Maryland, USA: evidence from radiocarbon, chlorine-36 and helium-4. *Hydrogeology Journal*, volume 20, 26 pages, [doi:10.1007/s10040-012-0871-1](https://doi.org/10.1007/s10040-012-0871-1).
- Prasetyo, R., Y. Daud, J. Hutabarat, and H. Hendarmawan, 2021, Fluid geochemistry and isotope compositions to delineate physical processes in Wayang Windu geothermal

- reservoir, Indonesia. *Geosciences Journal*, volume 25, 17 pages, [doi:10.1007/s12303-020-0039-2](https://doi.org/10.1007/s12303-020-0039-2).
- Pu, T., D. Qin, S. Kang, H. Niu, Y. He, and S. Wang, 2017, Water isotopes and hydrograph separation in different glacial catchments in the southeast margin of the Tibetan Plateau. *Hydrological Processes*, volume 31, 17 pages, [doi:10.1002/hyp.11293](https://doi.org/10.1002/hyp.11293).
- Qu, S., M. Zhou, P. Shi, H. Liu, W. Bao, and X. Chen, 2014, Differences in oxygen-18 and deuterium content of throughfall and rainfall during different flood events in a small headwater watershed. *Isotopes in Environmental and Health Studies*, volume 50, 10 pages, [doi:10.1080/10256016.2014.845565](https://doi.org/10.1080/10256016.2014.845565).
- Rai, S.P., D. Singh, N. Jacob, Y.S. Rawat, M. Arora, and B. Kumar, 2019, Identifying contribution of snowmelt and glacier melt to the Bhagirathi River (Upper Ganga) near snout of the Gangotri Glacier using environmental isotopes. *Catena*, volume 173, 13 pages, [doi:10.1016/j.catena.2018.10.031](https://doi.org/10.1016/j.catena.2018.10.031).
- Lord Rayleigh, 1902, On the distillation of binary mixtures. *The London, Edinburgh and Dublin Philosophical Magazine and Journal of Science*, volume 4, 17 pages, [doi:10.1080/14786440209462876](https://doi.org/10.1080/14786440209462876).
- Reeburgh, W.S., 1994, Global water reservoirs, fluxes and turnover times, <http://www.ess.uci.edu/~reeburgh/fig8.html>.
- Remenda, V., J.A. Cherry, and T.W. Edwards, 1994, Isotopic composition of old ground water from Lake Agassiz: Implications for Late Pleistocene Climate. *Science*, volume 266, number 5193, 4 pages, [doi:10.1126/science.266.5193.1975](https://doi.org/10.1126/science.266.5193.1975).
- Ronen, D., M. Magaritz, H. Gvirtzman, and W. Garner, 1987, Microscale chemical heterogeneity in groundwater. *Journal of Hydrology*, volume 92, 6 pages, [doi:10.1016/0022-1694\(87\)90094-1](https://doi.org/10.1016/0022-1694(87)90094-1).
- Rozanski, K., C. Sonntag, and K.O. Munnich, 1982, Factors controlling stable isotope composition of European precipitation. *Tellus*, volume 34, 9 pages, [doi:10.3402/tellusa.v34i2.10796](https://doi.org/10.3402/tellusa.v34i2.10796).
- Rozanski, K., L. Araguas-Araguas, and R. Gonfiantini, 1993, Isotopic patterns in modern global precipitation, editors, Swart P.K., K.C. Lohmann, J. McKenzie, and S. Savin, *Climate Change in Continental Isotopic Records*, American Geophysical Union, Geophysical Monograph 78, chapter 1, 36 pages.
- Salati, E., A. Dall'Olio, E. Matsui, and J.R. Gat, 1979, Recycling of water in the Amazon Basin: an isotopic study. *Water Resources Research*, volume 15, 9 pages, [doi:10.1029/WR015i005p01250](https://doi.org/10.1029/WR015i005p01250).
- Sanchez-Murillo, R., C. Birkel, K. Welsch, G. Esquivel-Hernandez, J. Corrales-Salazar, J. Boll, E. Brooks, O. Rouspard, O. Saenz-Rosales, I. Katchan, R. Arce-Mesen, C. Soulsby, and L.J. Araguas-Araguas, 2016, Key drivers controlling stable isotope variations in daily precipitation of Costa Rica: Caribbean Sea versus Eastern Pacific Ocean moisture sources. *Quaternary Science Reviews*, volume 131, 237 pages, [doi:10.1016/j.quascirev.2015.08.028](https://doi.org/10.1016/j.quascirev.2015.08.028).

- Schimmelmann, A. and M.J. DeNiro, 1993, Preparation of organic and water hydrogen for stable isotope analysis: Effects due to reaction vessels and zinc reagent. *Analytical Chemistry*, volume 65, 4 pages, [doi:10.1021/ac00054a024](https://doi.org/10.1021/ac00054a024).
- Sharp, Z., 2007, *Principles of Stable Isotope Geochemistry*. Pearson Prentice Hall, <https://www.abebooks.com/9780130091390/Principles-Stable-Isotope-Geochemistry-Sharp-0130091391/plp>.
- Sinclair, K.E., S.J. Marshall, and T.A. Moran, 2011, A Lagrangian approach to modelling stable isotopes in precipitation over mountainous terrain. *Hydrological Processes*, volume 25, 11 pages, [doi:10.1002/hyp.7973](https://doi.org/10.1002/hyp.7973).
- Sklash, M.G. and R.N. Farvolden, 1979, The role of groundwater in storm runoff. *Journal of Hydrology*, volume 43, 21 pages, [doi:10.1016/0022-1694\(79\)90164-1](https://doi.org/10.1016/0022-1694(79)90164-1).
- Smith, G.I., I. Friedman, G. Veronda, and C.A. Johnson, 2002, Stable isotope compositions of waters in the Great Basin, United States: 3. Comparison of groundwaters with modern precipitation. *Journal of Geophysical Research*, volume 107, issue D19, 16 pages, [doi:10.1029/2001JD000567](https://doi.org/10.1029/2001JD000567).
- Socki, R.A., H.R. Karlsson, and E.K. Gibson Jr., Extraction technique for the determination of oxygen-18 in water using preevacuated glass vials. *Analytical Chemistry*, volume 64, 3 pages, [doi:10.1021/ac00031a026](https://doi.org/10.1021/ac00031a026).
- Sonntag, C.E., E.P. Klitzoch, K.O. Löhnert, K.O. Münnich, O. Junghaus, K. Thorweihe, K. Weistroffer, and F.M. Swailen, 1979, Paleoclimatic information from deuterium and oxygen 18 in C14 date north Saharan groundwaters: groundwater formation in the past. *In: Isotope Hydrology 1978*, International Atomic Energy Agency, Vienna, Austria, 13 pages.
- Steur, P.M., H.A. Scheeren, D.D. Nelson, J.B. McManus, and H.A. Meijer, 2020, Simultaneous measurement of  $\delta^{13}\text{C}$ ,  $\delta^{18}\text{O}$  and  $\delta^{17}\text{O}$  of atmospheric  $\text{CO}_2$  - Performance assessment of a dual-laser absorption spectrometer. *Atmospheric Measurement Techniques*, 26 pages, [doi:10.5194/amt-14-4279-2021](https://doi.org/10.5194/amt-14-4279-2021).
- Stewart, M.K., 1985, *Isotopic geochemistry at Wairakei - Hydrological implications*. Institute of Nuclear Sciences, INS-R -345, Lower Hutt, New Zealand, 19 pages.
- Sultan, M., N.C. Sturchio, H. Gheith, Y. Abdel Hady, and M. El Anbeawy, 2000, Chemical and isotopic constraints on the origin of Wadi El-Tarfa groundwater, Eastern Desert, Egypt. *Groundwater*, volume 38, 9 pages, [doi:10.1111/j.1745-6584.2000.tb02710.x](https://doi.org/10.1111/j.1745-6584.2000.tb02710.x).
- Sumner, G., 1988, *Precipitation: Process and Analysis*. John Wiley and Sons, Inc. Singapore, <https://www.abebooks.com/9780471905349/Precipitation-Process-Analysis-Sumner-Graham-0471905348/plp>.
- Sunguro, S., K. Froehlich, B.Th. Verhagen, and W. Wagner, 2000, Geohydrology and isotope hydrology of the Lomagundi dolomite, Zimbabwe. In Sililo et al (editors): *Groundwater: Past Achievements and Future Challenges*, Balkema, Rotterdam.

- Tekleab, S., J. Wenninger, and S. Uhlenbrook, 2014, Characterisation of stable isotopes to identify residence times and runoff components in two meso-scale catchments in the Abay/Upper Blue Nile basin, Ethiopia. *Hydrology and Earth System Sciences*, volume 18, 17 pages, [doi:10.5194/hess-18-2415-2014](https://doi.org/10.5194/hess-18-2415-2014).
- Uemura, R., N. Yonezawa, K. Yoshimura, R. Asami, H. Kadana, K. Yamada, and N. Yoshida, 2012, Factors controlling isotopic composition of precipitation on Okinawa Island, Japan: Implications for palaeoclimate reconstruction in the East Asian Monsoon region. *Journal of Hydrology*, volume 475, 9 pages, [doi:10.1016/j.jhydrol.2012.10.014](https://doi.org/10.1016/j.jhydrol.2012.10.014).
- Uhlenbrook, S., M. Frey, C. Leibundgut, and P. Maloszewski, 2002, Hydrograph separations in a mesoscale mountainous basin at event and seasonal timescales. *Water Resources Research*, volume 38, 4 pages, [doi:10.1029/2001WR000938](https://doi.org/10.1029/2001WR000938).
- Urey, H.C., 1947, The thermodynamic properties of isotopic substances. *Journal of the Chemical Society of London*, 20 pages, [doi:10.1039/JR9470000562](https://doi.org/10.1039/JR9470000562).
- Van Gelden, R., A. Baier, H.L. Subert, S. Kowol, L. Balk, and J.A. Barth, 2014, Pleistocene paleo-groundwater as a pristine fresh water resource in southern Germany - evidence from stable and radiogenic isotopes. *Science of the Total Environment*, volume 496, 9 pages, [doi:10.1016/j.scitotenv.2014.07.011](https://doi.org/10.1016/j.scitotenv.2014.07.011).
- Vargas, A.I., B. Schaffer, L. Yuhong, and L. da Silveira Lobo Sternberg, 2017, Testing plant use of mobile vs immobile soil water sources using stable isotope experiments. *New Phytologist*, volume 215, 13 pages, [doi:10.1111/nph.14616](https://doi.org/10.1111/nph.14616).
- Vogel, J.C. and H. van Urk, 1975, Isotopic composition of groundwater in semi-arid regions of southern Africa. *Journal of Hydrology*, volume 25, issues 1-2, 4 pages, [doi:10.1016/0022-1694\(75\)90036-0](https://doi.org/10.1016/0022-1694(75)90036-0).
- Wang, C., 2007, Plasma-cavity ringdown spectroscopy (P-CRDS) for elemental and isotopic analysis. *Journal of Analytical Atomic Spectroscopy*, volume 22, 17 pages, [doi:10.1039/B701223C](https://doi.org/10.1039/B701223C).
- Wang, J., N. Lu, and B. Fu, 2019, Inter-comparison of stable isotope mixing models for determining plant water source partitioning. *Science of the Total Environment*, volume 666, 9 pages, [doi:10.1016/j.scitotenv.2019.02.262](https://doi.org/10.1016/j.scitotenv.2019.02.262).
- West, A.G., G.R. Goldsmith, P.D. Brooks, and T.E. Dawson, 2010, Discrepancies between isotope ratio infrared spectroscopy and isotope ratio mass spectrometry for the stable isotope analysis of plant and soil waters. *Rapid Communications in Mass Spectrometry*, volume 24, 7 pages, [doi:10.1002/rcm.4597](https://doi.org/10.1002/rcm.4597).
- Xie, Y., P.G. Cook, and C.T. Simmons, 2016, Solute transport processes in flow-event-driven stream-aquifer interaction. *Journal of Hydrology*, volume 538, 11 pages, [doi:10.1016/j.jhydrol.2016.04.031](https://doi.org/10.1016/j.jhydrol.2016.04.031).
- Yakir, D., M.J. de Niro, and J.E. Ephrath, 1990, Effects of water stress on oxygen, hydrogen and carbon isotope ratios in two species of cotton plants. *Plant, Cell and Environment*, volume 13, 7 pages, [doi:10.1111/j.1365-3040.1990.tb01985.x](https://doi.org/10.1111/j.1365-3040.1990.tb01985.x).

- Yang, X., T. Yao, W. Yang, W. Yu, and D. Qu, 2011, Co-existence of temperature and amount effects on precipitation  $\delta^{18}\text{O}$  in the Asian monsoon region. *Geophysical Research Letters*, volume 38, issue 21, article L21809, 6 pages, [doi:10.1029/2011GL049353](https://doi.org/10.1029/2011GL049353).
- Yidana, S.M., O.F. Fynn, D. Adomako, L.P. Chegbeleh, and P.M. Nude, 2016, Estimation of evapotranspiration losses in the vadose zone using stable isotopes and chloride mass balance method. *Environmental Earth Sciences*, volume 75, 208 pages, [doi:10.1007/s12665-015-4982-6](https://doi.org/10.1007/s12665-015-4982-6).
- Yin, L., G. Hou, Y. Dou, Z. Tao and Y. Li, 2011, Hydrogeochemical and isotopic study of groundwater in the Habor Lake Basin of the Ordos Plateau, NW China. *Environmental Earth Sciences*, volume 64, 10 pages, [doi:10.1007/s12665-009-0383-z](https://doi.org/10.1007/s12665-009-0383-z).
- Yonge, C.J., L. Goldenberg, and H.R. Krouse, 1989, An isotopic study of water bodies along a traverse of southwestern Canada. *Journal of Hydrology*, volume 1989, 11 pages, [doi:10.1016/0022-1694\(89\)90075-9](https://doi.org/10.1016/0022-1694(89)90075-9).
- Yurtsever, Y. and J.R. Gat, 1981, Atmospheric Waters, Gat J.R. and R. Gonfiantini, *Stable Isotope Hydrology*. International Atomic Energy Agency, Vienna, Technical Report 20, 40 pages, [https://inis.iaea.org/collection/NCLCollectionStore/ Public/13/677/13677657.pdf](https://inis.iaea.org/collection/NCLCollectionStore/Public/13/677/13677657.pdf).

## 13 Exercise Solutions

### Solution Exercise 1 - Meteoric Water Lines

Step-by-step calculation is shown in the tables and calculations that follow.

Calculation of a meteoric water line							
Location	Date	Precipitation mm	$\delta^{18}\text{O}$ ‰	$\delta\text{D}$ ‰	$(\delta^{18}\text{O}_i - \overline{\delta^{18}\text{O}})^2$	$(\delta\text{D}_i - \overline{\delta\text{D}})^2$	$(\delta^{18}\text{O}_i - \overline{\delta^{18}\text{O}})(\delta\text{D}_i - \overline{\delta\text{D}})$
UCT	Jan 2010	9	0.75	9.7	8.619	342.87	54.36
UCT	Feb 2010	12	-0.54	-5.8	2.709	9.10	4.96
UCT	Mar 2010	7	-0.83	0.4	1.838	84.95	12.50
UCT	Apr 2010	44	-2.25	-12.1	0.004	10.78	0.21
UCT	May 2010	277	-2.78	-8.4	0.353	0.17	-0.25
UCT	Jun 2010	222	-3.31	-17.0	1.264	66.97	9.20
UCT	Jul 2010	166	-3.69	-15.0	2.263	38.23	9.30
UCT	Aug 2010	121	-1.74	-4.9	0.199	15.34	1.75
UCT	Sep 2010	100	-2.24	-3.3	0.003	30.43	-0.30
UCT	Oct 2010	102	-2.15	-3.3	0.001	30.43	0.20
UCT	Nov 2010	73	-2.39	-6.2	0.042	6.85	-0.53
UCT	Dec 2010	17	-5.06	-39.9	8.261	966.17	89.34
		<b>Total</b>	<b>Mean</b>	<b>Mean</b>	<b>SS-<math>\delta^{18}\text{O}</math></b>	<b>SS-<math>\delta\text{D}</math></b>	<b>SP-<math>\delta^{18}\text{O}</math>-<math>\delta\text{D}</math></b>
		<b>1150</b>	<b>-2.19</b>	<b>-8.82</b>	<b>25.56</b>	<b>1602.30</b>	<b>180.74</b>

SS = sum of squares; SP = sum of products.

For the best fit line by RMA (reduced major axis) regression:

$$\text{the gradient} = \sqrt{\frac{SS\delta\text{D}}{SS\delta^{18}\text{O}}} = \sqrt{\frac{1602.30}{25.56}} = 7.92$$

$$\text{the intercept} = \overline{\delta\text{D}} - (7.92 \overline{\delta^{18}\text{O}}) = -8.8 - (7.92 (-2.19)) = 8.49$$

therefore, the  $\text{LMWL}_{\text{UCT-2010}}$  is  $\delta\text{D} = 7.92\delta^{18}\text{O} + 8.49$

Pearson's  $r$ , the sample correlation coefficient

$$= r_{\delta^{18}\text{O}\delta\text{D}} = \frac{SP\delta^{18}\text{O}\delta\text{D}}{\sqrt{SS\delta^{18}\text{O}}\sqrt{SS\delta\text{D}}} = \frac{180.74}{\sqrt{25.56}\sqrt{1602.30}} = 0.893$$

Calculation of a precipitation-weighted meteoric water line

Location	Date	Precipitation mm	$\delta^{18}\text{O}$ ‰	$\delta\text{D}$ ‰	Rain- fraction (rf)	$rf \times \delta\text{D}$	$rf \times \delta^{18}\text{O}$	$rf \times (\delta^{18}\text{O}_i - \delta^{18}\text{O})^2$	$rf \times (\delta\text{D}_i - \delta\text{D})^2$	$rf \times (\delta^{18}\text{O}_i - \delta^{18}\text{O}) \times (\delta\text{D}_i - \delta\text{D})$
UCT	Jan 2010	9	0.75	9.7	0.0078	0.0059	0.0759	0.067	2.68	0.43
UCT	Feb 2010	12	-0.54	-5.8	0.0104	-0.0056	-0.0605	0.028	0.09	0.05
UCT	Mar 2010	7	-0.83	0.4	0.0061	-0.0051	0.0024	0.011	0.52	0.08
UCT	Apr 2010	44	-2.25	-12.1	0.0383	-0.0861	-0.4630	0.000	0.41	0.01
UCT	May 2010	277	-2.78	-8.4	0.2409	-0.6696	-2.0233	0.085	0.04	-0.06
UCT	Jun 2010	222	-3.31	-17.0	0.1930	-0.6390	-3.2817	0.244	12.93	1.78
UCT	Jul 2010	166	-3.69	-15.0	0.1443	-0.5326	-2.1652	0.327	5.52	1.34
UCT	Aug 2010	121	-1.74	-4.9	0.1052	-0.1831	-0.5156	0.021	1.61	0.18
UCT	Sep 2010	100	-2.24	-3.3	0.0870	-0.1948	-0.2870	0.000	2.65	-0.03
UCT	Oct 2010	102	-2.15	-3.3	0.0887	-0.1907	-0.2927	0.000	2.70	0.02
UCT	Nov 2010	73	-2.39	-6.2	0.0635	-0.1517	-0.3936	0.003	0.43	-0.03
UCT	Dec 2010	17	-5.06	-39.9	0.0148	-0.0748	-0.5898	0.122	14.28	1.32
		<b>Total</b>	<b>Mean</b>	<b>Mean</b>	<b>Sum</b>	<b>Sum</b>	<b>Sum</b>	<b><math>SS \times rf \delta^{18}\text{O}</math></b>	<b><math>SS \times rf \delta\text{D}</math></b>	<b><math>SP \times rf \delta^{18}\text{O} \delta\text{D}</math></b>
		1150	-2.19	-8.82	1.00	-2.73	-9.99	0.909	43.98	5.08

SS = sum of squares; SP = sum of products; rf = rain fraction (i.e., weighted by precipitation).

For the best fit line by RMA (reduced major axis) regression:

$$\text{the gradient} = \sqrt{\frac{SS \times rf \delta\text{D}}{SS \times rf \delta^{18}\text{O}}} = \sqrt{\frac{43.98}{0.909}} = 6.95$$

$$\text{the intercept} = \sum rf \cdot \delta\text{D} - 6.95 \sum rf \cdot \delta^{18}\text{O} = -9.99 - (6.95 (-2.73)) = 8.96$$

the **precipitation weighted LMWL**<sub>UCT-2010</sub> is  $\delta\text{D} = 6.95\delta^{18}\text{O} + 8.96$

Pearson's *r*, the sample correlation coefficient

$$r_{rf \delta^{18}\text{O} \delta\text{D}} = \frac{SPrf \delta^{18}\text{O} \delta\text{D}}{\sqrt{SSrf \delta^{18}\text{O}} \sqrt{SSrf \delta\text{D}}} = \frac{5.08}{\sqrt{0.909} \sqrt{43.87}} = 0.805$$

[Return to Exercise 1](#) ↑

## Solution Exercise 2 - Recharge Altitude

1. The mean stable isotope composition for the Kirstenbosch spring is:

$$\bar{\delta} = \frac{\sum_i^n \delta_i}{n}$$

where:

$\delta_i$  = value for a given sample

$n$  = total number of samples

the means are -11.45‰ and -3.11‰ for  $\delta^2\text{H}$  and  $\text{d}^{18}\text{O}$  respectively.

2. The weighted means for the precipitation stations are:

$$\bar{\delta} = \sum_i^n \delta_i \times rf_i$$

where:

$\delta$  = denotes a year

$\delta_i$  =  $\delta$  value for a given month

$rf_i$  = fraction of the total precipitation

(over 3 years) for that month, calculated as:

$$rf_i = \frac{r_i}{r_t}$$

where:

$r_i$  = rain amount for a month

$r_t$  = total rain for the period of the study

For months with missing data, the total precipitation amount must exclude those months. Final answers of -9.15‰ and -2.90‰ for  $\delta^2\text{H}$  and  $\delta^{18}\text{O}$  at University of Cape Town and -14.34‰ and -3.73‰ similarly for the Table Mountain Cableway.

3. The altitude effect per isotope pair is calculated as:

$$\frac{\Delta\delta}{m} = \frac{\bar{\delta}_{TMC} - \bar{\delta}_{UCT}}{h_{TMC} - h_{UCT}}$$

where:

$\Delta\delta/m$  = change in  $\delta$  values per meter of altitude

$\delta_x$  = mean stable isotope composition for a station

$h_x$  = elevation of that station

giving answers of -0.0055‰/m for  $\delta^2\text{H}$  and -0.00089‰/m for  $\delta^{18}\text{O}$ . These answers are more reasonably displayed for  $\delta^2\text{H}$  and  $\delta^{18}\text{O}$  as -0.55‰/100 m and -0.089‰/100 m.

4. The recharge elevation for Kirstenbosch can be calculated by addition of the isotopic altitude effect to the starting elevation at UCT, as follows:

$$h_{Kb} = h_{UCT} + \frac{(\bar{\delta}_{Kb} - \bar{\delta}_{UCT})}{(\Delta\delta/m)}$$

or by using the same formula with the  $h_{TMC}$  and  $\delta_{TMC}$  values, which will produce a subtraction, both of which should give the same answer. Using  $\delta^2\text{H}$  gives 591 m and  $\delta^{18}\text{O}$  gives 368 m, the average of which is 479 m. This means the recharge area is 319 m above the spring at 160 m. This is obviously an average elevation as recharge occurs over an area and not at one point.

[Return to Exercise 2](#) ↑

## Solution Exercise 3 - Hydrograph Separation

Using the mass balance equation for a 2-component system:

$$Q_p \times \delta_p + Q_g \times \delta_g = Q_s \times \delta_s$$

where:

$Q$  = flow

$\delta$  = stable isotope composition

$p$  = precipitation

$g$  = groundwater

$s$  = surface water

and recognizing:

$$Q_p + Q_g = Q_s$$

and if fractions are used instead of actual flow:

$$Q_s = 1, \text{ then } Q_p + Q_g = 1$$

$$\therefore Q_p = 1 - Q_g$$

$$\therefore (1 - Q_g)\delta_p + Q_g\delta_g = \delta_s$$

$$\therefore \delta_p - Q_g\delta_p + Q_g\delta_g = \delta_s$$

$$\therefore Q_g(\delta_g - \delta_p) = \delta_s - \delta_p$$

$$\therefore Q_g = \frac{(\delta_s - \delta_p)}{(\delta_g - \delta_p)}$$

which, for  $\delta^2\text{H}$  gives 0.82 for groundwater, which translates to the surface water flow being 82 percent groundwater and 18 percent precipitation derived. For  $\delta^{18}\text{O}$ , the answers are 63 percent groundwater and 37 percent precipitation.

The measurement errors (given by Hu et al., 2020), especially for precipitation, are so large, it is possible precipitation has the same isotope composition as groundwater, in which case hydrograph separation is not possible. Similarly, the river water could have the same isotope composition as the groundwater, again negating the ability to perform a hydrograph separation. More measurements would lower the error and improve the estimate.

[Return to Exercise 3](#) ↑

## 14 Notations

$\text{‰}$	parts per thousand (permil)
$1,2,3,\dots$	subscript for input streams
$a,b,c$	fitting constants ( $K^2$ , $K$ , dimensionless, respectively)
$\alpha$	equilibrium fractionation factor for the reaction at a given temperature (dimensionless)
$\alpha_{X,Y}$	fractionation factor for transition from X to Y (dimensionless)
$c$	y-intercept (dimensions of y-axis values)
$d$	deuterium excess (D-excess)
$\delta$	deviation of stable isotope composition from a standard
$\varepsilon$	enrichment factor
$f$	fraction (1 to 0) of water that remains (dimensionless)
$f$	subscript for output stream
$g$	subscript indicating groundwater
$m$	gradient, i.e., slope of the line (dimensions of y-axis values over dimensions of x-axis values)
$m_{RMW}$	gradient, i.e., slope of the Reduced Major Axis Regression (dimensions of y-axis values over dimensions of x-axis values)
$p$	subscript indicating precipitation
$Q$	flow rate ( $\text{MT}^{-1}$ )
$R$	isotope ratio such as $^2\text{H}/^1\text{H}$ (dimensionless)
$r_{final}$	isotope composition of the pool of water with fraction $f$ remaining (dimensionless)
$r_{initial}$	original isotope composition of the pool (dimensionless)

$s$	subscript indicating resultant total stream flow
$SP_{xy}$	sum of product of deviations from the mean of $x$ and deviations from mean of $y$ (dimensions are product of $x$ and $y$ dimensions)
$SS_x$	sum of the squared deviations from the mean of $x$ (squared dimensions of the $x$ variable)
$SS_y$	sum of the squared deviations from the mean of $y$ (squared dimensions of the $y$ variable)
$T$	temperature (K)
$X$	subscript indicating reactant compound or state
$x, y$	regression variables
$Y$	subscript indicating product compound or state

## 15 About the Author



**Dr. Roger Diamond** studied geology at the University of Cape Town, receiving his Master of Science in 1997, after which he worked in Australia as a gold exploration geologist and then a hydrogeologist for the Western Australian state government. After returning to South Africa in 2002, he worked for the Western Cape government and as a consultant for Environmental Science Associates in various aspects of environmental management, before returning to University of Cape Town in 2010 to study for a Doctor of

Philosophy degree, which was awarded in 2014. He then moved to Pretoria where he lectures hydrogeology and geochemistry at the University of Pretoria, focusing his research on water quality and hydrochemistry, including work on nitrates, uranium, radon, and of course stable isotopes! He has been an active member of the Groundwater Division of the Geological Society of South Africa for many years, and takes part in several environmental and conservation actions, especially removal of invasive alien plants with the Mountain Club of South Africa. When not looking at rocks, he is out climbing up them.

Please consider signing up for the GW-Project mailing list to stay informed about new book releases, events and ways to participate in the GW-Project. When you sign up for our email list it helps us build a global groundwater community. [Sign up](#)<sup>↗</sup>.

